IAEA
International Atomic Energy Agency

IAEA TECDOC SERIES

No. 2063

Advancing the State of the Practice in Uncertainty and Sensitivity Methodologies for Severe Accident Analysis in Water Cooled Reactors of the BWR Type

Final Report of a Coordinated Research Project

ADVANCING THE STATE OF THE PRACTICE IN UNCERTAINTY AND SENSITIVITY METHODOLOGIES FOR SEVERE ACCIDENT ANALYSIS IN WATER COOLED REACTORS OF THE BWR TYPE

The following States are Members of the International Atomic Energy Agency:

AFGHANISTAN
ALBANIA
ALGERIA
ANGOLA
ANTIGUA AND BARBUDA
ARGENTINA
ARMENIA
AUSTRALIA
AUSTRIA
AZERBAIJAN
BAHAMAS
BAHRAIN
BANGLADESH
BARBADOS
BELARUS
BELGIUM
BELIZE
BENIN
BOLIVIA, PLURINATIONAL STATE OF
BOSNIA AND HERZEGOVINA
BOTSWANA
BRAZIL
BRUNEI DARUSSALAM
BULGARIA
BURKINA FASO
BURUNDI
CABO VERDE
CAMBODIA
CAMEROON
CANADA
CENTRAL AFRICAN REPUBLIC
CHAD
CHILE
CHINA
COLOMBIA
COMOROS
CONGO
COSTA RICA
CÔTE D'IVOIRE
CROATIA
CUBA
CYPRUS
CZECH REPUBLIC
DEMOCRATIC REPUBLIC OF THE CONGO
DENMARK
DJIBOUTI
DOMINICA
DOMINICAN REPUBLIC
ECUADOR
EGYPT
EL SALVADOR
ERITREA
ESTONIA
ESWATINI
ETHIOPIA
FIJI
FINLAND
FRANCE
GABON
GAMBIA
GEORGIA
GERMANY
GHANA
GREECE
GRENADA
GUATEMALA
GUINEA
GUYANA
HAITI
HOLY SEE
HONDURAS
HUNGARY
ICELAND
INDIA
INDONESIA
IRAN, ISLAMIC REPUBLIC OF
IRAQ
IRELAND
ISRAEL
ITALY
JAMAICA
JAPAN
JORDAN
KAZAKHSTAN
KENYA
KOREA, REPUBLIC OF
KUWAIT
KYRGYZSTAN
LAO PEOPLE'S DEMOCRATIC REPUBLIC
LATVIA
LEBANON
LESOTHO
LIBERIA
LIBYA
LIECHTENSTEIN
LITHUANIA
LUXEMBOURG
MADAGASCAR
MALAWI
MALAYSIA
MALI
MALTA
MARSHALL ISLANDS
MAURITANIA
MAURITIUS
MEXICO
MONACO
MONGOLIA
MONTENEGRO
MOROCCO
MOZAMBIQUE
MYANMAR
NAMIBIA
NEPAL
NETHERLANDS, KINGDOM OF THE
NEW ZEALAND
NICARAGUA
NIGER
NIGERIA
NORTH MACEDONIA
NORWAY
OMAN
PAKISTAN
PALAU
PANAMA
PAPUA NEW GUINEA
PARAGUAY
PERU
PHILIPPINES
POLAND
PORTUGAL
QATAR
REPUBLIC OF MOLDOVA
ROMANIA
RUSSIAN FEDERATION
RWANDA
SAINT KITTS AND NEVIS
SAINT LUCIA
SAINT VINCENT AND THE GRENADINES
SAMOA
SAN MARINO
SAUDI ARABIA
SENEGAL
SERBIA
SEYCHELLES
SIERRA LEONE
SINGAPORE
SLOVAKIA
SLOVENIA
SOUTH AFRICA
SPAIN
SRI LANKA
SUDAN
SWEDEN
SWITZERLAND
SYRIAN ARAB REPUBLIC
TAJIKISTAN
THAILAND
TOGO
TONGA
TRINIDAD AND TOBAGO
TUNISIA
TÜRKİYE
TURKMENISTAN
UGANDA
UKRAINE
UNITED ARAB EMIRATES
UNITED KINGDOM OF GREAT BRITAIN AND NORTHERN IRELAND
UNITED REPUBLIC OF TANZANIA
UNITED STATES OF AMERICA
URUGUAY
UZBEKISTAN
VANUATU
VENEZUELA, BOLIVARIAN REPUBLIC OF
VIET NAM
YEMEN
ZAMBIA
ZIMBABWE

The Agency's Statute was approved on 23 October 1956 by the Conference on the Statute of the IAEA held at United Nations Headquarters, New York; it entered into force on 29 July 1957. The Headquarters of the Agency are situated in Vienna. Its principal objective is "to accelerate and enlarge the contribution of atomic energy to peace, health and prosperity throughout the world''.

IAEA-TECDOC-2063

ADVANCING THE STATE OF THE PRACTICE IN UNCERTAINTY AND SENSITIVITY METHODOLOGIES FOR SEVERE ACCIDENT ANALYSIS IN WATER COOLED REACTORS OF THE BWR TYPE

FINAL REPORT OF A COORDINATED RESEARCH PROJECT

INTERNATIONAL ATOMIC ENERGY AGENCY
VIENNA, 2024

COPYRIGHT NOTICE

For further information on this publication, please contact:

Nuclear Power Technology Development Section
International Atomic Energy Agency
Vienna International Centre
PO Box 100
1400 Vienna, Austria
Email: Official.Mail@iaea.org

Printed by the IAEA in Austria
July 2024
https://doi.org/10.61092/iaea.i33x-g2lq

IAEA Library Cataloguing in Publication Data

Names: International Atomic Energy Agency.
Title: Advancing the state of the practice in uncertainty and sensitivity methodologies for severe accident analysis in water cooled reactors of the BWR type / International Atomic Energy Agency.
Description: Vienna : International Atomic Energy Agency, 2024. | Series: IAEA TECDOC series, ISSN 1011-4289 ; no. 2063 | Includes bibliographical references.
Identifiers: IAEAL 24-01696 | ISBN 978-92-0-123324-0 (paperback : alk. paper) | ISBN 978-92-0-123224-3 (pdf)
Subjects: LCSH: Boiling water reactors. | Water cooled reactors. | Nuclear facilities — Safety measures. | Nuclear reactor accidents.

FOREWORD

In January 2023 there were a total of 439 operating nuclear reactors worldwide; 304 were pressurized water reactors and 61 were boiling water reactors. Although some core degradation phenomena are shared by these light water reactors, the evolution of severe accidents is dependent on the reactor technology due to factors such as the use of different materials and their proportions in reactor fuel, equipment configuration in the reactor pressure vessel above and below the core, reactivity control components, and operating conditions. Severe accident scenarios need to be thoroughly studied for each design, including those of the same technology as they have evolved over time, to identify possible mitigation strategies using different systems. Additionally, given the incomplete knowledge of some of the severe accident phenomena, the uncertainty and sensitivity analysis need to be included in every comprehensive reactor safety assessment study.

In 2019 the IAEA launched a coordinated research project entitled Advancing the State of Practice in Uncertainty and Sensitivity Methodologies for Severe Accident Analysis in Water Cooled Reactors. By bringing together experts from Member States with relevant technologies, the primary objectives of the coordinated research project were to advance the understanding and characterization of sources of uncertainties and their effects on the key figure of merit predictions in severe accident codes for water cooled reactors, improve capabilities and expertise in Member States to perform the state of the art uncertainty and sensitivity analysis with severe accident codes, and support graduate students in their relevant research. The participating Member State organizations contributed to two major exercises: the Quench-06 test application uncertainty exercise and a plant application uncertainty exercise that was divided into five subtasks addressing the existing reactor lines (i.e. boiling water reactors; pressurized water reactors, including small modular reactor designs; pressurized heavy water reactors; and water cooled, water moderated power reactors). This publication addresses the studies of relevance to boiling water reactor designs in which institutions from four Member States participated: Research Centre for Energy, Environment and Technology (Spain), Ghana Atomic Energy Commission (Ghana), Sandia National Laboratories (United States of America), National Commission for Nuclear Safety and Safeguards (Mexico) and National Institute for Nuclear Research (Mexico). This publication summarizes contributions from the Research Centre for Energy, Environment and Technology, Ghana Atomic Energy Commission, National Commission for Nuclear Safety and Safeguards, and National Institute for Nuclear Research.

The IAEA acknowledges the efforts and assistance provided by the contributors listed at the end of this publication. The IAEA officer responsible for this publication was T. Jevremovic of the Division of Nuclear Power.

EDITORIAL NOTE

This publication has been prepared from the original material as submitted by the contributors and has not been edited by the editorial staff of the IAEA. The views expressed remain the responsibility of the contributors and do not necessarily represent the views of the IAEA or its Member States.

Guidance and recommendations provided here in relation to identified good practices represent expert opinion but are not made on the basis of a consensus of all Member States.

Neither the IAEA nor its Member States assume any responsibility for consequences which may arise from the use of this publication. This publication does not address questions of responsibility, legal or otherwise, for acts or omissions on the part of any person.

The use of particular designations of countries or territories does not imply any judgement by the publisher, the IAEA, as to the legal status of such countries or territories, of their authorities and institutions or of the delimitation of their boundaries.

The mention of names of specific companies or products (whether or not indicated as registered) does not imply any intention to infringe proprietary rights, nor should it be construed as an endorsement or recommendation on the part of the IAEA.

The authors are responsible for having obtained the necessary permission for the IAEA to reproduce, translate or use material from sources already protected by copyrights.

The IAEA has no responsibility for the persistence or accuracy of URLs for external or third party Internet web sites referred to in this publication and does not guarantee that any content on such web sites is, or will remain, accurate or appropriate.

CONTENTS

1. INTRODUCTION 1
1.1. BACKGROUND 1
1.2. OBJECTIVE 2
1.3. SCOPE 2
1.4. STRUCTURE 3
2. SEVERE ACCIDENT SCENARIOS AND SENSITIVITY AND UNCERTAINTY ANALYSIS METHODOLOGIES 3
2.1. OVERVIEW OF THE ACCIDENT SCENARIOS AND UNCERTAINTY AND SELECTED SENSITIVITY METHODOLOGIES 3
2.2. SEVERE ACCIDENT CODES 6
2.2.1. MELCOR Code 6
2.2.2. MAAP Code 6
2.3. PARTICIPANTS CONTRIBUTIONS 7
2.3.1. Centro de Investigaciones Energéticas, Medioambientales y Tecnológicas (CIEMAT), Spain 7
2.3.2. Ghana Atomic Energy Commission (GAEC), Ghana 21
2.3.3. Comisión Nacional de Seguridad Nuclear y Salvaguardias (CNSNS), Mexico 27
2.3.4. Instituto Nacional de Investigaciones Nucleares (ININ), Mexico 36
3. SUMMARY AND CONCLUSIONS 64
REFERENCES 67
ABBREVATIONS 71
CONTRIBUTORS TO DRAFTING AND REVIEW 73

1. INTRODUCTION

1.1. BACKGROUND

The severe accident codes are complex tools; they require expertise in multiple disciplines to use them correctly. It is not uncommon for users to be unsure about the accuracy of a nuclear power plant (NPP) accident analyses, especially when dealing with scenarios that are outside of the exciting experience. Additionally, understanding the importance and impact of uncertainty and variability on predicted code results is critical for ensuring the accuracy of the results interpretation. The Technical Meeting on the Status and Evaluation of Severe Accident Simulation Codes for Water Cooled Reactors, held in October 2017 as a response to the Member States interests in information exchange on the status of severe accident simulation and modelling codes and tools of relevance to water cooled reactors pointed to the need for the status of these codes and associated uncertainties to be addressed.

In 2019, the International Atomic Energy Agency (IAEA) established the coordinated research project (CRP) on Advancing the State-Of-Practice in Uncertainty and Sensitivity Methodologies for Severe Accident Analysis in Water Cooled Reactors. By bringing together the experts from the IAEA Member States with relevant technologies, the primary objectives of this CRP were to advance the understanding and characterization of sources of uncertainties and their effects on the key figure-of-merit (FOMs) predictions in severe accident codes for water cooled reactors, improve capabilities and expertise in Member States to perform state-of-the-art uncertainty and sensitivity analysis with severe accidents codes, and support graduate students relevant research. This CRP was specifically aimed at improving the state of practice in severe accident analyses by examining and characterizing the impact of uncertainty and variability on severe accident simulation and modelling. The reactor technologies considered for this CRP include pressurized water reactors (PWRs) and small modular reactors, boiling water reactors (BWRs), pressurized heavy water reactors of CANDU (Canada Deuterium Uranium) type, and water-cooled water-moderated energy reactors (VVERs). Described in a separate technical document, the uncertainty and sensitivity analysis of the QUENCH-06 experiment was also performed. This publication describes the uncertainty and sensitivity methodologies applied to BWR technologies in which institutions from five Member States participated: Centro de Investigaciones Energéticas, Medioambientales y Tecnológicas (CIEMAT, Spain), Ghana Atomic Energy Commission (GAEC, Ghana), Sandia National Laboratory (SNL, USA), Comisión Nacional de Seguridad Nuclear y Salvaguardias (CNSNS, Mexico), and Instituto Nacional de Investigaciones Nucleares (ININ, Mexico). This publication summarizes contributions from CIEMAT, GAEC, ININ and CNSNS. The first three institutions addressed severe accident scenarios in a BWR/3 with Mark I primary containment, while the last two used models of a BWR/5 with Mark II containment. Except for CNSNS, the participants selected a short term (unmitigated) station blackout (SBO) scenario for analysis, and the scope of the analysis was limited to only in-vessel phenomena. In case of CNSNS, depressurization and reactor core isolation cooling (RCIC) system injection are considered as mitigating measures and the analysis refers to ex-vessel phenomena. The MELCOR code was used by the first four participants for the severe accident simulations, and the MAAP5 code was used by ININ. DAKOTA was chosen as a tool for the sensitivity and uncertainty calculations by CIEMAT, GAEC and CNSNS, while in-house developed tools are used by SNL and ININ.

1.2. OBJECTIVE

The objective of this publication is to detail the specifics and findings for the performed BWR benchmark calculations. The exercises were aimed at consolidating the existing experience in the development of a strong technical basis for establishing uncertainty and sensitivity methodologies in severe accident analyses for the BRWs being accumulated by experienced analysts with the aim of increasing the sophistication and competency of the practitioners in this field. The insights gained from this exercise lead towards high level suggestions on uncertainty and sensitivity analysis and methods, and with capturing the best practices and lessons learned. Further objective of this publication is to highlight the diverse methodologies developed by the participating institutions with the aim to quantify uncertainties and sensitivities associated to relevant FOMs, such as hydrogen generation and reactor pressure vessel (RPV) breach time, resulting from the incomplete knowledge of the phenomena occurring during the progression of severe accidents. However, the objective of this publication is not only to describe the state-of-the-art methodologies applied to BWR severe accident code predictions, but also to present major issues remaining and pointing to the needs for further research.

1.3. SCOPE

The scope of this publication is focused on description of a framework of the uncertainty and sensitivity analysis, as applicable to the development and/or review of the technical basis for severe accident management guidelines (SAMGs) and the severe accident scenarios for a reference BWR plant, and includes:

- Description of the FOMs used in the analyses;
- List of uncertainties relevant to severe accident code input parameters, the probability density function (PDF) assigned to them, and the rationale for their selection;
- Description of the reference BWR plant, and associated nodalization;
- Description of the severe accident code used for simulations and the associated computational tool for uncertainty and sensitivity analysis;
- Key assumptions of the severe accident scenario/s and the results;
- Uncertainty and sensitivity analyses results and lessons learned.

The CRP exercises were developed as per flow diagram shown in Fig. 1 indicating five separate technical publications, each addressing a specific plant application exercise and outlining relevant research technical results with lessons learned and best practices. The participating organizations in this exercise and contributors to this publication were:

- Centro de Investigaciones Energéticas, Medioambientales y Tecnológicas (CIEMAT, Spain);
- Ghana Atomic Energy Commission (GAEC, Ghana);
- Comisión Nacional de Seguridad Nuclear y Salvaguardias (CNSNS, Mexico);
- Instituto Nacional de Investigaciones Nucleares (ININ, Mexico).

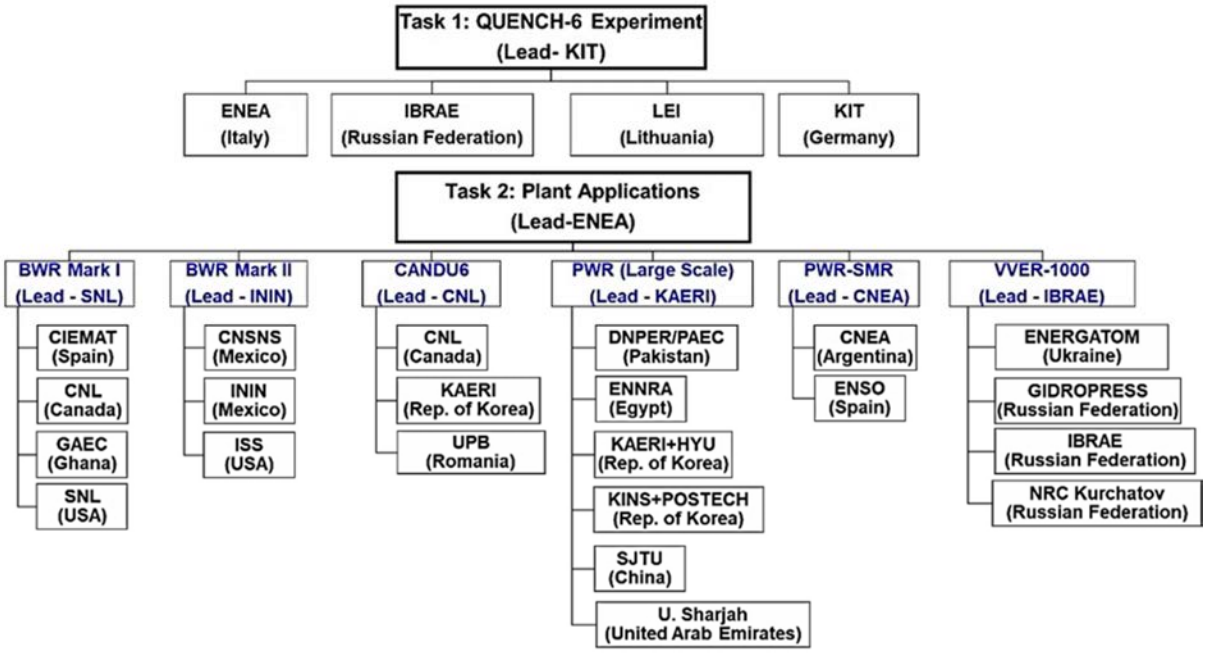

FIG. 1. CRP tasks and participants (refer to Abbreviations for the organizations full names).

1.4. STRUCTURE

Section 1 provides the necessary antecedents of this CRP, and the objective and content of this publication. In Section 2, a summary of the reference BWR plant and selected accident scenarios are presented, followed by description of the uncertainty and sensitivity methods employed, the severe accident simulation codes and coupling tools for input and output data processing, information about the FOMs, and the uncertain input variables along with their selected PDFs. This section concludes with contribution from each of the participant institutions including information about technical aspects and main lessons learned. Finally, Sections 3 presents a summary and the conclusions reached by all participants.

2. SEVERE ACCIDENT SCENARIOS AND SENSITIVITY AND UNCERTAINTY ANALYSIS METHODOLOGIES

This Section describes the accident scenarios, uncertainty and sensitivity methods used, severe accident simulation codes and coupling tools for input and output data processing, selected FOMs, and the uncertain input variables along with their chosen PDFs. The reference plant is described in detail by each participant in the context of the severe accident scenario selected.

2.1. OVERVIEW OF THE ACCIDENT SCENARIOS AND UNCERTAINTY AND SELECTED SENSITIVITY METHODOLOGIES

In the context of this CRP the modelling of BWR plants and simulation of the selected severe accident scenarios with relevant information are summarized in Tables 1–5. It can be seen from Table 1 that in all

cases the initiating event is SBO, which evolves to severe accident because no emergency cooling is provided or it is stopped sometime after the accident starts, as it is the case of simulation performed by CNSNS, where the RCIC is initially allowed to operate. This institution is also the only one who was studying the ex-vessel phenomena. Three participants used the MELCOR code, with different versions, as severe accident simulation tool, and only ININ used the MAAP code.

TABLE 1. REFERENCE PLANT AND ACCIDENT SCENARIO, SIMULATION TOOL AND FRAMEWORK OF ANALYSIS

Institution	Reference plant	Reference scenario and scope	Severe accident code	Framework of the analysis
GAEC	BWR3 / Mark I	SBO unmitigated, in-vessel	MELCOR 2.2.	Development of SAMGs
CIEMAT	BWR3 / Mark I	SBO, in-vessel	MELCOR	Development of SAMGs
CNSNS	BWR5 / Mark II	SBO with RCIC injection and ADS actuation, ex-vessel	MELCOR 2.1.	Support technical basis on regulation issues
ININ	BWR5 / Mark II	Unmitigated high pressure SBO, in-vessel	MAAP 5.03	Support development and review of technical basis of SAMGs

As shown in Table 2, DAKOTA is the preferred uncertainty and sensitivity tool, mainly because it can be used directly with the MELCOR code (GAEC, CIEMAT, and CNSNS), while ININ used the AZTUSIA code. In all cases, the common Pearson and Spearman correlation coefficients were calculated, although ININ also included the Partial and Partial Rank correlation coefficients. This institution additionally used the Monte Carlo filtering technique for sensitivity analyses. For the uncertainty and sensitivity quantification, the two sampling methods were used: the Latin Hypercube sampling and the simple random sampling. Table 3 lists the main points of interest for analysis per participating institutions, while the FOMs are provided in Table 4. The uncertain code input variables and types of PDFs per participating institution are provided in Table 5.

TABLE 2. UNCERTAINTY AND SENSIBILITY METHODS FOR ANALYSIS

Institution	Uncertainty quantification method	Uncertainty quantification tool	Sensitivity methodology
GAEC	Monte Carlo, Latin Hypercube sampling	DAKOTA	Pearson and Spearman correlation coefficients
CIEMAT	Monte Carlo and Wilks approach, Simple Random sampling	DAKOTA	Pearson and Spearman correlation coefficients
CNSNS	Monte Carlo and Wilks approach, Latin Hypercube sampling	DAKOTA	Pearson and Spearman correlation coefficients
ININ	Monte Carlo, Simple Random Sampling, $N = 1000$	AZTUSIA via Phyton scripts	Pearson, Spearman, Partial, and Partial Rank coefficients + Monte Carlo filtering technique

TABLE 3. MAIN POINTS OF INTEREST FOR ANALYSIS

Institution	Points of interest
GAEC	Provide insight to code users on the effect of uncertainty in selected input parameters on the key FOMs.
CIEMAT	How uncertainties in core degradation affect fission product release from fuel rods.
CNSNS	Determine the propagation of uncertainties in models due to key parameters.
ININ	Investigate the range of valid application of the different physical models involved in the accident progression.

TABLE 4. FIGURES OF MERIT SELECTED BY THE PARTICIPANTS

Institution	FOMs
GAEC	In-vessel hydrogen generation
CIEMAT	Everything referred to noble gases, I, and Cs: 1) Total amount of fission products released 2) Onset of fission products release 3) Fission products release rates 4) End time of fission products release
CNSNS	Containment failure time
ININ	1) Hydrogen mass 2) Fission product mass fractions 3) Time to core damage criterion 4) Core support plate failure 5) Debris mass in lower head 6) RPV breach time

TABLE 5. UNCERTAIN CODE INPUT VARIABLES AND TYPES OF PDFs

Institution	Number of input variables	Types of PDFs used
GAEC	11 related to core degradation and relocation to lower plenum; variables are also connected to zirconium cladding oxidation and are generally known to impact in-vessel hydrogen generation	Beta, uniform, log uniform and triangle
CIEMAT	Around 150 uncertain input variables were included, from initial and boundary conditions to physical model parameters and correlations used in the MELCOR code	Various
CNSNS	6 related to temperatures for failure of fuel elements and RPV, RCIC time life, and temperatures related to the state of pedestal concrete	Normal
ININ	28 related to the phenomena found as the core degradation occurs, the dynamics of corium in lower head, and variables directly impacting failure criteria; both quantitative and qualitative input variables were included in the analysis	Normal, uniform, triangular, and discrete.

2.2. SEVERE ACCIDENT CODES

As shown in Table 1, only MELCOR (different versions) and MAAP codes are used to simulate selected severe accident scenarios. Some brief information about these two widely used codes is presented in the following subsections.

2.2.1. MELCOR Code

Relevant features of the MELCOR code applicable to severe accident analysis are presented in detail in [1]. MELCOR is a fully integrated, engineering level computer code developed by Sandia National Laboratories for the United States Nuclear Regulatory Commission to model the progression of severe accidents in NPPs. The code was developed in response to the need for a more advanced modelling tool following the Three Mile Island accident and the Wash1400 report. MELCOR integrates various mechanistic codes such as CORCON, VANESSA, and CONTAIN, making it a comprehensive tool for performing probability risk analysis and evaluating the full reactor accident sequence. The code is designed to model different types of reactors, including BWRs and PWRs, high-temperature gas reactors, sodium containment fires, and spent fuel pools. To make the code user-friendly, Sandia National Laboratories has taken the approach of integrating the modelling for various reactor types within a single code executable. This means that users can specify the reactor type and develop input decks within a familiar syntax for various reactor types. From a developer's perspective, this means designing the code in a generalized manner that allows code components to represent different reactor parts with characteristics that depend on the reactor type being modelled.

2.2.2. MAAP Code

The Modular Accident Analysis Program (MAAP) is developed and maintained by the Electric Power Research Institute of the United States of America. This code has also been described in detail in [1]. simulates the response of light water reactors and CANDU during severe accidents. The code models a full range of important phenomena that could occur during an accident, including those related to thermal hydraulics and fission products. It also models the primary system, core, containment, and reactor/auxiliary building simultaneously.

MAAP5 results are primarily used to determine Level 1 and 2 success criteria and accident timing for probabilistic risk assessment analysis. The code is also used for investigating accident management strategies, equipment qualification analyses, fission product large early release frequency determinations, integrated leak rate test evaluations, emergency planning and training, simulator verification, analyses to support plant modifications, generic plant issue assessments (such as significance determinations), and other similar applications.

MAAP5 is widely used in the nuclear industry because it can model a wide range of severe accident scenarios and has been validated against numerous experimental data and actual accident data. The code is user-friendly and includes a graphical user interface that allows users to set up and run simulations easily. Additionally, MAAP5 provides visualization capabilities to aid in understanding the progression of the accident.

2.3. PARTICIPANTS CONTRIBUTIONS

In this section, each participating institution provides descriptions about the nodalization model, and the simulation tools used, along with the base case scenarios and sensitivity and uncertainty analysis results.

2.3.1. Centro de Investigaciones Energéticas, Medioambientales y Tecnológicas (CIEMAT), Spain

2.3.1.1. Motivation and objectives

Numerical codes are widely used in the nuclear community to assess the behaviour of NPPs during postulated accidents, including severe accidents. They are a central element of the safety demonstration where the compliance of the main safety features of a NPP is assessed against safety requirements. Among the key parameters to predict are the time of failure of safety barriers and the potential radiological source term to the environment. However, these computations used to be based on simplifications, assumptions, and bias, mainly because of the limitation in the computational resources and the inherent uncertainties of the complex severe accident phenomena. Therefore, it becomes necessary to bound the simulation results to account for the inaccuracy of the computations. The objective of this analysis is to obtain a tolerance interval over the FOMs selected to identify not only the prediction capabilities of the evaluation model developed, but also the major uncertainty sources that influence the results.

2.3.1.2. Reference plant

The NPP design selected for the study correspond to a BWR3 with a Mark-I containment. These kind of NPPs rule around five main elements (Fig. 2):

1) Reactor core, which includes nuclear fuel in zirconium alloy clad assemblies, bounded also by zirconium cannisters, along with the control rods of B_4C;
2) Reactor pressure vessel, which encloses the reactor core and water/steam used to transfer the heat;
3) Primary containment vessel consisting in a free-standing bulb-shaped steel dry well backed by a reinforced concrete shell, and the wet well;
4) Pressure suppression pool, formed by a torus shaped steel tank holding liquid water inside (the wet well) to condense the steam delivered from the RPV or the dry well, and therefore, to suppress pressure;
5) Safety systems, mainly formed by high and low active powered injection systems, safety valves, passive isolation condensers, and the venting system, among others.

2.3.1.3. Accident scenario and severe accident code

Based on the analyses carried out with the MELCOR 2.2 code, this study explores the evolution of an unmitigated SBO in a BWR3 with a Mark-I containment plant accounting for the uncertainties in the estimation of the in-vessel fission products release. The sequence analysed corresponds to a 24 h SBO with no mitigation measures assumed. The FOMs included in the analysis are the I2 classes defined in MELCOR, corresponding to all the halogen species, the CS class, referred to the alkali metals, and finally the XE class, which represents all the noble gases.

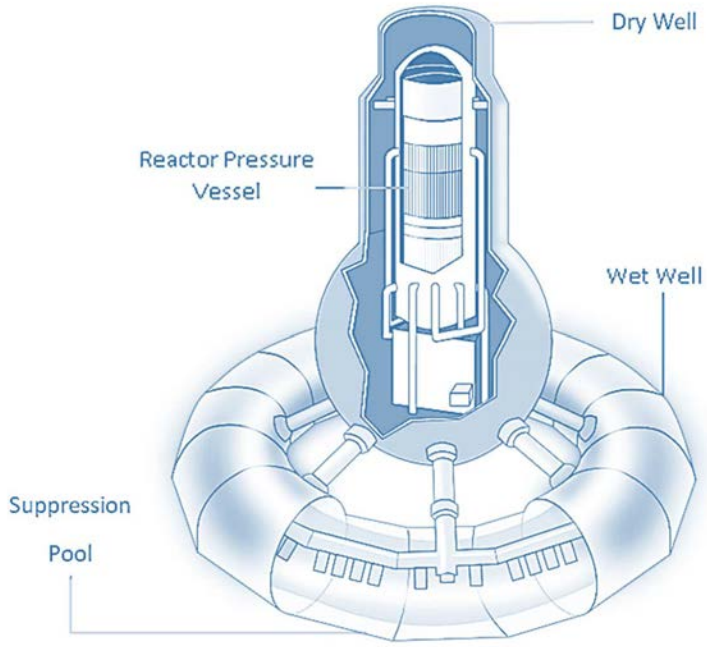

FIG. 2. Major components of GE BWR Mark-I (modified from https://en.wikipedia.org/wiki/GE_BWR).

MELCOR [1], as described in Section 2.2.1, is fully integrated, engineering level computer code that models the progression of severe accidents in light water reactors. It models a broad spectrum of phenomena, from core degradation to source term to the environment: thermal-hydraulic response in the reactor coolant system, reactor cavity, containment, and confinement buildings; core heat-up, degradation, and relocation; core-concrete interactions; hydrogen production, transport, and combustion; fission product release, transport and behaviour. Since MELCOR is a fully integrated code, there is no need of employing any other code to feed its input data file (input deck). MELCOR only allows the lumped parameters approach, except for the COR package[1] where a two dimensional axisymmetric nodalization is employed for capturing the core behaviour and its degradation.

2.3.1.4. Plant modelling and nodalization

The MELCOR EM is based on a Fukushima Unit 1 input deck employed in previous studies [2], which was setup following the best practices modelling guidelines from the SOARCA project [3]. Several modifications were applied to convert such Fukushima Unit 1 input deck, initially thought for forensic analysis, into a predictive evaluation model by removing or modifying most of the failure criteria and

[1] The MELCOR Core (COR) package provides calculation of the thermal response of the core and lower plenum internal structures, including the portion of the lower head directly below the core. Additionally, it models the relocation of core and lower plenum structural materials during melting, slumping, and debris formation, including failure of the reactor vessel and ejection of debris into the reactor cavity.

explicitly modelling some safety systems, as the isolation condensers. The nodalization applied is shown in Fig. 3 for the RPV and in Fig. 4 [2] for the primary containment vessel.

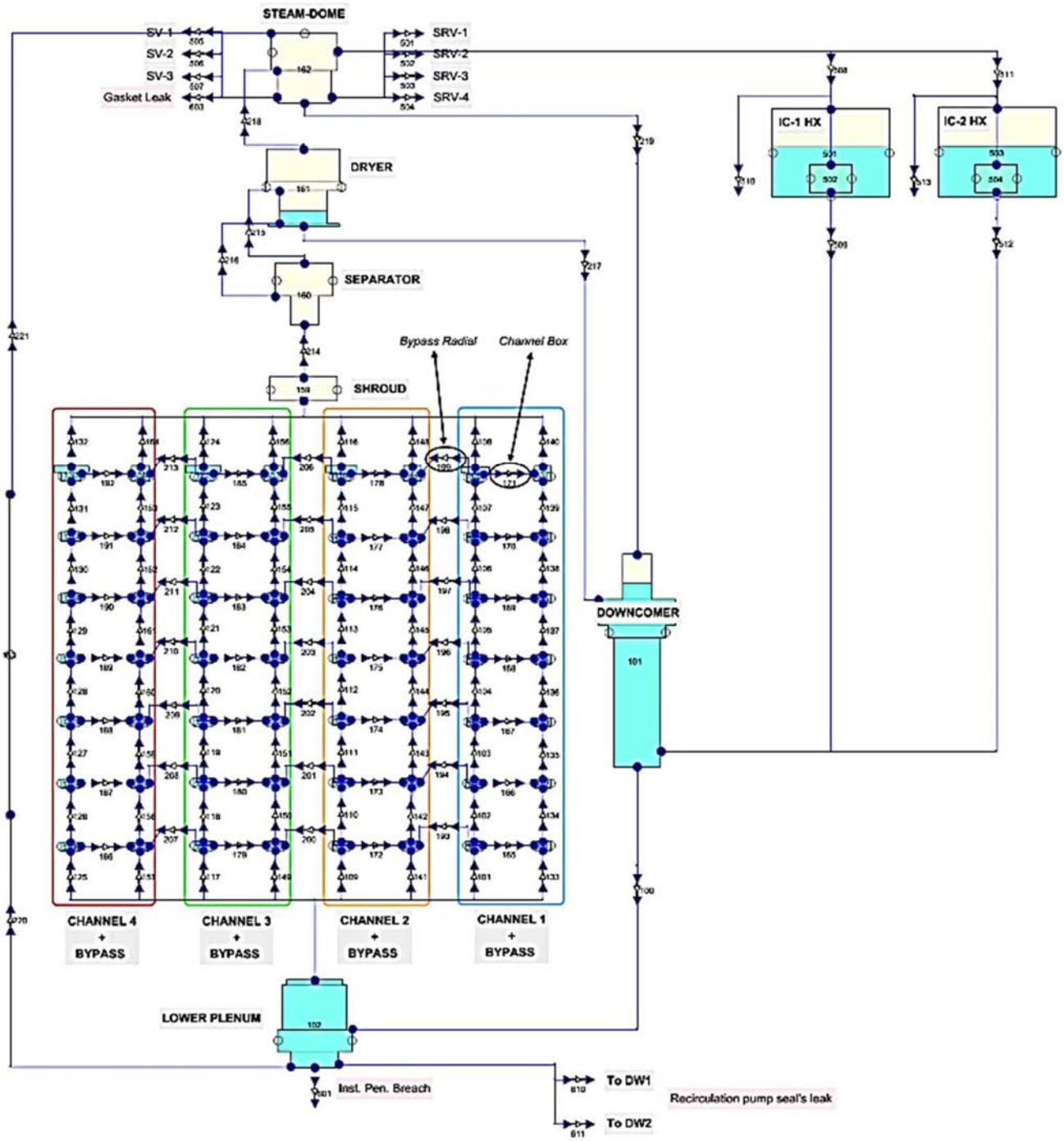

FIG. 3. RPV MELCOR nodalization.

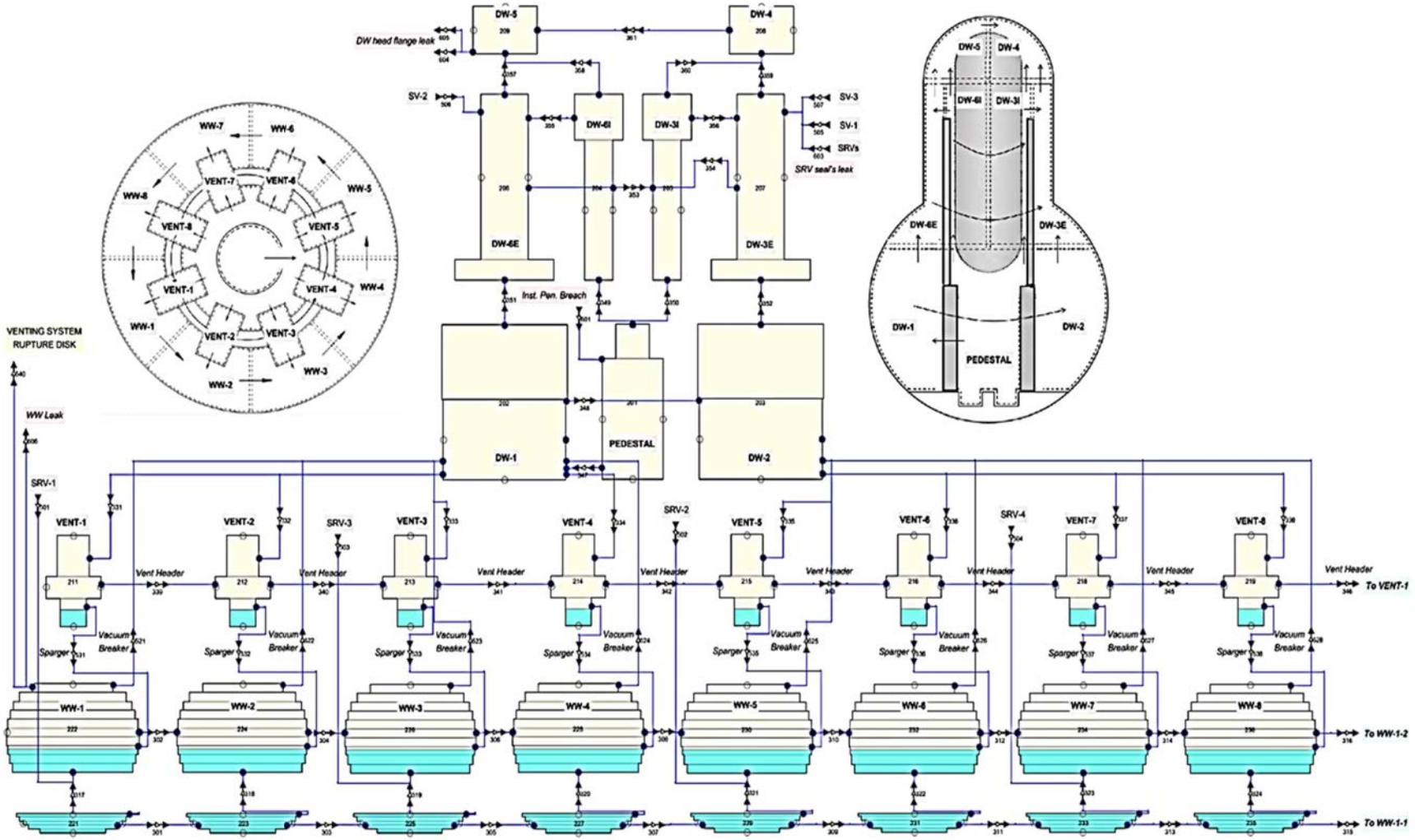

FIG. 4. MELCOR nodalization of the primary containment vessel.

The MELCOR Model of a reactor building is based on a single control volume since the goal of the study is the in-vessel fission product release. The two figures at the top and the bottom on the left hand side (drywell and wetwell) are to be used as the legend of the different cells in the modelling. As shown, each sector of the circumferential torus (8 in total) has MELCOR description, so that MELCOR users can fully understand the rationale behind the containment model (even with the separation of two layers of water in the wetwell according to the injection point).

2.3.1.5. Uncertainty and sensitivity analysis methodology and code

The Best Estimate plus Uncertainty (BEPU) methodology employed by CIEMAT in the framework of this analysis is based on the BEPU-CSA methodology [4]. It is a method originally developed for high fidelity containment safety analyses. However, as it presents a generic structure based on the Regulatory Guide 1.203 [5], it can be applied to other kind of analyses such as severe accidents. The codes employed are the MELCOR code for modelling and calculation of the severe accident phenomena, and the DAKOTA tool for the statistical analysis. The uncertainty assessment consists of identification, quantification, and interpretation:

— ***Identification****:* the response (FOM) uncertainty is produced by combination of different uncertainty and error sources. Experimental data[2], plant data[3], model inadequacy[4], numerical schemes[5], geometry simplification[6], and user effect[7] are the main sources of uncertainty and errors, generally grouped as follows:

Aleatory uncertainties come from the natural variability of a phenomenon (i.e., droplet sizes from a flashing liquid, or number of resultant neutrons from a fission reaction) and measurements (instrument accuracy). In the latest, it may be differentiated between instrument calibration, which add a bias (error) to the measurement; and the instrument precision, which adds dispersion (randomness). In some cases, there may be lack of information for a correctly characterizing of an aleatory uncertainty (i.e., only the mean is known, or the PDF parameters are based on a sample set instead of the whole population). In such situations, the uncertainty of this parameter may be considered as an imprecise uncertainty.

Epistemic uncertainties are those produced due to the lack of knowledge. Usually, availability of real plant schematics and documentation is not trivial. Hence, the information for plant modelling

[2] Experimental data used in developing the models can have inherent uncertainties due to limitations in the experimental techniques, measurement errors, or other sources of variability.
[3] Experimental data used in developing the models can have inherent uncertainties due to limitations in the experimental techniques, measurement errors, or other sources of variability.
[4] The models used in the code may not be fully representative of the physical phenomena, and this can result in uncertainties. For example, simplified models may neglect important physical phenomena or fail to capture the complexity of the system.
[5] The numerical methods used in the code can also contribute to uncertainty, particularly if they are not well-suited to the problem being solved.
[6] Simplifications made in the geometric modelling can also contribute to uncertainty. These can include assumptions made about the geometry, such as modelling components as cylinders instead of more complex shapes, or neglecting small features of the geometry.
[7] This can include user errors in input data, incorrect assumptions, or lack of experience in using the code.

could be incomplete, and incompleteness of data is by definition is an epistemic uncertainty. Consequently, these uncertainties may affect critical parameters, such as the definition of free volume and/or heat sink areas.

Numerical and systemic errors are usually produced due to the lack of control over the code structure, inadequacy of physical models used, and/or the complexity of the simulated phenomena. Therefore, code errors are related to physical models' adequacy (including scale distortions), discretization schemes (spatial and temporal), iterative process (residuals), round-off error, and user effect [6]. Errors are not considered by CIEMAT.

For determining uncertain input parameters, the MELCOR models of relevant phenomena for the scenario to be addressed are studied.

The ranges and probability distributions are generally used to characterize parameter uncertainties. There are different methods to characterize input uncertainties, remarking SAPIUM [7] and part of the SOARCA project [8] outcomes. When characterizing the uncertainties, the case of aleatory uncertainties is clear, since the most appropriate mathematical representation for them is classical probabilistic framework. Therefore, if the information is complete, uncertainty of parameters can be characterized with an adequate PDF applying the classical probability theory, whose basis can be found in almost every textbook related to statistics and probability, such as in [9]. The data for characterizing the parameter uncertainty are extracted from the experiments, in a similar way as it was in the SAPIUM project [7]. However, it is not common to have all the information needed available. Or maybe, there are different sources of information for a parameter. In these cases, the uncertainty becomes incomplete or imprecise. In such situation, the characterization is driven by the principle of minimal specificity [10], and a method based on bounded probabilities (or probability boxes) may be employed. Instead of a single value of probability, the parameter uncertainty will be represented by a bound defined by upper and lower probability values [11, 12].

For the case of purely epistemic uncertainties (total ignorance about the value(s) of a parameter), there is no other way but applying the expert judgment for estimating the uncertainty range. The uncertainty characterization in these cases is driven by the principle of insufficient reason [13] by assigning a uniform distribution to it.

— ***Quantification:*** To account for the additional uncertainties during the execution of the evaluation model, it is necessary to execute the model multiple times with different input values [6]. The Monte Carlo method is one way to obtain a sample set from the input uncertain variables distributions, by randomly generating values from these distributions according to a probability density function [14]. Once a set of input values is generated, the model is run with each set of input values to obtain a set of output values. This process is repeated many times to obtain a large sample set of output values. Statistical techniques are then used to analyse this sample set of output values and to obtain uncertainty bands for the FOMs, which provide a measure of the variability and uncertainty in the predictions. The Monte Carlo method is widely used for uncertainty quantification and sensitivity analysis in many fields, including nuclear engineering, due to its ability to handle complex models with a large number of uncertain parameters. By using this method, it is possible to account for the

uncertainties associated with the different sources of uncertainty and errors in severe accident codes and to obtain more realistic predictions with quantified uncertainties.

To reduce the computational resources needed for the statistical analysis, the Wilks approach is applied [15, 16]. In that manner, the number of iterations needed depends only on the tolerance and confidence limits established, being for instance, 93 runs to establish the 95th percentile at 95% confidence (95/95) for a tolerance interval (two-sided).

— ***Interpretation****:* the Wilks approach being a statistical method used to obtain tolerance intervals with a specified level of confidence or probability for the output quantities of interest, it does not provide information on the influence of each input uncertainty on the output uncertainty. Therefore, a sensitivity analysis is needed to identify the most important input parameters or uncertainties that contribute the most to the output uncertainty. By running a large number of Monte Carlo simulations with a randomly generated set of input values, the effect of each input uncertainty on the output uncertainty can be quantified. This allows the identification of the most important input uncertainties and their contribution to the overall output uncertainty. Using a reduced set of Monte Carlo iterations, it is possible to obtain uncertainty statements and sensitivity measures for all single-value output quantities of interest simultaneously. This provides a more complete understanding of the uncertainties and sensitivities associated with the severe accident codes, allowing for more informed decisions to be made regarding reactor safety and risk management.

  The Pearson product-moment correlation coefficient [17] will be employed to observe the linear correlation between the FOM(s) and the input parameters. The Spearman's correlation coefficient [18] is used to analyse the monotonic correlation between them (a monotonic correlation is considered when a perturbation in one of the two parameters implies a change in the other parameter, but not necessarily at a proportional rate). However, since these two regression coefficients are obtained from a relatively small sample, a p −values analysis is performed to check its consistency. Confidence Intervals is also estimated to consider the so-called statistical error.

DAKOTA is a toolkit developed by Sandia National Laboratories for performing optimization and uncertainty quantification of complex systems. It provides a set of algorithms and methods for design optimization, parameter estimation, sensitivity analysis, and uncertainty quantification. It is designed to be flexible and modular, so that it can be easily integrated with other software tools and workflows. It also provides a range of user interfaces, including a command-line interface and a graphical user interface, to accommodate different user preferences and skill levels. One of the main features of DAKOTA is the ability to perform forward uncertainty propagation, which involves mapping probability information for input parameters to probability information for output response functions. This allows users to explore the effects of input uncertainty on the output of a simulation or model. DAKOTA also includes the capability to perform nested models, which involves layering one DAKOTA method over another. This allows users to apply more advanced algorithms such as mixed epistemic-aleatory or second order uncertainty quantification. In mixed epistemic-aleatory uncertainty quantification, both aleatory (random) and epistemic (systematic) uncertainties are taken into account. Second order uncertainty quantification involves incorporating the effect of uncertainty in the model parameters themselves, as well as the uncertainty in the

model output due to the input parameters. In addition, DAKOTA supports a range of optimization methods, including gradient-based and gradient-free algorithms, as well as surrogate modelling techniques for dealing with expensive simulation codes. It also includes methods for global optimization and multi-objective optimization.

Aleatory uncertainty quantification methods included in DAKOTA are mostly sampling based approaches, such as simple random sampling or Latin Hypercube sampling used to sample the input set and propagated throughout the Monte Carlo method. They are both included in the Latin Hypercube sampling package. The variable distributions allowed are limited to normal, log-normal, uniform, log-uniform, triangular, exponential, beta, gamma, Gumbel, Frechet, Weibull, Poisson, binomial, negative binomial, geometric, hypergeometric, and user-supplied histograms.

DAKOTA provides several sampling methods that generate sets of input samples based on the PDF of the uncertain variables. These samples are then propagated through the simulation or model to obtain a set of response functions, which represent the output of the model for each input sample. Once the response functions are computed, DAKOTA can compute various statistical measures to characterize the uncertainty in the output. These measures can include the mean, standard deviation (std), coefficient of variation, and confidence intervals of the response functions. The mean is simply the average value of the response functions across all the input samples, while the standard deviation measures the spread or variability of the response functions around the mean. The coefficient of variation is the ratio of the standard deviation to the mean and provides a measure of the relative variability of the response functions. Confidence intervals represent the range of values within which the true mean of the response functions is expected to lie with a specified level of confidence. By computing these statistical measures for the response functions, DAKOTA provides a quantitative characterization of the uncertainty in the model output, which can be used to make more informed decisions and assess the reliability of the simulation or model.

If random sampling is selected, order statistics methods can be employed for determining the number of samples that ensures a particular confidence level in a quantile of interest. The most used between these methods in the BEPU collective is that proposed by Wilks[8] [16]. The run cases required are shown in Table 6 as a function of the coverage and confidence levels for a tolerance interval.

TABLE 6. WILKS' TOLERANCE INTERVAL SAMPLE SIZES AS A FUNCTION OF COVERAGE AND CONFIDENCE LEVEL

Wilks' tolerance interval sample size		**$\beta \times 100\%$ (Confidence level)**		
		90	95	99
$\alpha \times 100\%$ (Coverage level)	90	38	46	64
	95	77	93	130
	99	388	473	662

[8] Wilks' approach, also known as Wilks' theorem, is a mathematical result in statistics that provides a way to test whether two statistical models are significantly different from each other. It was developed by Samuel Wilks in the 1930's and is widely used in hypothesis testing and model comparison.

The epistemic uncertainty quantification methods include interval analysis and evidence theory. In interval analysis, it is assumed that nothing is known about an epistemic uncertain variable except that its value lies somewhere within an interval. It must be remarked that it is no assumption that the value has a uniform PDF within the interval. Instead, any value within the interval is a possible value of that variable. The uncertainty quantification goal is to determine the resulting bounds on the output (defining the FOM interval) given interval bounds on the inputs. Any output response that falls within the output interval is a possible output with no frequency information assigned to it, like that supplied by the Wilks' approach. The handicap is that this method is highly computer demanding when there are many input parameters to study. DAKOTA has the capability to perform interval analysis using either global or local methods.

In the evidence theory, also referred as Dempster-Shafer theory[9], the belief function represents the lower bound of the probability of an event, while the plausibility function represents the upper bound of the probability of the same event. These functions can be used to derive measures of uncertainty such as the degree of belief, the degree of uncertainty, and the degree of disbelief. One of the advantages of evidence theory is that it can handle conflicting evidence and combine it in a principled way. However, it can be computationally expensive and requires careful consideration of the assignment of basic probability assignments to the intervals. As the interval analysis, the Dempster-Shafer theory is as well highly computationally demanding.

DAKOTA is also applicable to the problems with a mixture of epistemic and aleatory uncertainties, which requires the segregation of uncertainty types within a nested analysis. An outer epistemic level selects realizations of epistemic parameters, and the inner level of aleatory parameters. This is quite interesting since it allows the use of interval analysis or Dempster-Shafer theory methods to characterize the epistemic uncertainties and then perform a nested sampling process to perform the global uncertainty analysis applying, for example, the Wilks' approach.

In the analysis presented here, only a single sampled based method applying the Wilks' approach is used to obtain the tolerance interval of 95% coverage with 95% confidence on the FOMs of interest.

To compute the Monte Carlo sequence and perform the sampling pairing of input parameters, several scripts in Python were developed for the DAKOTA-MELCOR coupling as depicted in Fig. 5. The whole process is governed by a Python script denominated "*MUQPy_Director*", which refers to "MELCOR Uncertainty Quantification Director for Python". As it can be seen in Fig. 5, the uncertainty quantification begins with a parameter identification table. This table contains the –{parameters ids} to locate every parameter wherein the MELCOR input deck, the uncertainty range (lower and upper bound), the PDF it follows and the expected value, which is dependent on the PDF (mean for a normal distribution, mode for triangular distributions, etc…). This table needs to be in *csv* format to be readable by next subroutine. The next step is the parameter identification table processing and the DAKOTA input deck generation. Since it is expected

[9] Dempster-Shafer theory, also known as the theory of belief functions, is a mathematical framework for reasoning with uncertainty and combining evidence from multiple sources. It was developed by Arthur Dempster and Glenn Shafer in the 1960s and 1970s as an alternative to classical probability theory, which assumes that probabilities can be assigned to all possible outcomes.

to being managing a huge quantity of input parameters, this process is automatized. However, it may be done by the user following the guidance in (https://dakota.sandia.gov/content/manuals). Automatizing the process not only save the time, but also avoids the user errors. Once DAKOTA input deck is ready, the code is executed. All input parameters are sampled following it characteristics. At first, MUQ Director checks if there is an existing MELCOR template corresponding to the base case to analyse. If not, a standard MELCOR input deck is used to generate it. The MELCOR input deck is read and all parameters with ids coincident with these in the Parameter Identification Table are replaced with {parameter id}. On the other hand, if the template already exists (i.e. second iteration round), the marked parameters in the MELCOR template are replaced with the corresponding value of the sample set.

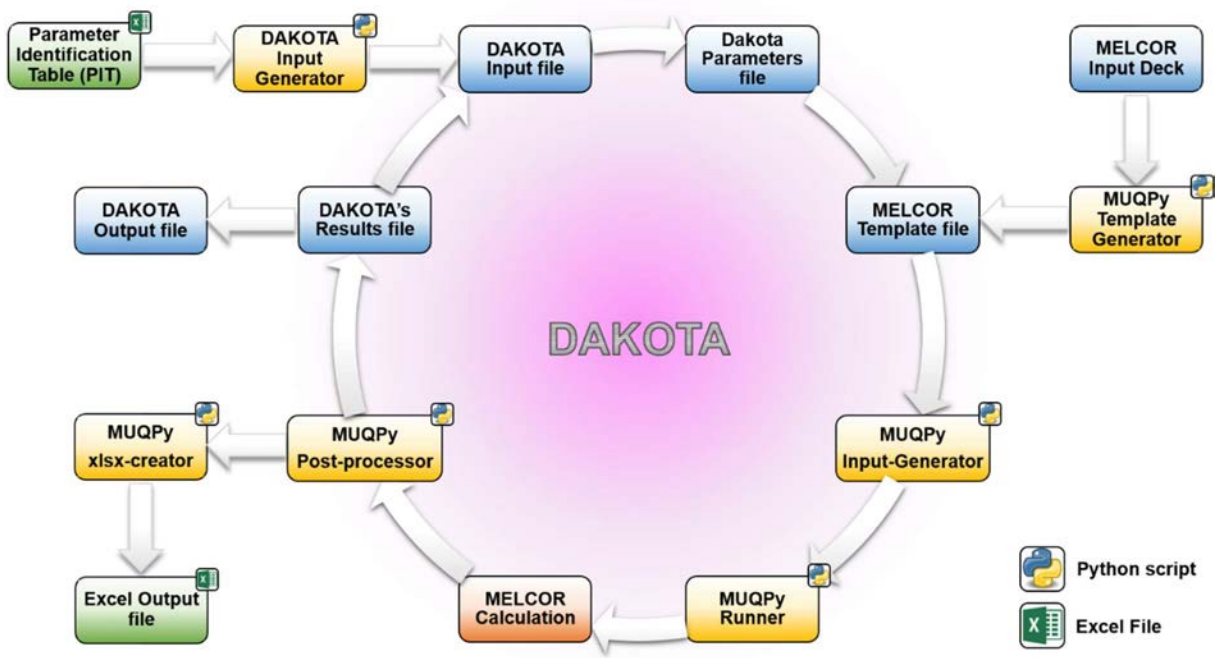

FIG. 5. Uncertainty quantification with DAKOTA-MELCOR.

With the MELCOR input deck set with the parameter values, a new subroutine calls both MELCOR executables, the MELGEN and the MELCOR files. The system is prepared to run several cases simultaneously, but it is highly recommended to leave at least one CPU core free for the operating system and Python scripts manage. The MELCOR output is then post processed by another subroutine to generate a file with the FOMs results in the adequate format for DAKOTA, which processes the output responses to derive the statistical information required, being in this case the lower and upper bound at a 95% probability and 95% confidence. In addition, an extra post processing is performed to obtain extra data in an Excel file format. The data of all the cases are read and written in an .xlsx file with its correspondent plots. Around 150 uncertain input variables are included in the analysis, from initial and boundary conditions to physical model parameters and correlations used in the MELCOR code. A total of 93 cases were launched as it is the minimum sample size needed to infer a tolerance interval with a 95% content and 95% confidence (95/95) according to the Wilks' approach [15, 16].

2.3.1.6. Results

Results obtained in the uncertainty quantification analysis are discussed here. Figure 6 shows the I2 class of radioactive elements release rate as a function of initial mass in the fuel rods. The bound lines correspond to the limits of the tolerance interval according to the Wilks' approach and the in-between curve represents the values obtained in the base case run. As it can be seen, the release begins in a time interval between 1,500 s (25 min) and 38,280 s (10.5 h), being the base case onset at 18,800 s (5 h). This prompt release is relatively small in its magnitude and represents the timing of the fuel clad failure. The reasons for the fuel cladding failure may be related to heat transfer phenomena in the core, as well as the liquid level within the RPV, which is dependent on the performance of the isolation condensers. Nevertheless, it becomes necessary to perform a regression analysis to quantify the contribution of each of the mechanisms affecting the fuel cladding failure. The release continues while more fuel rods fail, and more fission products are released from the fuel pellets as its temperature increases. At 24 h after the reactor SCRAM, it is estimated that the release of I2 class from the fuel is between 7% and 73% of the initial I2 class inventory.

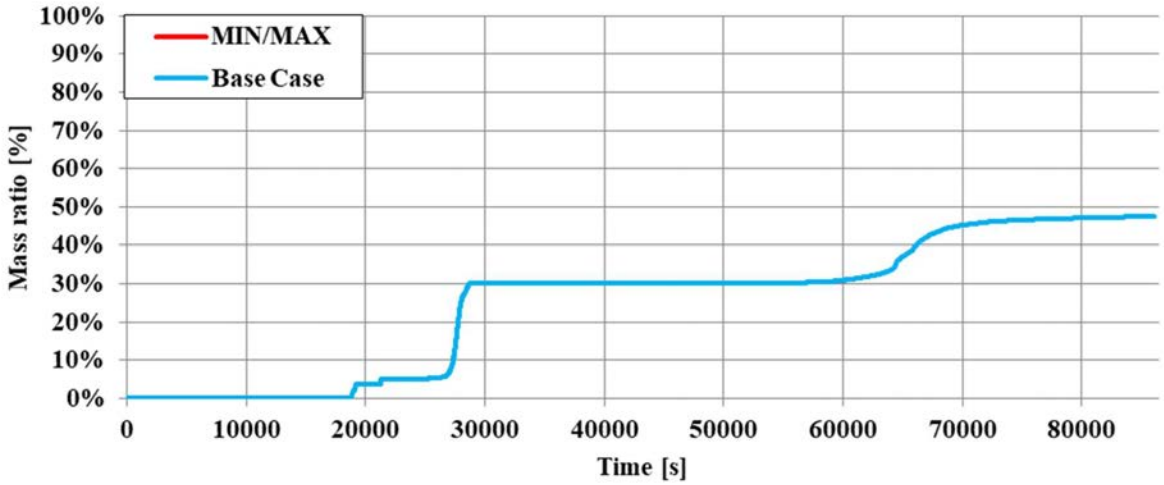

FIG. 6. Release of the I2 class of radioactive elements as a function of the initial I2 class inventory.

Analogously, Fig. 7 shows the Cs class of radioactive elements released from fuel, which results in an interval between 40% and 97%. The released Cs at the end of the transient is within 40–97%. It is not surprising that the released ratio of Cs resulted greater than that of I2 since its diffusion coefficient is higher than that for the I2, and the model included in the MELCOR code to derive the release rate from the fuel is the same for both. This model assumes a correlation with the Arrhenius equation, which is commonly used in chemistry and physics to describe the temperature dependence of reaction rates. In this model, the release rate is mainly dependent on the activation energy and the temperature in the fuel. The higher the activation energy, the greater the energy required for the reaction to occur, and the lower the release rate. The temperature also plays a key role, as higher temperatures generally lead to higher reaction rates and hence a higher release rate. The model only calculates the release rate for the Cs class of radioactive elements. The release rate for other classes is calculated relative to that of Cs by applying a correction factor, which is dependent on the diffusion coefficient. The diffusion coefficient is a measure of how quickly a substance

can move through a medium, and it affects the rate at which the radioactive element can escape from the fuel. That makes the release rate differences between classes in MELCOR calculations dependent basically on the diffusion coefficients of each of the fission product species.

Figure 8 shows the release of Xe class of radioactive elements. In this case, the released ratio at the end of the transient is even higher than that for the Cs class of radioactive elements, resulting within 48–100% of the Xe class initial inventory. The maximum is reached sooner than the other FOMs analysed mainly due to diffusion coefficient of noble gases, that makes these fission products much more volatiles than the others.

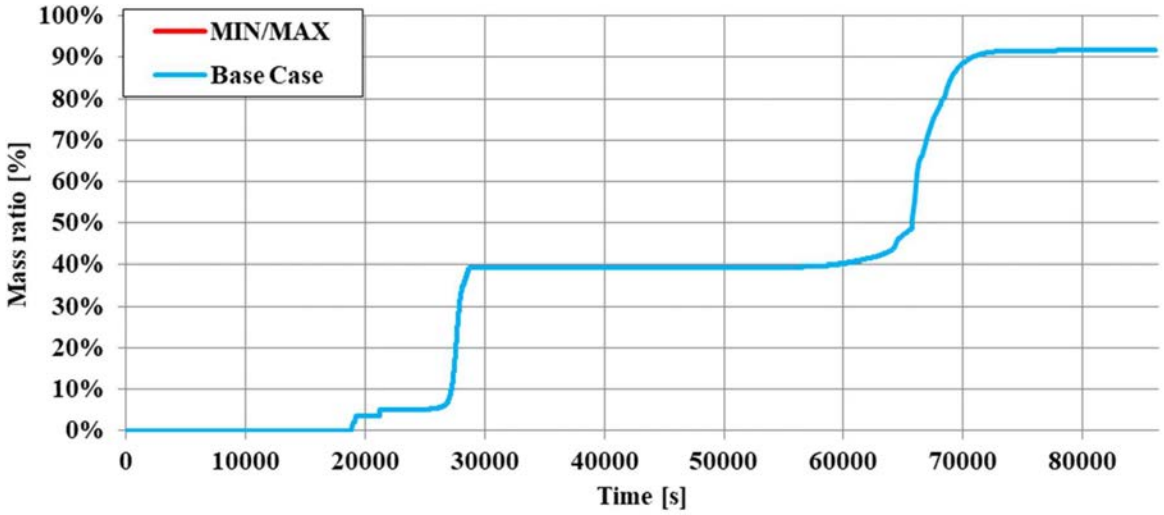

FIG. 7. Release of Cs class of radioactive elements as a function of the initial Cs class inventory.

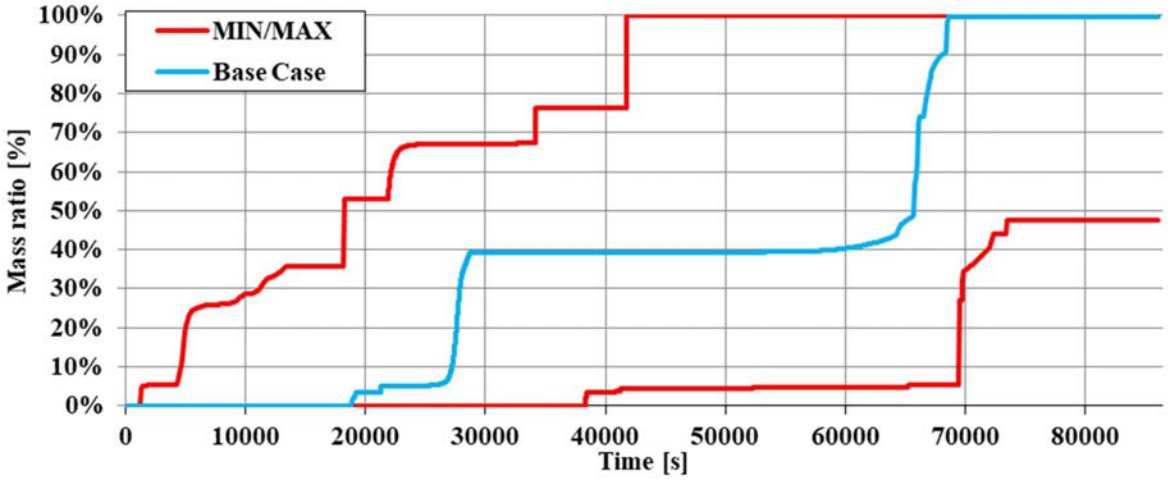

FIG. 8. Release of Xe class of radioactive elements as a function of the initial XE class inventory.

Figure 9 shows the mass of generated hydrogen by in-vessel oxidation reactions. The mass of hydrogen generated by in-vessel oxidation reactions in nuclear accidents depends on a variety of factors, including the specific accident scenario, the properties of the fuel and coolant, and the conditions within the reactor.

However, in general, the primary source of hydrogen in nuclear accidents is the oxidation of zirconium-based fuel cladding material, which can release hydrogen gas as a byproduct of the reaction. The amount of hydrogen generated by in-vessel oxidation reactions can vary widely depending on the conditions of the accident. For example, the temperature and pressure within the reactor can have a significant impact on the rate and extent of fuel cladding oxidation, and therefore on the amount of hydrogen released. In addition, the presence of impurities or other materials within the fuel or coolant can affect the rate of oxidation and the amount of hydrogen generated. In general, the mass of hydrogen generated by in-vessel oxidation reactions in nuclear accidents can range from a few kilograms to tens of kilograms, depending on the specific conditions and circumstances of the accident (Fig. 9).

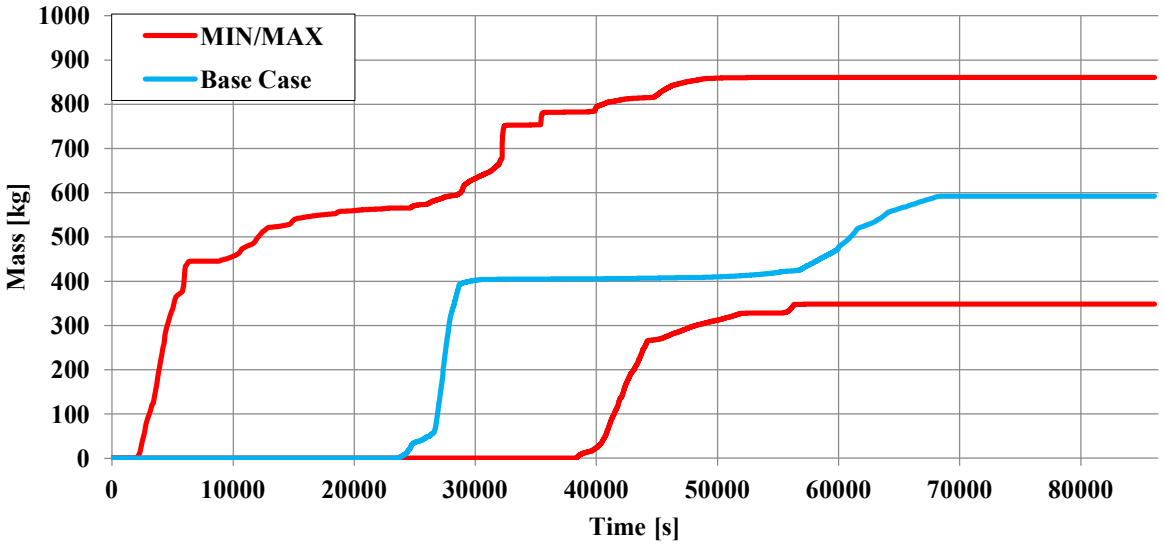

FIG. 9. Hydrogen generated by in-vessel oxidation reactions.

2.3.1.7. Summary and conclusions

The uncertainty quantification analysis was performed for a 24 h SBO in a BWR3 with a Mark-I containment reactor using the MELCOR 2.2 code. The FOMs included in the study are the released ratio of I2, Cs and Xe classes of radioactive elements in relation to the initial inventory at the moment of a reactor SCRAM. Around 150 uncertain input variables are included in the analysis, from initial and boundary conditions to physical model parameters and correlations used in the MELCOR code.

The results show that the released ratios range in more than one order of magnitude in the case of I2 class of radioactive elements (7–73% of initial inventory) and slightly fewer for the Cs class of radioactive elements (40–97% of initial inventory) and Xe class of radioactive elements (48–100% of initial inventory). Differences between the released ratios are mainly due to diffusion coefficients of the classes. Although it is meaningful and according to the physics, the model employed in MELCOR for the estimation of release rates of fission products is somehow simple, but effective, as was largely demonstrated in the decades of the MELCOR code applications. The release onset due to fuel cladding failure ranges from 25 min to around 10 h. There are different mechanisms causing the cladding to fail, and most of them are directly related to

the cladding temperature. Therefore, in this case, it can be said that the core/plant thermal hydraulics, along with the material properties of the cladding, are main contributors to the fission products release onset. It has to be also considered that thermal behaviour of the cladding also affects the conditions of the fuel, and therefore it also has impact on the fission products release from the fuel pellet.

2.3.1.8. Lessons learned and best practices

The presented results suggest that in uncertainty and sensitivity analysis of the reference plant's accident scenario, a cascade effect on the uncertainties in the system does occur indicating that small uncertainties in certain input parameters can have a significant impact on the overall analysis, highlighting the importance of accounting for all uncertain input parameters to some extent. Furthermore, the study suggests that variables not directly related to the FOMs chosen may have a significant effect on the analysis and need to be considered. However, given the limitations in numerical robustness and computational power, it can be challenging to propagate uncertainties of a comprehensive selection of uncertain input deck parameters in a full scope uncertainty and sensitivity analysis of an NPP severe accident scenario.

The study suggests that soundly grounded expert judgment can provide useful support in this part of the uncertainty and sensitivity analysis. This highlights the importance of combining both quantitative and qualitative methods in the analysis of complex systems such as NPPs, to ensure a comprehensive understanding of the uncertainties involved and their potential impact on the system.

The uncertainties characterization of input deck parameters needs to be based on scientific knowledge as much as feasible. However, in many cases, such information may not be available, and expert judgment may be required. It is essential to consider all available information, including both scientific knowledge and expert judgment, to ensure a comprehensive and accurate characterization of uncertainties in input parameters. Also, it is important to consider the limitations of the BEPU code being used in the analysis. In some cases, defining a PDFs that is untruncated may cause unexpected code crashes. Therefore, it may be necessary to truncate the PDFs suitable for the BEPU code being used. This means that the characterization of uncertainties may be, to some extent, code dependent. It is important to consider the capabilities and limitations of the BEPU code being used in the analysis and to ensure that the characterization of uncertainties is consistent with these capabilities and limitations. By taking these factors into account, it is possible to perform a robust uncertainty analysis that provides a comprehensive understanding of the uncertainties involved in the analysis. Finally, when handling a huge number of calculations, it is indispensable to keep track of the physics of the scenario and its unfolding, particularly in case of bifurcations, outliers and/or code crashes. Understanding should be guaranteed so that right decisions can be made along the results analyses. This is also of utmost relevance when coming to the sensitivity analysis and the integral interpretation of the BEPU analysis. Once again, expert judgement should be deeply involved in this final part of the analyses.

When performing many calculations in a BEPU analysis, it is important to maintain a clear understanding of the physics of the scenario being modelled and how it is unfolding. This is particularly important when dealing with bifurcations, outliers, and code crashes, which can significantly affect the results and interpretation of the analysis. To ensure a comprehensive understanding of the analysis results, it is important to keep track of the physics of the scenario and its unfolding throughout the analysis process. This includes monitoring the behaviour of the BEPU code and identifying any anomalies or unexpected results.

In addition, sensitivity analysis and integral interpretation of the BEPU analysis require a deep understanding of the analysis results and their implications. Expert judgment needs to be involved in this final part of the analysis to ensure that the results are properly interpreted, and the right decisions are made based on the analysis.

Overall, a successful BEPU analysis requires a combination of scientific knowledge, expert judgment, and careful monitoring of the analysis process to ensure a comprehensive understanding of the analysis results and their implications.

2.3.2. Ghana Atomic Energy Commission (GAEC), Ghana

2.3.2.1. Motivation and objectives

Two categories of uncertainties as already described in Section 2.3.1 are: aleatory and epistemic uncertainties. The focus of this study was to analyse the epistemic uncertainties associated with severe accident code simulations in terms of input parameters for a specific defined severe accident scenario. In-vessel hydrogen generation was the FOMs investigated due to direct correlation between this parameter and cladding oxidation, which provides an indication of the extent of fuel failure due to high temperatures in the reactor core. Additionally, hydrogen production provides an indication of fission product release from the fuel, since hydrogen generation is an indicator of cladding oxidation and fuel temperatures rising above 1,500 K. This is the temperature range where thermally driven release of the volatile fission products, caesium, iodine, and tellurium, occurs. Hydrogen may also lead to explosions when it comes into contact with air. Therefore, in-vessel hydrogen generation was investigated to provide insights that would support SAMG development for NPPs.

2.3.2.2. Reference plant

The Fukushima Daiichi unit 1 NPP was a BWR Mark I containment design with an installed capacity of 460 MWe. The containment structure was comprised of a drywell, which contained the RPV and was connected to a suppression chamber. The suppression chamber was filled with water, which was used to condense steam in case of over pressurization and to remove fission products in case of fuel damage. Safety relief valves (SRVs) were the primary pressure control system in the reactor, automatically actuating when pressure exceeded present values. In case of isolation from the power conversion system, an isolation condenser system was used to remove decay heat from the RPV. An isolation condenser system, which consisted of large heat exchangers and their piping was used to remove decay heat when the RPV became isolated from the power conversion system. Emergency power was provided from both alternating current and direct current power sources. Alternating current power was obtained from either offsite or onsite sources. If offsite power is lost, alternating current power could be generated using onsite emergency diesel generators automatically. These generators could provide power for several days. Direct current power was also available through banks of batteries onsite to provide power to safety related equipment such as selected valves, instruments, lighting, and communications for up to 8 h following a loss of offsite power.

2.3.2.3. Accident scenario and severe accident code

The analysed severe accident scenario is that of the Fukushima Daiichi unit 1 NPP that occurred in March 2011. The accident was initiated by a magnitude 9 earthquake, followed by a tsunami that submerged the emergency diesel generators and caused a total loss of power. The loss of power resulted in the failure of the two isolating condenser systems that were designed to remove heat from the reactor during shutdown. The operators managed to shutdown the isolation condenser as per the normal procedures, but they could not restart it due to the loss of power. Two isolating condenser systems were designed in unit 1 to remove the heat from the reactor during shutdown. This sequence of events led to core melt under high system pressure. The inability to restart the isolation condenser system caused a build-up of pressure inside the reactor, which led to the core's meltdown. The core meltdown resulted in the release of radioactive materials into the environment and a massive evacuation of the surrounding areas. The detailed accident progression events timelines as modelled in MELCOR can be found in [19].

MELCOR version 2.2, a modular system-level computer code primarily developed to model the progression of severe accidents in light water reactor nuclear power plants, was used. The control volume hydrodynamics, flow path and heat structure packages are used to model thermal hydraulic behaviour of the primary and secondary circuits as well as the containment [20].

2.3.2.4. Plant modelling and nodalization

The reactor nodalization is illustrated in Fig. 10 as used for uncertainty and sensitivity analyses following descriptions provided in [19].

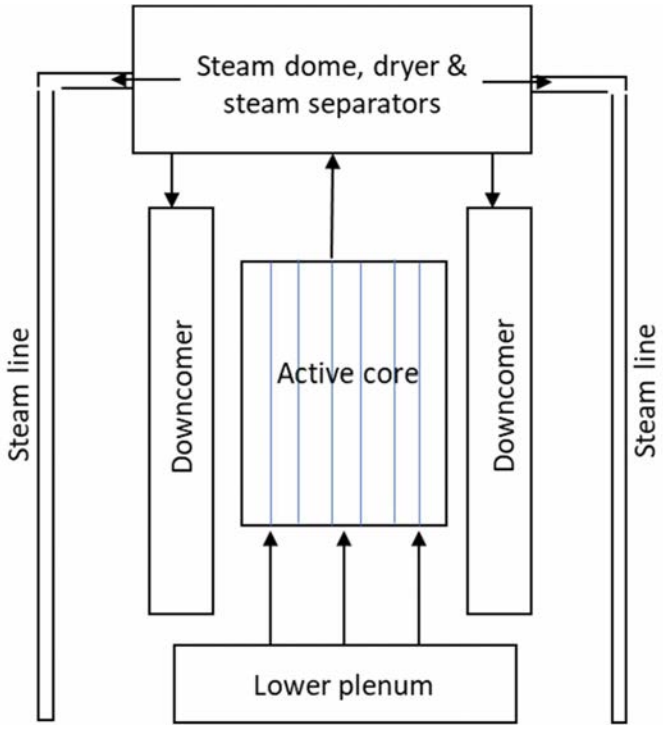

FIG. 10. Nodalization scheme.

2.3.2.5. Uncertainty and sensitivity analysis method

The uncertainty quantification method was based on the coupling between MELCOR and DAKOTA in the stand-alone architecture as shown in Fig. 11. The parameters used for DAKOTA input file include the uncertain input parameters, the sampling technique, the sample size for the analysis (*N*) and the PDFs assigned to the uncertain input parameters. Total of 11 uncertain input parameters were selected based on previous studies that identified them as potentially having the most significant effect on in-vessel hydrogen generation. The input parameter descriptions, ranges and assumed PDFs are shown in Table 7.

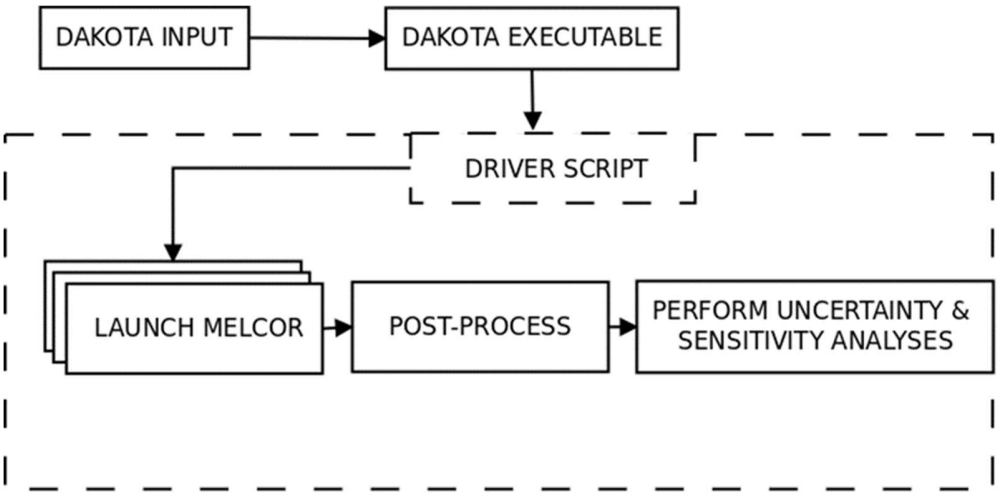

FIG. 11. MELCOR-DAKOTA workflow.

The simulation driver script consists of three main steps: the pre-processing, the simulation, and the post-processing step. A number (*N*) of MELCOR input decks are created in the pre-processing step based on the information specified in the DAKOTA input file and a MELCOR template file containing special characters. The special characters are replaced with the parameter values obtained from DAKOTA run. Code execution commands are written to launch MELGEN and MELCOR at the simulation step for each sample. After the successful execution of each MELGEN/MELCOR input deck, the results are retrieved from the MELCOR output files at the post-processing step using the 'EDF' option in the MELCOR input file. Uncertainty and sensitivity analysis was then performed using MATLAB scripts. The DAKOTA code can be applied in various disciplines including nuclear engineering, computational fluid dynamics, electrical circuits, heat transfer, nonlinear dynamics, shock physics as well as other science and engineering models [21]. The code as a computational tool enhances understanding in the behaviour of complex models as well as the capability to predict complex characteristics identified in physical systems. DAKOTA has capabilities that can be utilized in specific areas including parameter studies, uncertainty quantification, design of experiments, optimization and calibration. A useful and economical feature DAKOTA has is its ability to exploit the computational model in parallel computing, which could be applied either on a multiprocessor desktop or a high-performance computing architecture [22]. MELCOR was coupled with DAKOTA in this study to perform uncertainty quantification and sensitivity analysis.

TABLE 7. UNCERTAIN INPUT PARAMETERS (MELCOR VERSION 2.2)

Parameter	Description	Range & Mean/Mode	Assigned PDF
COR_SC 1131	Zirconium melt breakout temperature	2,098 – 2,550 K Mode = 2400 K	Uniform
COR_SC 1132	Fuel rod collapse temperature	2,400 – 2,800 K Mean = 2,800 K	Uniform
COR_CHT	Melt relocation heat transfer coefficient	2,000 – 22,000 W/m^2K 7,500 W/m^2K	Triangle
COR_CMT	Fractional local dissolution of UO_2 in molten Zircaloy	0.1 – 0.5 Mode = 0.2	Log Uniform
COR_EDR	Characteristic debris size in core region affecting subsequent heat transfer and oxidation surface areas	2 mm – 5 cm Mean = 10 mm	Log Uniform
COR_EDR	Characteristic debris size in lower plenum affecting subsequent heat transfer and oxidation surface areas	1 mm – 6 cm Mean = 2 mm	Log Uniform
COR_ZP	Porosity of fuel debris beds	0.1 – 0.5 Mean = 0.4	Log Uniform
DC Power Limit	Battery Duration	2.0 – 8.0 h Mean = 4.0 h	Triangle
SRV LAMDA	SRV Stochastic failure to reclose (per demand)	Alpha = 0.494 Beta = 133.2 LB= 0.0 UB = 1.0	Beta
COR_LP	Heat transfer coefficient for fuel debris falling through water filled lower plenum	1,250 – 4,000 W/m^2 K Mode = 2,000 W/m^2 K	Triangle
COR_SC 1141	Melt flow rate per unit width at breakthrough candling	– 1.0 kg/m smode = 0.2 kg/m s	Triangle

The uncertain input parameters investigated were selected based on previous studies in which uncertainty analysis was performed for the hydrogen source term for a SBO accident scenario in Sequoyah using MELCOR 1.8.5 [3]. The parameter values and ranges used were based on best practice recommendations as well as experimental results. The following is a brief description of selected input parameters:

— *Zirconium melt breakout temperature (SC1131)* is the temperature at which molten cladding is released from retaining oxide shell. The recommended range is 2,100–2,550 K. The default value used in the reference case is 2,400 K, which is thought to be a most likely value based on the Phebus FPT-1 test [23]. In this study, the PDF assigned to this parameter is the uniform distribution due to the assumption that all values of this parameter in the defined range are equally probable and values outside this range are impossible.

— *Duration of DC power (battery life)*: DC batteries are used as backup power to supply power for essential instrumentation in the reactor control room in the event of loss of power. For the Fukushima Daiichi accident, the reactor was cooled by the IC initially. The IC was momentarily stopped at the time of the SBO due to loss of DC power. Accordingly, the reactor lost all of its cooling approximately 50 min after the earthquake [19]. A triangular distribution was selected for this parameter in this study based on expert judgement with a mode of four hours [24]. The mean is presumed from the time of advent of the tsunami when all AC and DC power was lost.

— *Safety relief valve stochastic failure to reclose*: at the fixed pressures and specified flow rates, the MELCOR model is coded to cause the SRVs to open. The SRVs are expected to close when pressure decreases below 96% of their opening pressure. A beta distribution was assigned to this parameter, which is in line with the methodology presented in NUREG/CR-7037 [24]. If electric power is unavailable, the valve opens at 7.64 MPa_{gauge} and closes at 6.88 MPa_{gauge} with spring force. In the MELCOR model, the gauge pressure was calculated from steam line pressure subtracted from wetwell pressure. The impact of this parameter on accident progression is expected to be significant as a stuck-open SRV will depressurize the system, which significantly effects the accident progression.
— *Particulate debris characteristic size following core collapse (COR_EDR)*: The characteristic debris size in core region influences subsequent heat transfer and oxidation surface areas. According to best practices, the recommended range is from 2mm−5cm with a default of 10 mm [3], which was used in the reference case. A log uniform distribution was assigned to this parameter in this study, which assumes equal probability to the parameter values in the specified range. This distribution choice shows that the information available on the relative probabilities of different values of the parameter are not sufficient.

2.3.2.6. Results

All the results obtained from simulation of the reference MELCOR model for the key output parameters were consistent with the results obtained by VTT [19]. Details of the reference case results can be obtained from [25].

The number of samples was determined based on Wilks' formula for achieving a two-sided 95% confidence interval. The Latin Hypercube sampling technique was utilized due to its ability to give a good coverage of the solution space compared to the simple random sampling method. The assumed PDFs were assigned based on available information in literature as well as engineering judgment. Uncertainty quantification results are summarized in Fig. 12 and in Table 8, while a summary of sensitivity analysis results are presented in Table 9. The results indicate that the mean hydrogen generated is 433.85 kg with a standard deviation of 91.99. These results are with respect to the mean hydrogen generated over the entire simulation time of 39 h. The estimated uncertainty in the amount of hydrogen generated in-vessel during the severe accident simulated by MELCOR is approximately 22.46%, which was computed as a ratio between the standard deviation of results obtained by sampling and the standard deviation of hydrogen generation results obtained from simulating the reference case.

The sensitivity analysis results reveal that six input parameters are positively correlated with hydrogen FOM while five input parameters are negatively correlated with the FOM. The positively correlated parameters are COR_SC 1131 (zirconium melt breakout temperature), COR_CMT (fractional local dissolution of UO_2 in molten Zircaloy), COR_ZP (porosity of fuel debris beds), COR_CHT (Melt relocation heat transfer coefficient), COR_SC 1141 (melt flow rate per unit width at breakthrough candling) and *SRV LAMDA* (SRV stochastic failure to reclose (per demand)), while the following parameters are negatively correlated: *COR_LP* (heat transfer coefficient for fuel debris falling through water filled lower plenum), *BATT LIFE* (DC power limit), *COR_EDR* (characteristic debris size in the core region) and *COR_EDR-LP*

(characteristic debris size in the lower plenum), *COR_SC 1132* (fuel rod collapse temperature). Positive correlation implies an increase in these input parameter values results in increase in hydrogen generation while negative correlation implies an increase in such input parameters results in a decrease in hydrogen generation.

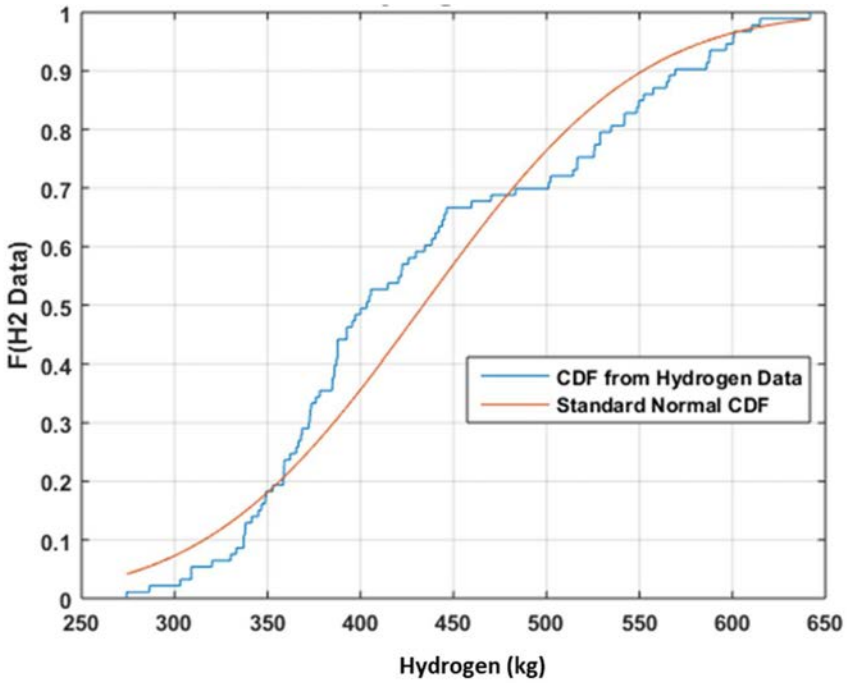

FIG. 12. In-vessel generated hydrogen fitted to a normal distribution.

TABLE 8. UNCERTAINTY QUANTIFICATION RESULTS

Metric	**Value**
Mean	433.85
Standard deviation	91.99
Uncertainty	~22.46%

TABLE 9. SENSITIVITY ANALYSIS RESULTS

Parameter	***ρ*-value**	***p*-value**
COR-SC 1131	0.0142	0.7365
COR-SC 1132	–0.0513	0.4765
COR-CMT	0.0156	0.7685
COR-EDR	–0.2871	0.0164
COR-EDR(LP)	–0.0778	0.3438
COR-ZP	0.4230	3.19×10^{-5}
BATT LIFE	–0.0216	0.6886
COR-CHT	0.0299	0.6453
COR-LP	–0.0389	0.7691
COR-SC 1141	0.5273	1.25×10^{-7}
SRV LAMDA	0.0046	0.7680

From the *p*-values presented in Table 9, it is observed that *COR-SC 1141* is the most important variable that affects hydrogen generation followed by *COR-ZP* and *COR-EDR* due to reported *p*-values less than 0.05 as well as high correlation coefficient (*ρ)* values. *COR-SC 1141* is known to be important to hydrogen generation, since it determines how long unoxidized molten zirconium is held behind an oxidized cladding shell. More hydrogen is produced when the zirconium is held for a longer period [24]. This phenomenon is further confirmed by the results shown in Table 9, in which *COR-SC 1141* has a positive correlation with hydrogen generation.

2.3.2.7. Summary and conclusions

A methodology for performing uncertainty and sensitivity analysis was developed and demonstrated using a severe accident scenario. The key FOMs investigated was hydrogen generated in-vessel during a severe accident. The uncertainty in hydrogen generated was estimated to be approximately 22.46%. A sensitivity analysis was also performed using linear multiple regression. The analysis estimated the contribution of each selected input parameter to the uncertainty in the response variable. The results show that three MELCOR input parameters (*COR_SC 1141, COR_ZP* and *COR_EDR*) considerably influenced hydrogen generated in-vessel. The results can provide further insight to severe accident code users and developers on the impact of their choice of input parameters on the results of simulations. In terms of SAMGs development, these results can help reactor operators in determining the right timing of key operator actions such as the automatic actuation of emergency systems.

2.3.2.8. Lesson learned and best practices

In the process of conducting this study the following valuable lessons were learned:

- Selection of uncertain input parameters and the assignment of probability distribution functions proved to be a significant task requiring extensive literature search to justify the choices made;
- Not all MELCOR samples were successful simulations, and the simulations were computationally expensive.

The best practices, in summary, are as follows:

- Sensitivity analysis is performed initially to rank the uncertain input parameters. The results from this analysis then form the basis for investigating the specific input parameters' contributions to the uncertainty in the key FOMs;
- In using Wilk's approach for determining the sample size, a higher number of samples need to be simulated in order to account for MELCOR samples that would not complete successfully.

2.3.3. Comisión Nacional de Seguridad Nuclear y Salvaguardias (CNSNS), Mexico

Uncertainty and sensitivity analysis was carried out for the BWR type plant with Mark II containment. In Mexico the uncertainty and sensitivity analyses are implemented for BWR transient and severe accident simulations, and they are performed by joint efforts between the National Commission of Nuclear Safety

and Safeguards (CNSNS – Mexican Nuclear Regulatory Authority) and the National Nuclear Research Institute of Mexico (ININ). These two organizations collaborate closely in order to stablish the basis and foundations of methodologies to be applied and used in the analysis of severe accidents for regulatory, nuclear safety evaluations, research on modelling and development of input decks purposes. *Motivation and objectives*

Development of modelling input deck for regulatory and supporting activities to nuclear safety analysis at government level has been advanced one more step to evaluate the impact on variations over some key parameters, in order to set a compilation of variables that impacts greatly the phenomena progression and the end state of scenarios. This is important because the uncertainty and sensitivity analysis reflects the degree of confidence and credibility of results for certain calculations. For the regulator, the uncertainty and sensitivity analysis have most importance because the results will support the decision making process. For instance, the Fukushima accident stated the importance of knowing the uncertainty for the analysis and evaluations, particularly for the severe accidents' scenarios.

2.3.3.1. Reference plant

This uncertainty and sensitivity analysis case of Mexico is intended for a BWR-5 with Mark II containment type. In comparison to the Fukushima Site, a Mark II containment is bigger than Mark I containment, but smaller than Mark III Containment. The objective of CNSNS evaluations was focused on the failure of primary containment due to overpressure (time as variable of interest). The BWR-5 reactor core consists of 444 fuel assemblies and 109 control rods, producing 2,317 MWth, under normal operating conditions.

2.3.3.2. Accident scenario and severe accident code

The SBO with irrecoverable loss offsite site power is modelled; it implies that the loss of offsite alternating current power to the essential and non-essential electrical buses, is concurrent with turbine trip and the unavailability of the redundant on-site emergency alternating current power systems. The postulated scenario states that RCIC and fire protection system are available systems, and the operating time is one of the parameters to be considered in the analysis in order to evaluate its impact in the output parameter of interest.

Safety relief valves operate in safety mode, due to loss of power. The SRVs actuation limitations are not considered (mechanical fatigue and back-pressure effect) since their direct effects due to the conditions in the primary containment are not taken into account. The RCIC is postulated to be lost at some point in time given the pressure increase in the suppression chamber. The loss of the RCIC is a key parameter in order to analyse its impact over the set of FOMs.

The MELCOR V2.1 code was used. Input deck files were developed including reactor vessel, fractional balance of plant, and containment, and improved to include un-collapsing volumes, pipes of main steam isolation valves, feed-water system, logic for automatic system actuation, logic of systems electric supply, control functions, among others.

The interface application SNAP as a platform to control externally the executions of MELCOR is used. DAKOTA is used to manage the execution of uncertainty analysis through automatic control, assignation, manipulation and organization of results for each output [26].

2.3.3.3. Plant modelling and nodalization

The nodalization of the RPV and recirculation system is illustrated in in Fig. 13 indicating the thermal-hydraulic volumes defined for the major reactor components.

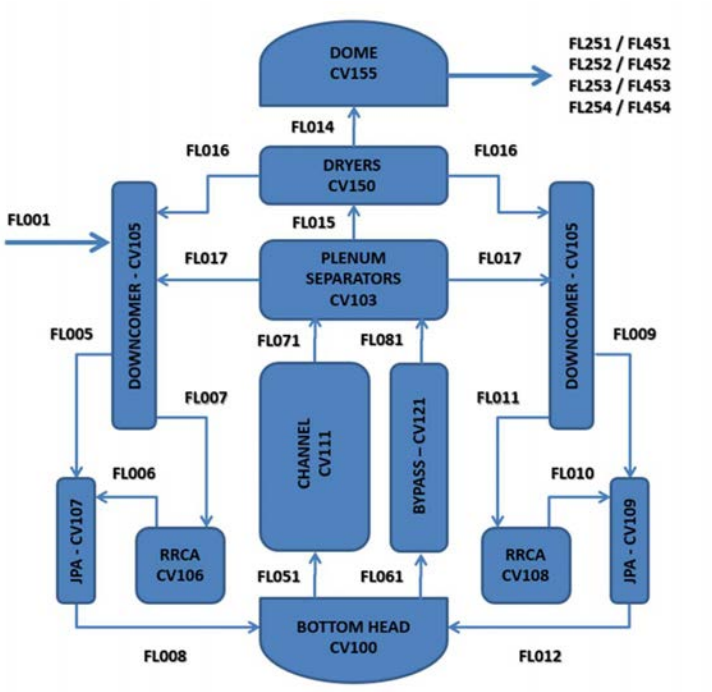

FIG. 13. MELCOR RPV and core region nodalization schemes.

2.3.3.4. Uncertainty and sensitivity analysis methodology

CNSNS used the GRS method of propagation of input uncertainties for the uncertainty and sensitivity analysis with the following step sequence:

1. Define the response variable (FOM);
2. Select the uncertainty input parameters set;
3. Specify the features of uncertainty analysis;
4. Assign a PDFs for each uncertainty input parameter;
5. Configure the output layout for uncertainty analysis;
6. Generate the random values set;
7. Generate an input deck file for each set of random values;
8. Execute each case in the selected code;

9. Extraction of FOM for each execution;
10. Perform the uncertainty analysis;
11. Generate the report of uncertainty analysis.

Correct random sampling is very important element for each uncertainty parameter. The Monte Carlo sampling was used, and sampling size was based on the requirements of the GRS uncertainty methodology [35, 36]. The number of code calculations is independent of the number of input uncertainty parameters, and it is determined by the Wilks' approach [15, 16]. The CNSNS used 59 executions (for one limit upper or lower) or 93 executions (for both limits upper and lower) for a 95/95 criteria. When any of the programmed executions did not finish, it was necessary to execute more than 59 or 93 cases, thus accounting for unfinished executions. The analysis of primary containment failure time due to overpressure included six uncertainty parameters for ex-vessel phenomena with their associated PDFs. Table 10 shows the selected uncertainty parameters. All six uncertain MELCOR input variables were sampled from a Gaussian distribution function. The necessary average (μ) and standard deviation (σ) parameters corresponding to each uncertain variables are also shown in Table 10. Selection of these variables are related with their importance to the analyst, in order to know their impact in the output variables of interest or FOMs, which in this study is just one, the containment failure time.

TABLE 10. UNCERTAINTY VARIABLES, PDFS AND DISTRIBUTION PARAMETERS

Variables	**PDF**	**Application Rule**	**Distribution Parameters**
TEM_FAIL_VAS	Normal	Scalar	μ = 1323.15, σ = 50.0 [1223.15, 1423.15]
TEM_GAP_RELEASE	Normal	Scalar	μ = 1173.15, σ = 50.0 [1073.15, 1273.15]
TIME_LIFE_RCIC	Normal	Scalar	μ = 16200.0, σ = 2700.0 [10800.0, 21600.0]
TEM_CON_SOL	Normal	Scalar	μ = 1420.0, σ = 25.0 [1370.0, 1470.0]
TEM_CON_LIQ	Normal	Scalar	μ = 1650.0, σ = 25.0 [1600.0, 1700.0]
TEM_ABLATION_CEM	Normal	Scalar	μ = 1540.0, σ = 25.0 [1490.0, 1590.0]

Though the uncertainty variables could simply be chosen randomly, this is not considered a good practice; instead, expert criteria must be applied to choose the most important elements to perform the analysis and avoid unnecessary calculations with overload of results. One of the main elements of uncertainty and sensitivity analysis is the phenomena identification and ranking table (PIRT). The PIRT allows to identify the importance in the variation of parameters by taking into account its impact over progression and end-state of scenario [27]. Selection of uncertainty variables requires a detailed study based on expert criteria and results of experience in the analysis of accident progression and impact of variation of different parameters over interest phenomena. The method employed does not restrict the number of input parameters to be considered. It is highly recommended to perform an initial analysis of a transient in order to determine and identify the phenomenology associated. The PIRT tables are very useful tool to identify and categorize, according its importance the physical phenomena occurred during a specific event. Other recommended sources include medium and high importance for specific phenomenology [28].

2.3.3.5. Results

The results include the output values for primary containment failure time due to overpressure and the type of analysis applied to these values. Reference case results are only briefly mentioned, because they basically showed the stability of input deck file, that is the steady state behaviour of model. In order to stablish a good level of numerical stability of input deck model, a 3,600 s simulation was performed. The key parameters such as level, pressure, temperature, reactor vessel and containment, did not show important variations; these values were almost constant in time. Parameters were not manipulated by using the fixed value option for steady state executions, the values of these parameters took its value from the natural iterative calculation process through the steady state modelling. Table 11 shows the progression of the event in order to provide a more comprehensive idea of phenomena for the postulated scenario taken to develop this uncertainty and sensitivity analysis.

TABLE 11. SBO EVENT PROGRESSION

Time	**Event**
00:00:00	SBO start
00:00:01	Reactor trip
00:00:58	Level 2 signal
00:01:28	First RCIC automatic startup due to level 2 signal
00:11:20	RCIC automatic trip
00:12:40	Second RCIC automatic startup due to level 2 signal
00:17:27	Manual opening of SRV C
00:17:40	RCIC automatic trip
00:20:15	Third RCIC automatic startup due to level 2 signal
00:25:20	Manual closure of SRV C
01:00:29	Manual opening of SRV C
01:12:10	RCIC automatic trip
01:24:30	Manual closure of SRV C
01:25:13	Fourth RCIC automatic startup due to level 2 signal
01:48:13	RCIC automatic trip
02:20:20	Manual opening of SRV C
02:28:25	Manual closure of SRV C
02:29:10	Fifth RCIC automatic startup due to level 2 signal
02:51:00	RCIC automatic trip
03:37:25	Manual opening of SRV C, stays open afterwards
03:47:30	Sixth RCIC automatic startup due to level 2 signal
03:51:30	Reactor core level oscillates around level 3
03:51:30	Reactor core level oscillates around level 3
04:00:00	RCIC automatic trip, batteries exhausted
04:01:40	Reactor core level oscillates around level 2
04:32:10	Reactor core level oscillates around level 1
05:36:08	Initial failure of fuel elements
11:57:30	Reactor vessel failure
31:11:00	Pressure in the primary containment above 10 kg/cm^2
31:11:02	Primary containment failure

In order to ensure that at least intended minimum of 59 MELCOR runs were satisfied, 62 executions were submitted to cover the potential gap of executions that could fail due un-convergence, execution time exceeded, boundary limits violated, etc. All 62 runs were successful, thus the uncertainty and sensitivity analysis was performed with the results from all the runs. Table 12 shows results of some of the 62 executions carried out to predict the primary containment failure time due to overpressure. This table includes resulting values of FOMs, the primary containment failure time (time), and the primary containment pressure at failure time, due to the variations of the input values of the six uncertain parameters: RPV Failure Time due to over-temperature (T_RPV_Fail), fuel element failure time due to over-temperature (T_Fuel_Fail), RCIC time life (Time_RCIC_life), concrete ablation temperature (T_Con_Abl), concrete solidification temperature (T_Con_Sol), and concrete liquefaction temperature (T_Con_Liq). Average and standard deviation values of the uncertain MELCOR input variables and the FOM, and its corresponding overpressure value, are also shown.

TABLE 12. RESULTS OF THE PRIMARY CONTAINMENT FAILURE TIME DUE TO OVERPRESSURE

Input Variables							**Output Variables**	
Exec No.	**T_RPV_ Fail (K)**	**T_ Fuel _Fail (K)**	**Time_RCIC _life (s)**	**T_Con_ Abl (K)**	**T_Con_ Sol (K)**	**T_Con_ Liq (K)**	**Time (s)**	**Primary containment pressure (MPa)**
1	1349.3	1170.3	15059.7	1540.2	1455.7	1666.1	122448.4	1.231
2	1319.2	1250.0	16841.4	1573.8	1446.9	1639.9	123219.8	1.231
3	1370.1	1172.0	18104.3	1525.1	1439.2	1635.5	123745.1	1.232
4	1329.5	1130.5	16369. 3	1549.9	1415.6	1660.5	127369.2	1.231
5	1396.6	1146.4	18332. 2	1519.2	1419.8	1663.3	128688.9	1.231
6	1245.2	1142.7	15354.5	1527.9	1425.8	1626.6	121993.3	1.232
7	1300.2	1179.8	15604.8	1550.9	1459.4	1646.2	131329.1	1.230
8	1312.8	1101.9	17681.8	1555.8	1453.2	1627.9	127656.9	1.231
9	1313.7	1150.3	14495.8	1578.5	1405.9	1636.3	119904.1	1.232
10	1300.3	1213.1	16527.6	1557.5	1418. 7	1655.0	131305.9	1.231
…	…	…	…	…	…	…	…	…
20	1335.3	1160.1	16844.4	1526.4	1411.2	1647.4	123553.9	1.231
21	1392.1	1205.9	16406.8	1550.9	1393.9	1632.9	133009.4	1.230
22	1333.3	1208.3	19532.4	1541.1	1393.8	1651.8	127874.5	1.231
23	1400.4	1142.9	15570.8	1543.9	1422.0	1695.6	129866.5	1.230
24	1392.9	1225.9	17211.6	1534.9	1424.9	1623.7	122448.2	1.231
25	1251.8	1143.1	13782.0	1540.0	1442.9	1649.4	115896.8	1.236
…	…	…	…	…	…	…	…	…
62	1280.9	1127.3	14195.3	1561.9	1463.7	1666.7	136540.7	1.230
AVG	**1333.8**	**1171.5**	**15770.3**	**1541.8**	**1424.3**	**1647.8**	**127320.6**	**1.231**
DEV	**43.314**	**42.264**	**2282.625**	**20.079**	**23.382**	**20.991**	**6514.466**	**0.0009**

Figure 14 shows the primary containment failure time from each of the 62 simulations. The lowest and the highest times were 111,696.5 s and 143,860.1 s, respectively. With the data in Table 12, the sensitivity

analysis was performed. A linear regression analysis of the FOM versus each of the six input variables was performed, in order to calculate the regression coefficient (R^2), to determine the ranking of impact of each uncertain variable on the FOM. The minimum and maximum values calculated for R^2 corresponded to the uncertain variables' concrete ablation temperature and concrete solidification temperature, that is R^2 = 0.0017 and 0.0354, respectively. These results are agreement with the expected conditions in the primary containment once the molten core – concrete interactions start, since it can be noticed that if concrete is in a quasi-liquid state, it stills irradiates heat to the containment. In regards of the ablation temperature, heat irradiation is negligible because concrete is absorbing heat instead irradiating.

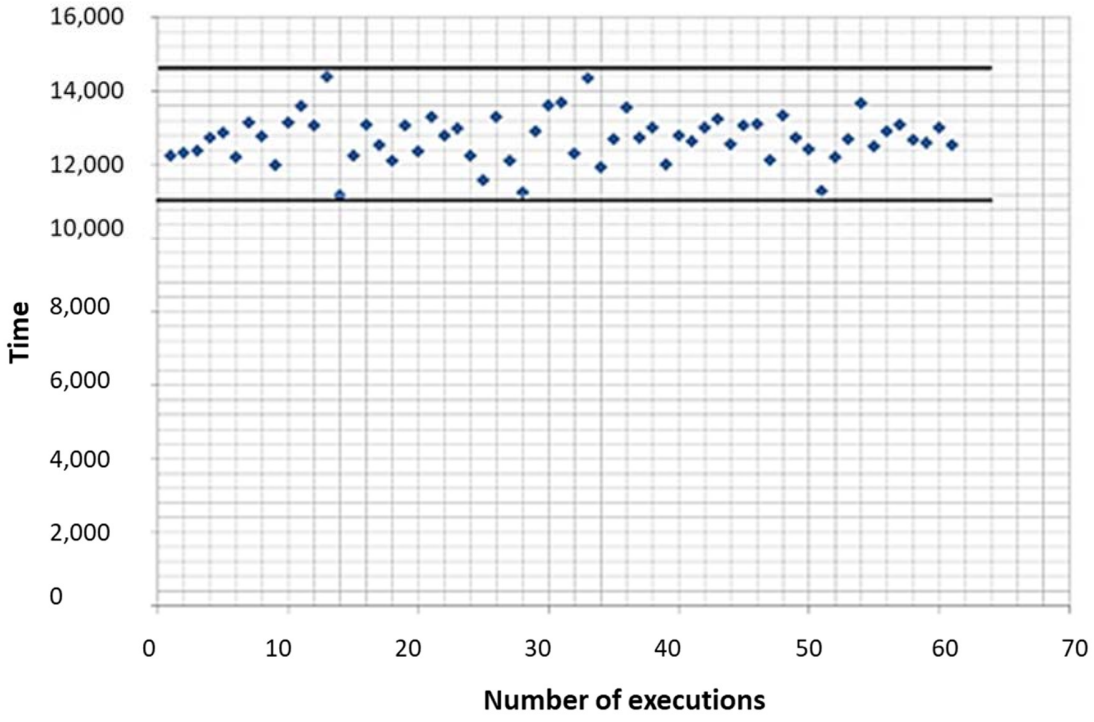

FIG. 14. Primary containment failure time from each of the MELCOR code executions.

In addition to the linear regression analysis, the correlation coefficient was calculated, and the results are shown in Fig. 15. Direct impact is represented as a positive bar, while inverse impact corresponds to a negative bar, and the bar height represents the level of impact over the variable of interest. Thus, the variable with the highest impact to the selected FOM is the variable concrete solidification temperature, and that with the lowest relevance is the variable fuel element failure temperature. These results are equivalent to the results from the linear regression analysis. The resulting ranking of all six uncertain MELCOR input variables was the same from both approaches.

Figure 16 shows the cumulative distribution function associated to the uncertainty over the primary containment failure time. The analysis was performed taking into account all the available data from output

variables provided in Table 12. The cumulative distribution function is defined as a probability that variable takes a value being less than or equal to x: $F(x) = P(X \leq x) = \sum_{x_i \leq x} p(x_i)$.

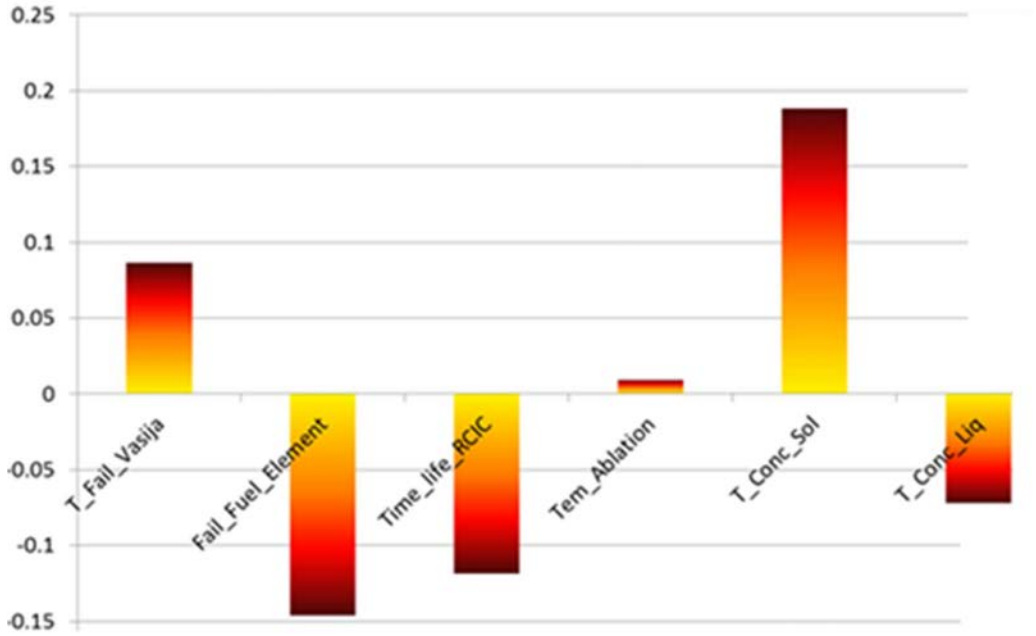

FIG. 15. Correlation coefficient results for the sensitivity analysis.

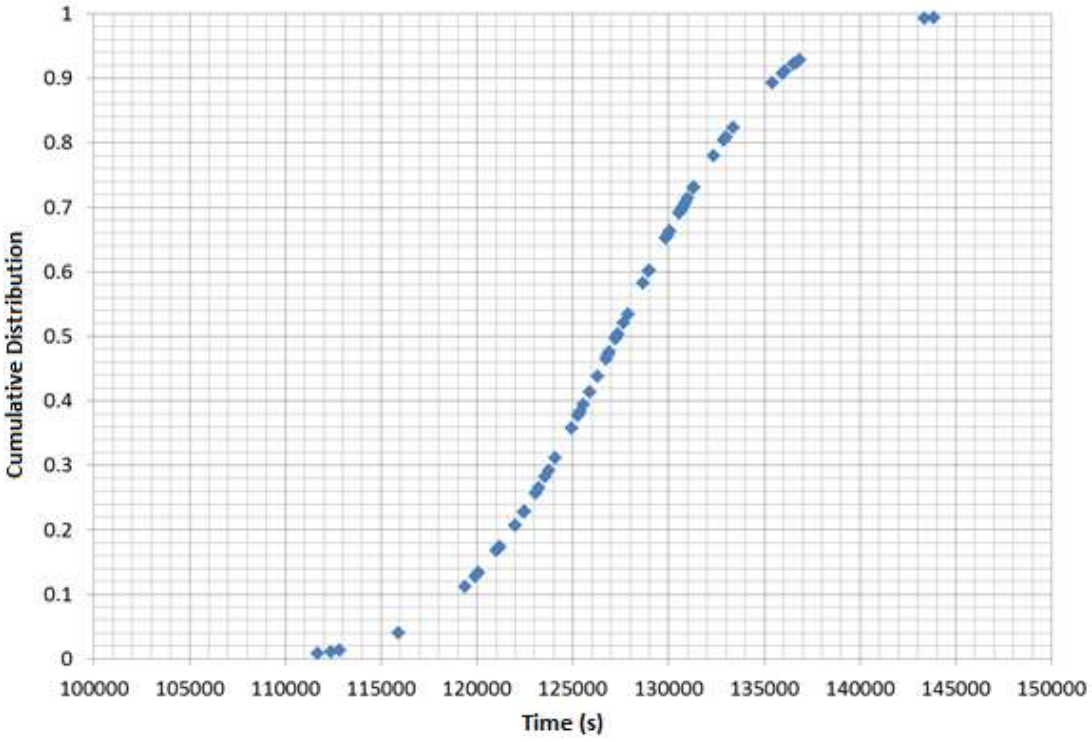

FIG. 16. Cumulative distribution function of the primary containment failure time.

The time interval for the failure time of the primary containment can be computed applying ordered statistics, however a simpler approach is to obtain the interval directly from the output values, thus only the maximum and minimum values are taken to determine the time range for containment failure due to overpressure. Figure 17 shows the uncertainty range of the FOM values obtained from the 62 successful code executions.

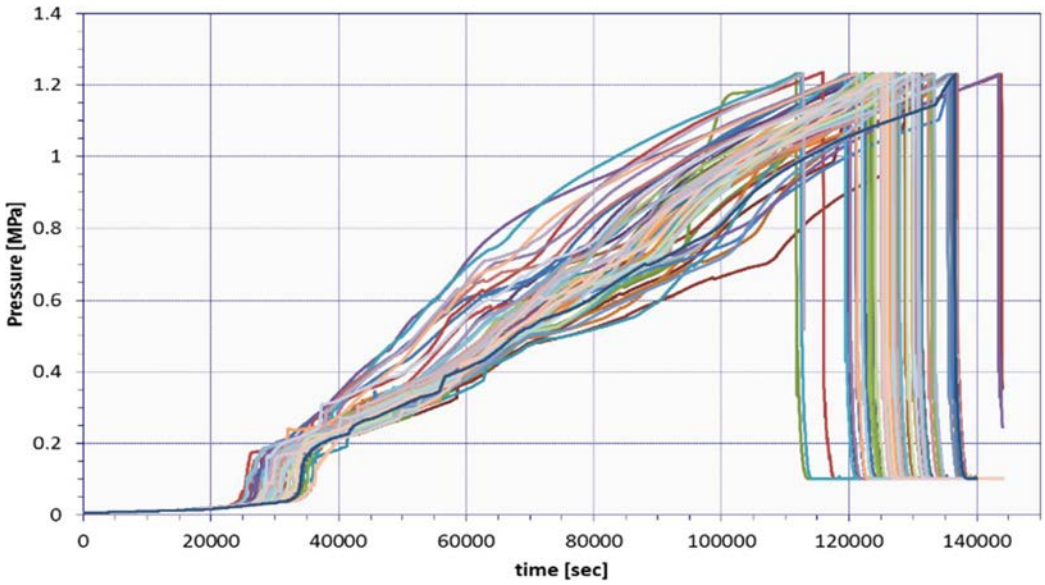

FIG. 17. Figure of merit uncertainty range.

Besides getting the whole uncertainty time range for containment failure time (see Fig. 17), the conservative and best estimate intervals of containment failure time (window time) can be determined too. These intervals were calculated from the containment failure time average and standard deviation values (see Table 12). Thus, the primary containment failure time conservative interval is given here by the range $[\mu-2\sigma, \mu+2\sigma]$ and for the best estimate interval it was used $[\mu-2.5\sigma, \mu+2.5\sigma]$, and the resulting ranges are [114291.6, 140349.5] and [111696.5, 143860.1], respectively.

2.3.3.6. Summary and conclusions

The uncertainty and sensitivity analysis were carried out to determine the time interval for the potential failure of the primary containment due to overpressure, in a BWR-5 with Mark II containment. The accident scenario under study was a SBO in which the depressurization is allowed, but only RCIC injection is available and just for a limited time. Thus, the scenario eventually evolves to the severe accident stage. The uncertainty and sensitivity methodology used was the forward propagation of input uncertainties with six uncertain code input variables, and the only FOM was the containment failure time. A total of 62 simulations were carried out with the MELCOR code and with DAKOTA as the uncertainty and sensitivity calculation tool. Two kinds of sensitivity analysis were performed: using a linear regression analysis and the calculation of the correlation coefficient. Both analyses led to the same results, which showed that three of the uncertain variables have relevant impact on the FOM, but the concrete solidification temperature was clearly the one

with the highest impact, which is considered a result being consistent with physical phenomena. It is important to mention that the uncertain code input variables were chosen in this study only from the physics point of view. Thus, more detailed analyses are still needed, taking into account not only more uncertainty variables related to the physical phenomena occurring in the different stages of the severe accident progression, but adding other uncertainty sources. Regarding the uncertainty analysis, besides obtaining the whole range of the FOM uncertainty band, it was also determined the best estimate and conservative intervals for primary containment failure time, based on the average and standard deviation values obtained from the whole set of simulations.

2.3.3.7. Lesson learned and best practices

For a Regulatory Body it is very important to consider all elements that have significant impact on the results of the analysis of different severe accident scenarios, because this organization has the responsibility of the assessment and surveillance of the compliance with the safety standards required for NPPs. Therefore, the results achieved and lessons learned provide support to a technically sound application of uncertainty and sensitivity analysis methodologies.

2.3.4. Instituto Nacional de Investigaciones Nucleares (ININ), Mexico

Uncertainty and sensitivity analysis applied to transient and accident scenarios in BWR with Mark II containment is performed. The Comisión Nacional de Seguridad Nuclear y Salvaguardias and the Instituto Nacional de Investigaciones Nucleares have carried out collaborative efforts to set the basis of a more comprehensive study of severe accident scenarios in BWRs, including uncertainty and sensitivity.

2.3.4.1. Motivation and objectives

In Mexico, the Laguna Verde NPP is the only site where nuclear power is generated from two BWR-5 units with MARK II primary containment. After the Fukushima Daiichi accident in 2011, the power station was required to present updated stress tests to show this station's capability to withstand beyond design basis accidents. The review of the severe accident guidelines was part of the stress test package. Such review includes the technical basis to support potential changes in reactor operatives and/or the new systems to mitigate the severe accident evolution. One of the lessons learned from the Fukushima accident indicates that probabilistic and deterministic approaches are required to get a more comprehensive analysis of beyond design basis accidents. For both approaches, uncertainty and sensitivity analysis have become an important part of an integral safety analysis. In reactor safety, the uncertainty and sensitivity analysis provide tools to investigate phenomena, via their associated analysis variables, leading to a significant impact on the accident's progression. Generally, for safety assessment, the FOMs are those parameters requiring continuous monitoring on the emergency operational procedures and SAMGs, as hydrogen concentration, RPV breaching time, etc. However, such parameters depend directly on the physical models implemented in the simulation tools to predict the rates of change of fundamental variables: temperature, pressure, flow rates, heat fluxes, etc., on volumes and materials. Therefore, it is quite necessary to investigate the range of valid applications of different physical models that strongly influence the sequence of an accident scenario.

2.3.4.2. Reference plant

BWR-5 and BWR-6 technologies do not differ much for practical applications in their core configuration, reactor vessel design and internals, emergency core cooling systems, and other accident mitigation systems. However, the primary containment of those two reactor types is quite different: BWR-6 has a Mark III containment, which has a larger volume than Mark II containment. Their configuration also differs notably. Since only in-vessel phenomena was investigated, information available for BWR-6 designs can be used as necessary. The reference BWR-5 core consists of 444 fuel assemblies. Each of these has 92 fuel rods in a 10×10 array. There are 109 control rods. The reactor generates 2,317 MWth. The plant is considered initially to be working at 100% power, 100% core flow, and rated pressure under nominal operating conditions.

2.3.4.3. Accident scenario and severe accident code

The base case is an unmitigated SBO at high pressure with loss of alternating current power systems, including diesel generators; only in-vessel phenomena are considered. However, the alternating current power to buses fed by station service batteries through inverters is still considered operable, plus all direct current loads [32]. In a BWR-5, an SBO implies the unavailability of the emergency systems and the feedwater system. The emergency core cooling systems are the high pressure core spray, the low pressure core spray, and the low pressure core injection. An unmitigated SBO is that scenario where all direct current power is also considered unavailable. In that case, the automatic depressurization system is also lost, and the SRVs cycle (open–close) in safety mode. For those plants with the RCIC system based on a steam turbine, this system is assumed to be unavailable because there is no control over it. Under such circumstances, an SBO will evolve into a severe accident. It can only be mitigated via some external emergency equipment (diesel generator, battery banks, emergency pumping, etc.).

The loss of offsite power and loss of all in-site alternating current power are assumed concurrent with the loss of all available in-site direct current power. This leads to an unmitigated SBO at high pressure from the very beginning of the simulation. Steam continues being generated due to decay heat and sent to the pressure suppression pool through those SRVs reaching their opening set-points (safety mode only). It is also assumed that there is no limitation to the number of cycles a SRV can operate. No external additional coolant injection equipment is considered, and no external additional power supply is available. The severe accident analysis code used in this study is the Modular Accident Analysis Program 5 (MAAP5), version 5.03 [33]. The MAAP5 code is used to study different operator's actions to support the development and review of emergency operational procedures and severe accident guidelines. It has physical models to simulate both in- and ex-vessel phenomena.

2.3.4.4. Plant modelling and nodalization

Since the presented simulation includes only in-vessel phenomena, the nodalization of the RPV and nuclear core is presented. Figure 18 shows the nine MAAP's thermal hydraulics components used for modelling the primary system. Some of those components are also nodalized to obtain a more detailed analysis of the transients and accidents; for example, the RPV lower head and the core regions. Figure 18 also shows 30 axial nodes and six radial nodes of the core region. The radial nodalization only corresponds to the fuel

assemblies. Still, the code does consider the total liquid water volume in that section. The first four axial nodes correspond to volumes of structures supporting fuel assemblies and their entrances. Node 30 corresponds to the top zone of the fuel channel.

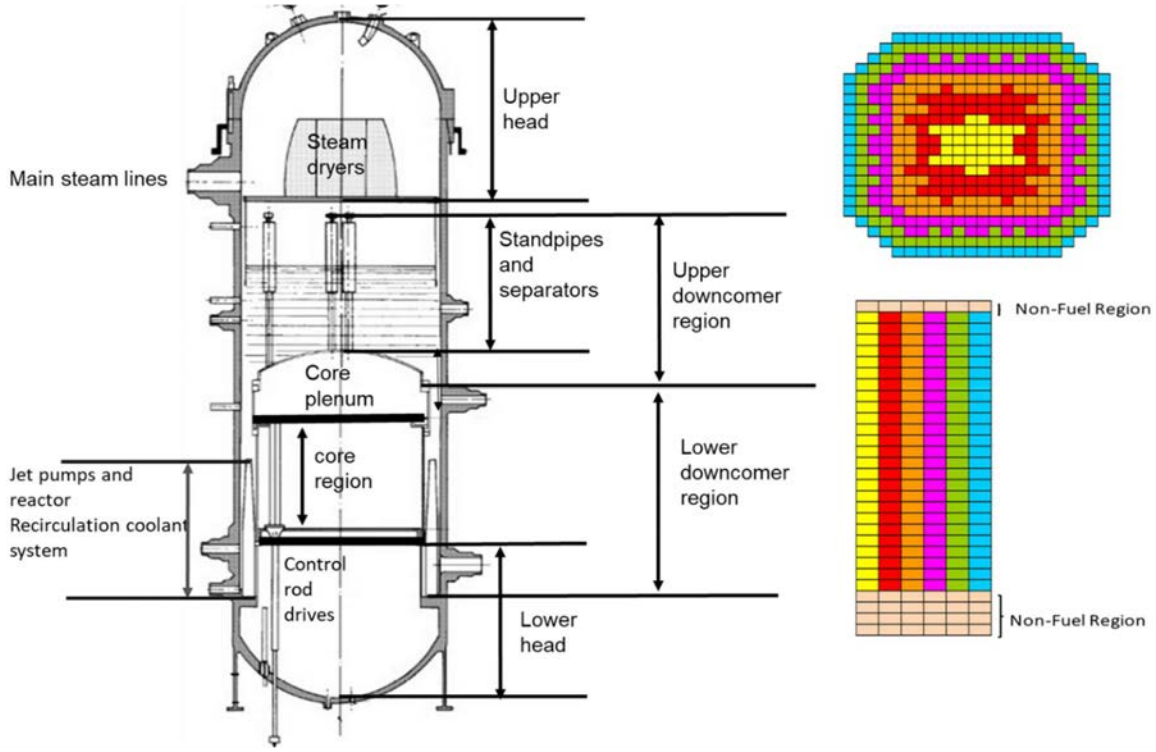

FIG. 18. MAAP5 BWR-5 reactor pressure vessel, core region, and non-active fuel region nodalization schemes.

2.3.4.5. Uncertainty and sensitivity analysis methodology

For most methodologies, the uncertainty and sensitivity analysis require a list of uncertain parameters and their associated PDFs. To select the uncertain parameters, it is important to identify the relevant physical phenomena for the chosen scenario and the severe accident code for simulations. The code should have models to adequately reflect the impact of accident progression on key physical variables and the FOMs previously chosen. To better exploit the benefits of uncertainty and sensitivity analysis, robust computational tools are required to generate the input decks for the severe accident code being used and then correctly handle the large amounts of data resulting from simulations. One aspect in particular that must be considered is to perform a correct random sampling within each uncertain parameter's PDF. Here the Monte Carlo sampling is applied. The sample size is determined based on the requirements of the uncertainty methodology being applied for a robust sensitivity analysis and/or the desired confidence level in the uncertainty analysis, as the case of the GRS method.

Several methodologies for uncertainty and sensitivity analysis applied to nuclear reactor safety have been used as described in [34]. The Monte Carlo filtering (MCF) technique was also applied to determine which uncertain variables had noticeable impact on the FOMs. Then, the final ranking of importance of the uncertain variables on the FOMs was determined by calculation of an indicator of degree of correlation, as shown later. In the aspect of uncertainty analysis, among all of methodologies in the literature, the GRS

approach has become practically the most widely used [35, 36]. This approach is based on the concept of propagation of input uncertainties. Figure 19 shows a scheme of how the GRS method can be applied, based on either the Wilks' or Wald's[10] approaches (Wilks' approach is preferably used for comparing nested models, while Wald's approach is more straightforward for testing individual parameter estimates). While the intended tolerance and confidence level for the FOMs are to satisfy at least the 95/95 criteria (a common requirement when using the GRS method), it was preferred to set the number of code executions for the uncertainty analysis as a large number that also satisfies other accurate sensitivity analysis techniques, such as the MCF technique.

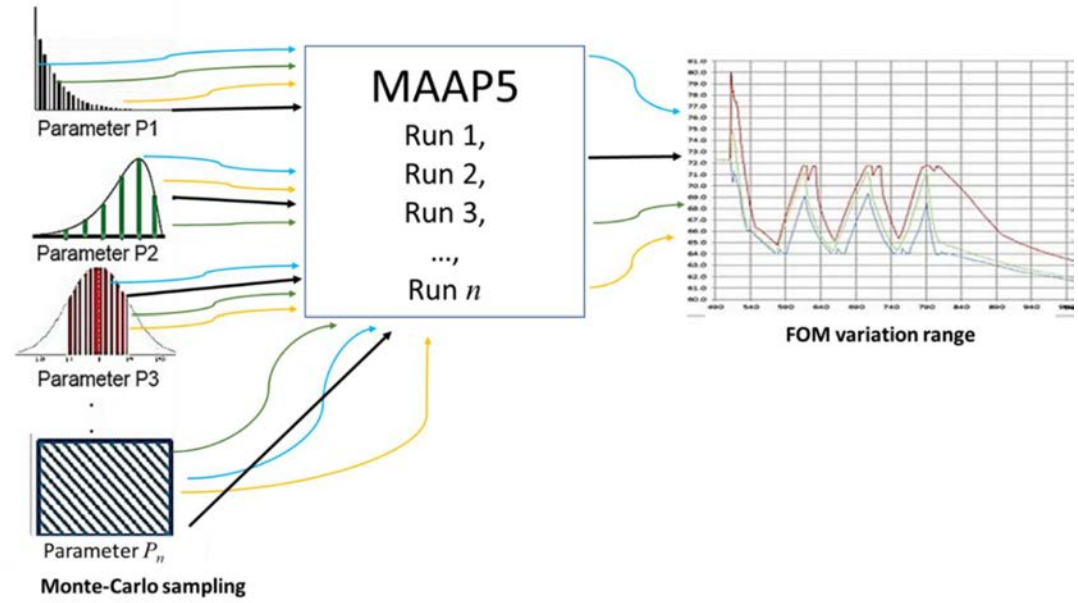

FIG. 19. Probabilistic method based on the propagation of input uncertainties (for illustration purposes).

For quantitative variables (physical parameters), correlation coefficients can be computed to measure the degree of correlation between the input and output variables. However, some of such coefficients are not directly applicable when the input parameters are qualitative variables, that is, options or flags available to the code's user to choose specific models. Among several common correlation coefficients, four of those of common use have been implemented in sensitivity computational procedures for calculating the degree of correlation when using physical parameters, that is, quantitative variables:

— Pearson simple correlation coefficient (PSCC);

[10] The Wald's approach, developed by the statistician Abraham Wald in early 1940's, is a method used in statistical hypothesis testing to assess the significance of estimated parameters. It involves comparing an estimated parameter to its standard error, forming a test statistic that follows a known distribution, typically the standard normal distribution for large sample sizes. This approach is particularly useful because it does not require the full specification of the likelihood function, making it more flexible and easier to apply in complex models.

— Spearman rank correlation coefficient (SRCC);
— Partial correlation coefficient (PCC);
— Partial rank correlation coefficient (PRCC).

The correlation coefficient PSCC, is a quantitative estimate of linear monotonic correlation between input and output values (correlation between x_i and y) is given by:

$$r = \frac{\sum_{i=1}^{n}(x_i - \bar{x})(y_i - \bar{y})}{\sqrt{\sum_{i=1}^{n}(x_i - \bar{x})^2 \sum_{i=1}^{n}(y_i - \bar{y})^2}} \tag{1}$$

where:
r – Pearson simple correlation coefficient;
x_i – uncertain input variable for x samples;
y_i - uncertain input variable for y samples;
$\bar{x}$ – mean value;
$\bar{y}$ - mean value;
n – number of samples.

If the data are not linear but still monotonic, one can still use correlation type methods, but it is necessary to reduce nonlinearity. One method is the rank transformation, which is a reliable tool if the dependent variable is a monotonic function of the independent variables. If the rank transformation is applied, the SRCC yields the degree of monotonicity between the input and output sample values, and it can be calculated using the equation for Pearson's r but operating on the rank transformed data, as follows:

$$\rho_S = \frac{\sum_{i=1}^{N}(R_i - \bar{R})(S_i - \bar{S})}{\sqrt{\sum_{i=1}^{N}(R_i - \bar{R})^2 \sum_{i=1}^{N}(S_i - \bar{S})^2}}; \bar{R} = \bar{S} = \frac{N+1}{2} \tag{2}$$

where:
ρ_S – Spearman rank correlation coefficient;
R_i – uncertain input variables;
S_i – FOM output variables;
N – number of samples.

Regarding the PCC, given random variables X_1 and X_2 as input and the output variable Y, this coefficient is a measure of the correlation between X_1 (or X_2) and Y, while eliminating indirect correlations due to relationships that may exist between X_1 and X_2, or X_2 and Y. In this example, the degree of correlation ($rXiY \mid X_2$) is given as:

$$r_{X_1Y|X_2} = \frac{r_{X_1Y} - r_{X_1X_2} r_{X_2Y}}{\sqrt{(1 - r_{X_1X_2}^2)(1 - r_{X_2Y}^2)}} \tag{3}$$

where:

$r_{X_1 Y|X_2}$ – partial correlation coefficient;

r_{xy} – correlation between the variables.

The PRCC refers to calculating a PCC, but after using a rank transformation, it is a monotonicity test between input and output variables while accounting for relationships between input parameters. In the rank based coefficient calculation it is required that the dependent variable is a monotonic function of the independent variables. This is not the case if the qualitative (discrete) variable corresponds to selecting code model options. Thus, when dealing with combinations of quantitative and qualitative input variables, rank transformation should not be directly performed (as in the SRCC) to determine the impact of these two types of uncertain variables on the FOMs. Alternatively, one can use a method as the MCF [37], in which it is determined the probability that the resulting FOM values fall into selected percentiles. If more detailed analysis is desired, there are alternatives such as the response surface method for determining the impact of two, or more, varying quantitative variables on the FOMs. For qualitative input uncertain variables, the Chi-square parameter can be also calculated for each of the available code options [38].

The AZtlan Tool for Uncertainty and SensItivity Analysis (AZTUSIA) is developed and validated [39] as a computational tool aimed to support the pre-processing and post-processing of input and output data sets respectively. AZTUSIA is a computational tool supporting the sensitivity and uncertainty analysis in the framework of the AZTLAN Platform project [40], a Mexican national initiative aiming to have a platform for the analysis and design of nuclear reactors. High performance computing capabilities are implemented in all the AZTLAN platform's modules (neutronics and thermal hydraulics codes). Several exercises for verification and validation have been performed. Figures 20 and 21 show the schemes of the role assigned to AZTUSIA in the input data pre-processing and output data post-processing sequences, respectively. For the preprocessing part, AZTUSIA mainly performs the uncertain variable random sampling to then generate the MAAP5 input files. Once the simulations are completed, AZTUSIA is used again to calculate correlation coefficients and to generate supporting plots for a more comprehensive analysis of the uncertainty and sensitivity results.

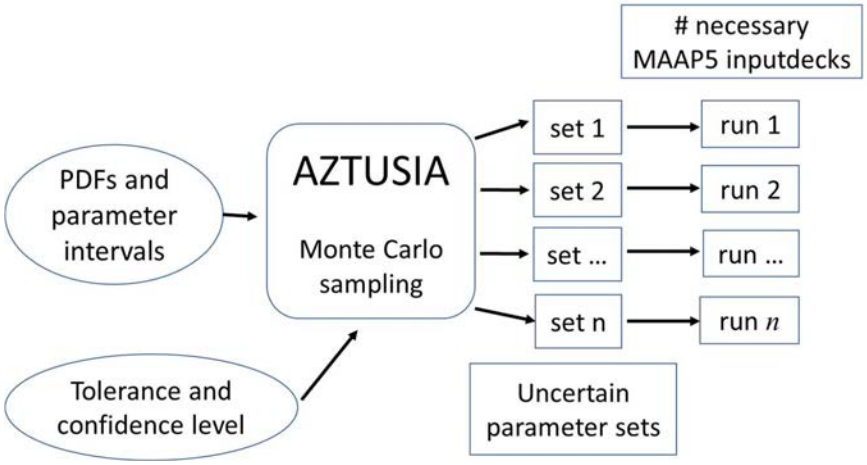

FIG 20. Schematic of AZTUSIA role in the input data pre-processing.

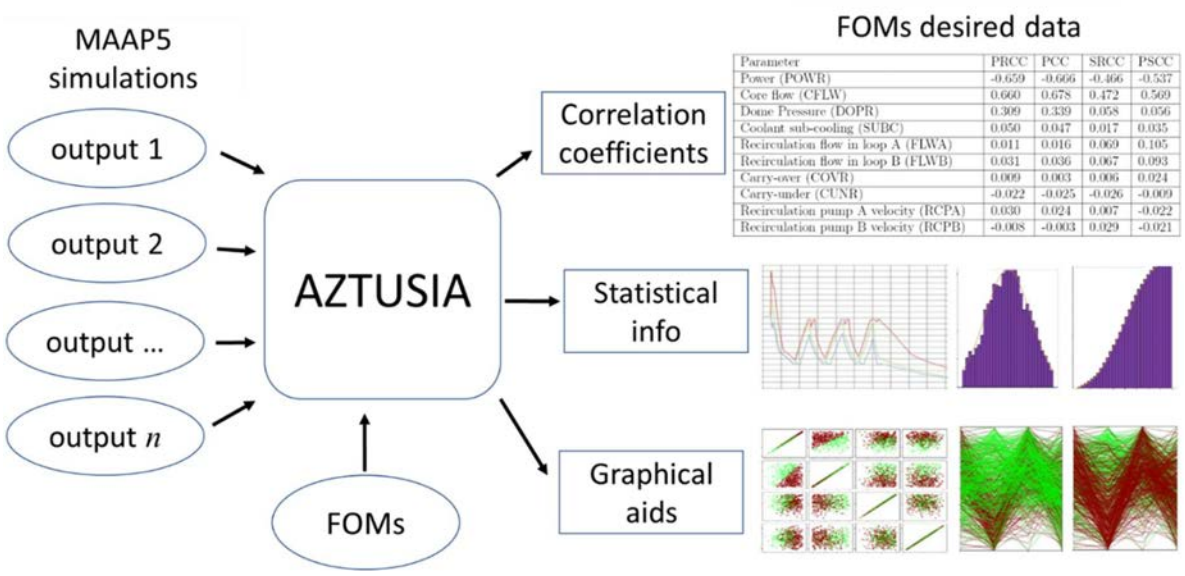

FIG. 21. Schematic of AZTUSIA role in the output data post-processing.

Table 13 shows the main features of AZTUSIA, as the MCF for sensitivity analysis, graphical aids, and correlation coefficients that can be obtained for a sensitivity and uncertainty analysis.

TABLE 13. AZTUSIA MAIN FEATURES

Features	**Options**	**Stage**
Sampling method	Monte Carlo	Pre-processing
Tolerance and confidence level	1. Wilks one-sided tolerance 2. Wilks two-sided tolerance 3. Wald 4. User's option of sample size	Pre-processing
PDF options	1. Uniform 2. Log-Normal 3. Triangular 4. Normal 5. Discrete	Pre-processing
Sensitivity analysis	1. Correlation coefficients: a. PSCC b. SRCC c. PCC d. PRC 2. MCF techniques	Post-processing
Uncertainty analysis	1. uncertainty bands 2. min, max, mean, median, standard deviation, skewness, and kurtosis values	Post-processing
Graphical aids	Scatter plots Histograms Cobweb plots	Post-processing

It is important to study in detail all phenomena that may occur during an SBO in a BWR, as it is often the initiating event that contributes the most to the core damage frequency parameter in probabilistic safety analysis. This can help in estimating the efficiency of various mitigating actions, such as depressurization and injection of external refrigerant, and determining the appropriate timing for such actions. In order to monitor the progression of the severe accident, several parameters need constant monitoring. These parameters include hydrogen concentrations in the dry well and the wet well, RPV level, pressure and temperature, and radiation levels in primary containment. Some of these variables can be taken directly as FOMs for severe accident uncertainty and sensitivity analysis, while others provide key information on the progression of core degradation. Six FOMs related mostly to accident management are considered:

1) Hydrogen mass generated;
2) Fission products mass fractions;
3) Time until core damage criterion;
4) Core support plate failure time;
5) Debris mass in the lower head;
6) RPV breach time.

These FOMs are important in assessing the effectiveness of accident management strategies. Additionally, other five key events are tracked: time to reach the top of active fuel, time to reach the bottom of active fuel, time to runaway oxidation reaction, time to first fuel rods failure, and time of core slumping to lower head. These events provide important information on the progression of the severe accident and can help in assessing the effectiveness of various accident management strategies. Selecting the uncertain code input variables is a critical step in uncertainty and sensitivity analysis and requires a detailed study of the accident progression and the most relevant phenomena.

The process of selecting these input variables often involves generating a PIRT, which is a systematic approach used to identify and rank the most important phenomena that contribute to the uncertainty of the FOMs. The level of knowledge for each of the phenomena occurring in the early and late phases of a severe accident progression is different, which means that the uncertainty of key parameters of physical and chemical phenomena needs to be reflected accordingly. For instance, parameters that are critical during the early phase of a severe accident, such as fuel-coolant interactions and steam explosions, may have a greater impact on the FOMs than those that are important during the late phase, such as the behaviour of the corium in the lower plenum. However, some of the key parameters that are identified during the PIRT may not be directly available as input variables in the code being used. In these cases, surrogate parameters or correlations may be used to represent the effects of these key parameters on the FOMs. The selection of appropriate surrogate parameters requires careful consideration of their relationship with the key parameters and their impact on the FOMs.

Figure 22 shows the process of selecting uncertain parameters as applied in this simulation. MAAP5 provides a proposed list of parameters that can be used for the uncertainty and sensitivity analysis [33]. One can choose other input variables as needed. The parameter information includes recommended values, their intervals, and expected phenomena that can be impacted. A sequential process is followed to narrow the number of variables from one stage to the next to obtain the final set of user input uncertain variables. Out

of initially considered 153 input variables based on Fig. 23 selection process, total of 28 input variables are selected.

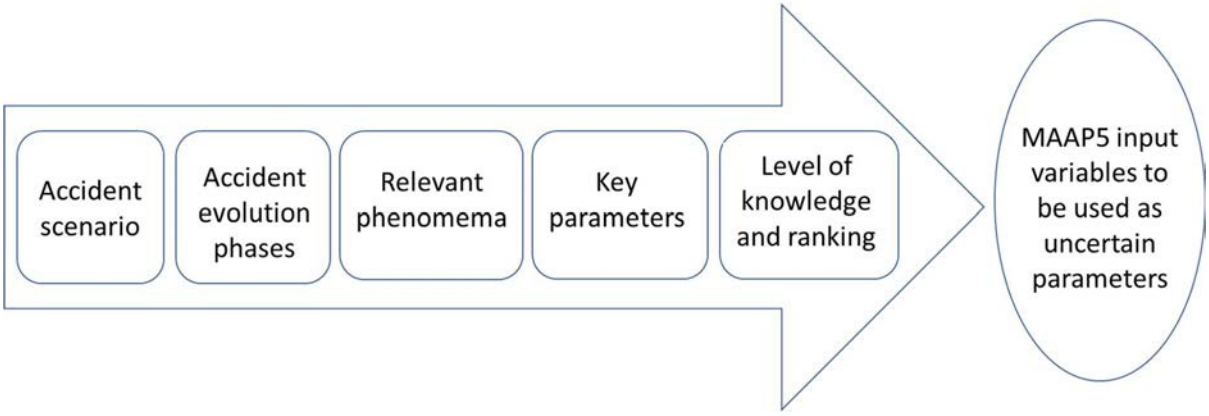

FIG. 22. Uncertain parameters selection process.

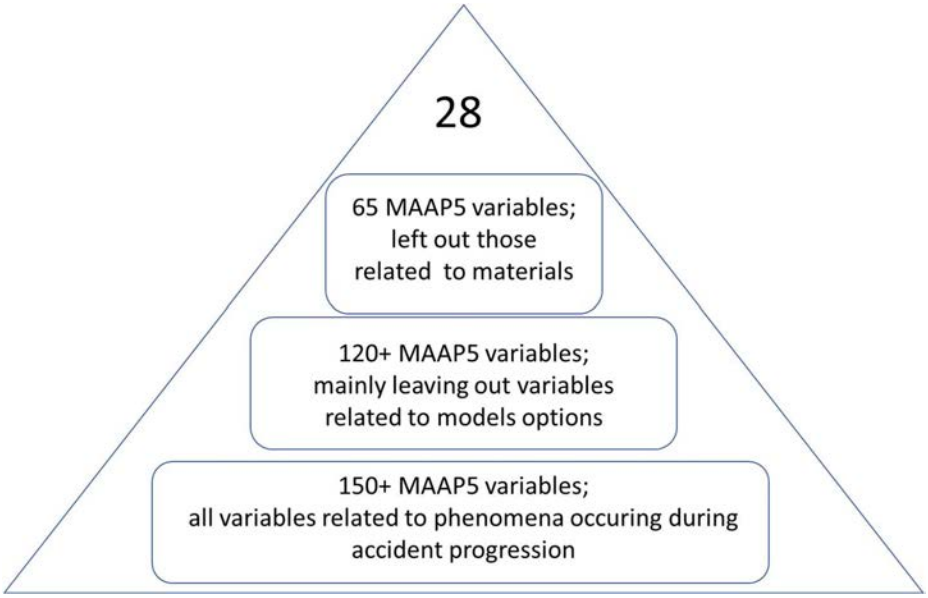

FIG. 23. Uncertain MAAP5 user-input variables selection process.

One of the sensitivity and uncertainty analysis's key issues is using the proper PDF for each uncertain parameter. Choosing a PDF frequently relies on experience and/or data found in the scientific literature; for example, normal (Gaussian), triangular and uniform PDFs are commonly used [41].

Table 14 shows the uncertain variables with short descriptions with intervals and associated PDFs chosen from [42–44] in combination with engineering judgment.

TABLE 14. UNCERTAINTY PARAMETERS USED FOR THE UNMITIGATED SBO ANALYSIS

Variables	MAAP variable	Description	Reference value	PDF	min value	max value
UV01	ASRV(1)	Effective flow area for the 1st S/RV. The discharge coefficient is hardwired.	1.04×10^{-2} $m^2 = \mu$	Normal, +/- 2σ	–2σ= 10 %	+2σ= 10%
UV02	HTCONC	Overall heat transfer coefficient between fuel and cladding for covered core nodes.	5.00×10^{3} W/m^2C	Uniform	–20 %	+20 %
UV03	HTCONR	Overall heat transfer coefficient between fuel and cladding for uncovered core nodes.	7.50×10^{2} W/m^2C	Uniform	–20 %	+20 %
UV04	HTBLAD	Correction for heat transfer from control blades to bypass flow.	0.00 W/m^2C	Triangular	0	500
UV05	FAOX	Multiplier for cladding surface area for oxidation.	1.00	Uniform	1.0	2.0
UV06	FZORUP	Minimum fraction of Zr oxidized to keep cladding intact.	7.00×10^{-1}	Triangular	0.45	0.75
UV07	TCLMAX	Temperature in time-at-temperature correlation for cladding rupture.	2.50×10^{3} K	Uniform	2000	2700
UV08	IUZROXID	Option for U-Zr-O mixture oxidation model. 2 models.		Discrete		
UV09	FACT	Multiplier to reduce hydraulic diameter and flow area when intact fuel node collapses.	3.00×10^{-1}	Triangular	0.1	1.0
UV10	IOXIDE	Specifies Zr oxidation model. 4 models.		Discrete		
UV11	TCLRUP	Temperature at which fuel cladding fails.	1.00×10^{3} K	Triangular	1000	1500
UV12	FGPOOL	Geometric factor for in-core molten pool.	7.38×10^{-1} = μ	Normal, +/- 2σ	–2σ= 10 %	+2σ= 10 %
UV13	TOXMP	Melting point of oxidic debris.	2.50×10^{3} K	Uniform	2300	2700
UV14	TMLMP	Melting point of metallic debris.	1.70×10^{3} K	Uniform	1600	1800
UV15	TSPFAL	Temperature for time-at-temperature correlations for core support plate failure.	1.65×10^{3} K	Uniform	1550	1750

TABLE 14. UNCERTAINTY PARAMETERS USED FOR THE UNMITIGATED SBO ANALYSIS (Cont.)

UV16	VFCRCO	Porosity of collapsed core region.	3.50×10^{-1} = μ	Normal, +/- 2σ	–2σ= 20%	+2σ= 20%
UV17	IADDB4CSTEEL	Option to add or not B4C to the top light metal layer.		Discrete		
UV18	IOCHF	Option for gap cooling CHF correlation. 3 models.		Discrete		
UV19	IPARTBEDMELT	Option for melting rate of particulates in lower plenum corium pool.		Discrete		
UV20	FRCOEF	Debris friction coefficient.	5.00×10^{-3}	Uniform	0.001	0.010
UV21	IOXIDHT	Specifies the model for heat transfer from oxidic debris to crust in the lower plenum. 3 models.		Discrete		
UV22	IQDPB	Specifies the model for heat transfer from debris bed particles to water in the lower plenum. 2 models.		Discrete		
UV23	FDAMLH	Lower head damage fraction for extensive failure.	4.00×10^{-1}	Uniform	0.3	0.5
UV24	FEQSIG	Multiplier to hoop stress for creep calculations.	1.00	Uniform	0.5	1.5
UV25	XLVP0	Initial length of the crack for the vessel lower head creep rupture.	5.00×10^{-1} m	Triangular	0.005	2.000
UV26	XROF0	Initial radius of localized lower head failures.	1.00×10^{-2} m	Triangular	0.005	0.250
UV27	XROF1	Initial radius of extensive lower head failures.	1.00×10^{-1} m	Triangular	0.05	0.50
UV28	XWIDVP0	Initial width of the crack for the vessel lower head creep rupture.	2.00×10^{-2} m	Triangular	0.001	0.250

The reasoning for choosing a PDF for each uncertain variable is provided in Table 15.

TABLE 15. ARGUMENTS TO SELECT SPECIFIC PDFs

Variables	Arguments	PDF rationale
UV01	Discharge coefficient is hardwired in MAAP5, so it is through the effective flow area that one can impact SRV flow.	Engineering judgment.
UV02	Heat transfer coefficients are commonly treated as uniform PDF since not enough information about dependency on several other fundamental variables can be obtained. It was preferred to choose the uniform PDF on base a literature survey.	Reference [44].
UV03	Heat transfer coefficients are commonly treated as uniform PDF since not enough information about dependency on several other fundamental variables can be obtained. It was preferred to choose the uniform PDF on base a literature survey.	Reference [44].
UV04	Heat transfer coefficients are commonly treated as uniform PDF since not enough information about dependency on several other fundamental variables can be obtained. It was preferred to choose the uniform PDF on base a literature survey.	Reference [44].
UV05	More surface area implies more oxidation, according to the model. No preference was considered for a particular value of this multiplier, so a uniform PDF was taken.	Engineering judgment and Reference [43].
UV06	Failure criteria usually take a uniform PDF, but given the minimum and maximum values allowed, it was preferred to use a triangular PDF. The reference value is chosen as the one with the highest probability and from it linearly decreasing to the minimum and maximum allowed values.	Engineering judgment and Reference [43]
UV07	Values of limiting temperature for failure criteria are commonly treated as uniform PDF. It was preferred choice based on literature survey.	Reference [44]
UV08	To test the 2 available options equally.	Engineering judgment and Reference [43]
UV09	Given the default, minimum and maximum values allowed, it was preferred to use a triangular PDF. The reference value is selected as the one with the highest probability and from it linearly decreasing to the minimum and maximum allowed values.	Engineering judgment and Reference [43]
UV10	To test the 4 available options. The default option is given a 40% probability, and the rest a 20% each of them.	Engineering judgment and Reference [43]
UV11	Uniform PDF was considered first, but given the default, minimum and maximum values allowed, it was preferred to use a triangular PDF.	Engineering judgment and Reference [43]
UV12	Shape of the molten core affects the heat transfer area.	Engineering judgment and Reference [43]
UV13	Values of limiting temperature for failure criteria are commonly treated as uniform PDF. It was preferred choice based on literature survey.	Reference [44]
UV14	Values of limiting temperature for failure criteria are commonly treated as uniform PDF. It was preferred choice based on literature survey.	Reference [44]

TABLE 15. ARGUMENTS TO SELECT SPECIFIC PDFs (Cont.)

UV15	The values of limiting temperature for failure criteria are commonly treated as a uniform PDF. It was preferred to choose the uniform PDF on base a literature survey.	Reference [44]
UV16	The porosity of the collapsed core region affects the coolability and heat transfer.	Engineering judgment and Reference [43]
UV17	To test the 2 available options equally.	Engineering judgment and Reference [43]
UV18	To test the 3 available options. The default option is given a 40% probability, and the rest a 30% each of them.	Engineering judgment and Reference [43]
UV19	To test the 2 available options equally.	Engineering judgment and Reference [43]
UV20	Friction coefficients are commonly treated as uniform PDF since not much information about dependency on other several fundamental variables can be obtained. It was preferred to choose the uniform PDF on base a literature survey.	Reference [44]
UV21	To test the 3 available options. The default option is given a 40% probability, and the rest a 30% each of them.	Engineering judgment and Reference [43]
UV22	To test the 2 available options equally.	Engineering judgment and Reference [43]
UV23	Failure criteria usually take a uniform PDF.	Reference [44]
UV24	No preference was considered for a particular value of this multiplier, so a uniform PDF was taken.	Engineering judgment and Reference [43]
UV25	Given the default, minimum and maximum values allowed, it was preferred to use a triangular PDF. The reference value is selected as the one with the highest probability and from it linearly decreasing to the minimum and maximum allowed values.	Engineering judgment and Reference [43]
UV26	Given the default, minimum and maximum values allowed, it was preferred to use a triangular PDF. The reference value is selected as the one with the highest probability and from it linearly decreasing to the minimum and maximum allowed values.	Engineering judgment and Reference [43]
UV27	Given the default, minimum and maximum values allowed, it was preferred to use a triangular PDF. The reference value is selected as the one with the highest probability and from it linearly decreasing to the minimum and maximum allowed values.	Engineering judgment and Reference [43].
UV28	Given the default, minimum and maximum values allowed, it was preferred to use a triangular PDF. The reference value is selected as the one with the highest probability and from it linearly decreasing to the minimum and maximum allowed values.	Engineering judgment and Reference [43]

2.3.4.6. Results

A numerical stability analysis is performed to ensure that the results of the BWR nuclear steam supply system plant model are accurate and reliable. The analysis involved varying the time step parameters used for iteration towards convergence and keeping one of the parameters fixed. The main parameters of the heat balance, which are crucial for the proper functioning of the BWR plant, were considered during the analysis. Fifteen different combinations of time steps were used in the analysis based on MAAP5, which indicates a thorough and comprehensive testing approach. This would help to identify any potential issues or errors in the numerical solution and ensure that the results are accurate and reliable.

As an example, Fig. 24 shows normalized results of the nominal vessel level and the nominal pressure in the reactor from 15 different time step combinations. All combinations quickly fall into a band bounded by less than 1%, but several of the combinations led to oscillations (most noticeable, the combinations 1, 6, and 11) in the vessel level profiles and the reactor pressure. The remaining combinations show a smoother quick convergence pattern towards steady state values. Similar trends were obtained for other relevant, steady-state parameters as steam flow and temperatures. According to the results shown in Fig. 24, combination 9 was the selected option for the base case simulations.

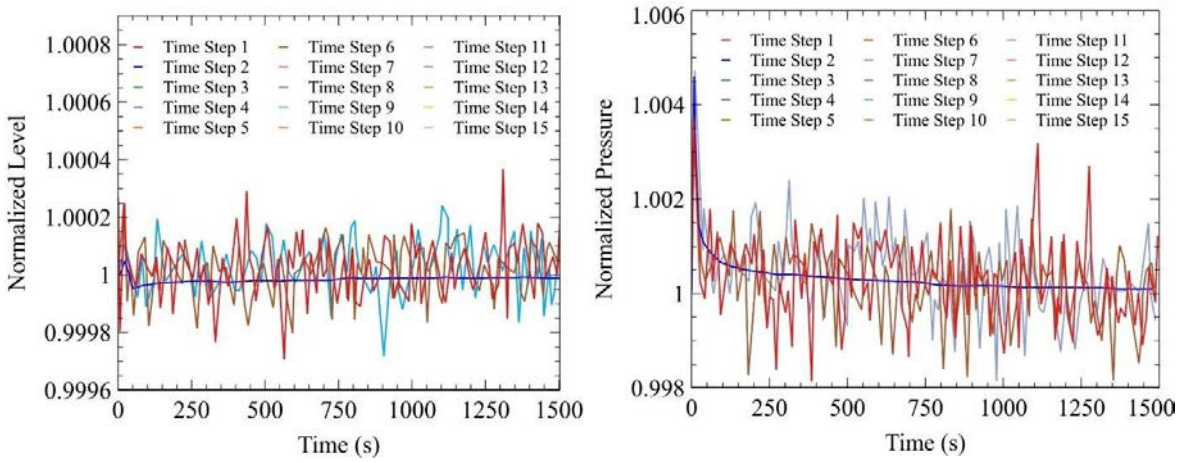

(a) *(b)*

FIG. 24. Normalized profiles of (a) reactor level and (b) pressure from 15 different time-step combinations.

Once it was determined the time step combination yielded more stable results, steady state results were compared against relevant reference data.

Table 16 shows this comparison, and Fig. 25 shows the convergence profile.

TABLE 16. COMPARISON BETWEEN STEADY STATE REFERENCE VALUES AND MAAP5 RESULTS

Parameter	Difference	Absolute percent relative error (%)
Main steam flow	+1.3769 kg/s	0.109
Steam enthalpy	+657.27 J/kg	0.024
Feed water flow	–9.0761 kg/s	0.715
Thermal power	0 MWt	0.000
Entering core flow	+2.3438 kg/s	0.030
Dome pressure	+0.008 MPa	0.111
Control rod drive flow	–0.011 kg/s	0.459
RPV level	+0.0154 m	0.110

The main postulates of the severe accident case are: a) the plant is considered initially working at 100% power, 100% core flow, and rated pressure, that is, nominal operating conditions; b) initial SBO; c) reactor scrammed at $t = 0$; d) loss of all direct current sources; e) no depressurization; f) SRVs cycling in safety mode, and g) RCIC unavailable because of no direct current for its control system. Table 17 shows the times of key events during the progression of the accident. Figure 26 shows normalized nominal dome pressure during the event; the colored region refers to the time after vessel failure.

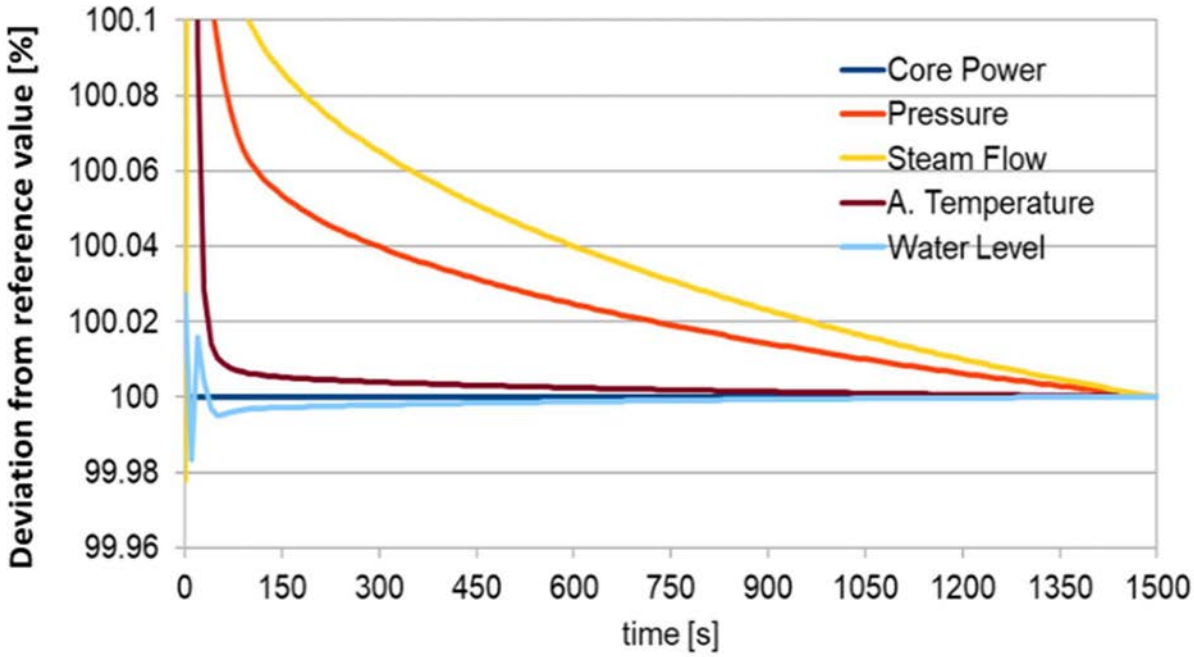

FIG. 25. MAAP5 steady-state results.

TABLE 17. TIMING OF KEY EVENTS DURING THE UNMITIGATED SBO

Event	Timing [s]
Loss of alternate and direct current power	0.0
Reactor scrammed	0.05
Recirculation pump tripped	0.3
Vessel level at top of active fuel	1,948.0
Hydrogen generation begins	3,002.3
Runaway oxidation reaction	3,402.0
Core damage criterion	3,410.4
Vessel level at bottom of active fuel	5,210.4
Corium at lower head	9,007.3
Support plate failure (ring 3)	9,606.5
Support plate failure (ring 4)	9,862.3
Support plate failure (ring 5)	9,988.3
First core slumping to lower head	10,007.5
Support plate failure (ring 1)	11,986.6
Big core slumping to lower head	12,107.0
Support plate failure (ring 2)	13,353.2
RPV failure	13,360.2

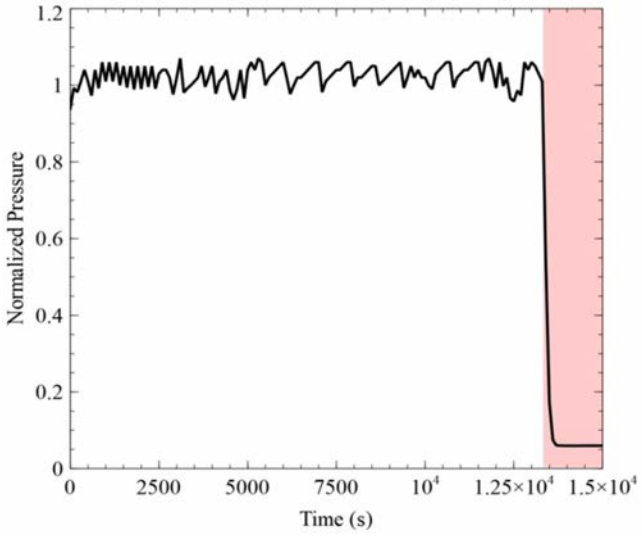

FIG. 26. Normalized nominal dome pressure showing SRVs cycling action.

Figure 27 shows the temperature profiles in the active core (mean and maximum values) and in the reactor structures (shroud and downcomer) at core height as a function of time. Shroud temperature is far from the steel melting point, and similarly is the downcomer wall temperature. The maximum temperatures for these

two structures are 1,094.7 K and 772.5 K, respectively. This figure also shows that the hydrogen starts to be generated at 2,904 s at which time the maximum core temperature is 815.7 K. The sharp generation rate increases at ~3,600 s, a phenomenon associated with the runaway oxidation reaction. Cladding temperature, at that time is ~1,500 K. At the time of the RPV failure, total accumulated mass of hydrogen is 308.5 kg.

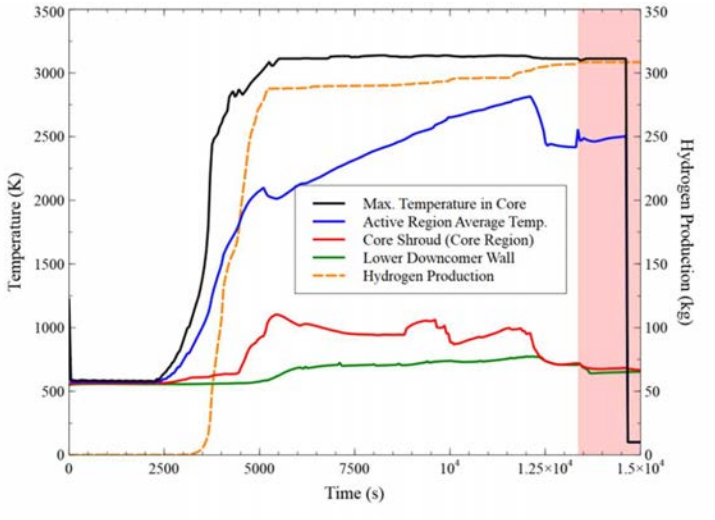

FIG. 27. Hydrogen mass generation and core temperature as a function of time.

The core damage criterion occurs at 3,410.4 s; this criterion is associated with the time when the maximum core temperature reaches 1,255 K and the core level is less than one third of its active part. For the FOM core support plate failure time, Fig. 28 shows the mass of debris in the RPV lower head (continuous line) and, the mass of steel of each of six rings composing the core support plate (dashed lines). It can be noted, that as each of the steel rings collapses, the mass of material increases in the lower head. The total mass of debris includes molten core and steel from the core plate and other supporting structures. Collapsing times for each ring are given in Table 17.

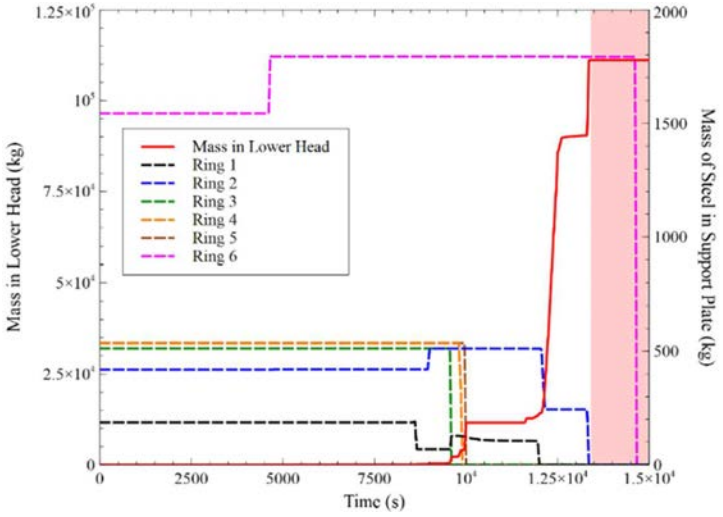

FIG. 28. Collapse of the six core support plate sections and mass of debris in RPV lower head.

Figure 29 shows the total amount of mass in the core, the generation of molten material as core degrades, and the debris mass in the lower head. The collapse of molten core material occurs at 12,000s, with the corresponding decrease of core mass and the consequent increase of debris mass in the lower head. By the time of the RPV breach, there would be over 100 tons of material in the lower head.

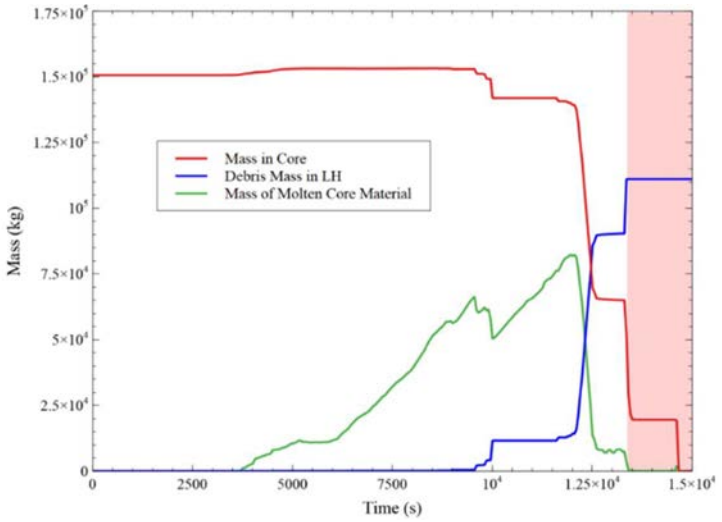

FIG. 29. Total mass of core material, molten core material, and debris in the lower head.

Figure 30 shows the debris temperature and its height in the lower head. The first noticeable increase of debris temperature corresponds to the initial fall of the molten core, as shown in Fig. 29. At this time the molten material falls mainly through the support pieces of the fuel assembly. The temperature jump is ~450 K. The temperature spikes occurring during 9,000–10,000 s correspond to the collapse of the core support plate sections (Fig. 28). The temperature increase is 500–600 K. The largest temperature rise is due to core slumping at 12,000 s.

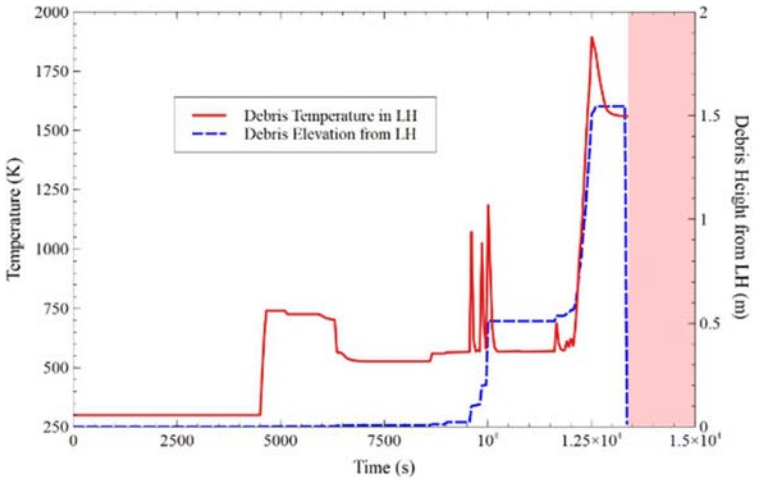

FIG. 30. Temperature and height of debris in the lower head.

Figure 31 shows the fission products mass fractions released in the whole primary system, considering products as noble gases (Xe, Kr), CsI, CsOH, and Cs2MoO4. The mass fraction is defined as the released mass divided by the initial total mass for each product at the beginning of the scenario.

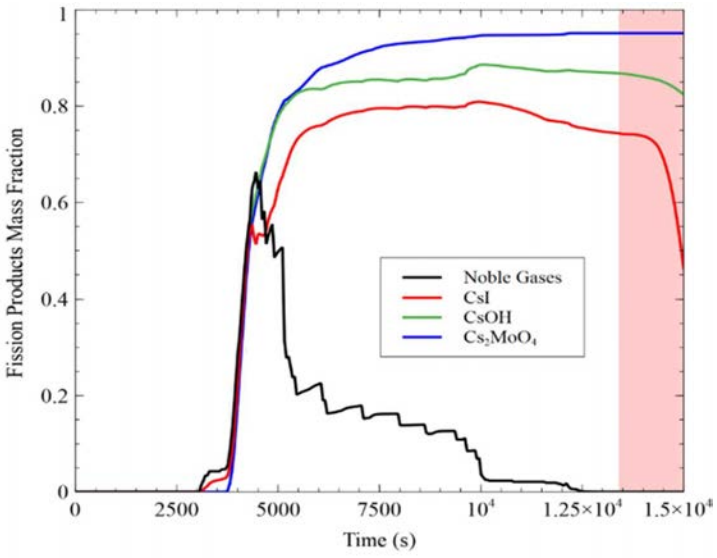

FIG. 31. Fission products mass fraction in the primary system.

Figure 32 shows the temperature field on the RPV lower head wall and the location where the breach would occur. MAAP5 predicts the cause of failure to be due to degradation of the control rod drive tubes near node 2, just besides the middle plane. As shown in Table 17, the time of failure is at 13,360.2 s.

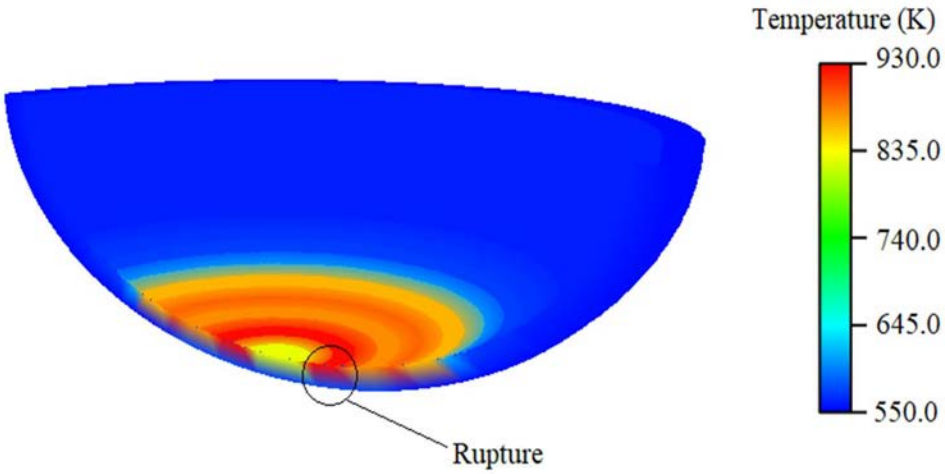

FIG. 32. Temperature field on the lower head wall and location of RPV failure.

The sensitivity analysis was performed to determine which of the uncertain parameters significantly impact the FOMs. All of the uncertain variables shown in Table 14 are set to a uniform PDF. This analysis is based on a sample of 1,000 MAAP5 simulations, although eight of them crashed. Figure 33 shows a scatter plot

of the total amount of hydrogen mass being generated in the core, from 992 successful MAAP5 simulations. The figure also presents the maximum, minimum, and average values.

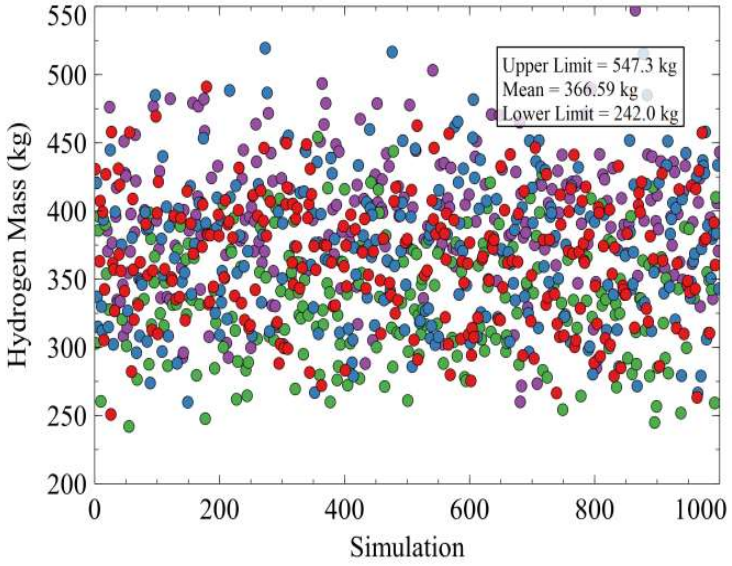

FIG. 33. Accumulated hydrogen mass values obtained from 992 MAAP5 simulations.

When only dealing with quantitative (physical) parameters, any of the correlation coefficients described before can be computed. Thus, the SRCC was computed for all six FOMs, because it is a standard practice. The results are presented in Table 18 for only five variables with the highest rankings. For the calculation, the range of variation of the uncertain variables was divided into ten equal intervals (bins).

TABLE 18. RESULTS OF THE SRCC FOR THE SIX FIGURES OF MERIT

FOM	**UVi / SRCC**				
Hydrogen mass	UV16 / 0.358	UV07 / 0.328	UV05 / 0.067	UV11 / –0.047	UV13 / –0.044
RPV failure time	UV16 / 0.192	UV01 / 0.054	UV14 / –0.053	UV02 / –0.052	UV24 / 0.051
Volatile FPs mass fraction	UV12 / 0.124	UV15 / 0.058	UV26 / 0.043	UV27 / 0.042	UV24 / 0.039
Debris mass in lower head	UV16 / –0.164	UV12 / 0.078	UV07 / 0.053	UV09 / 0.052	UV02 / 0.048
Core damage criterion time	UV01 / –0.553	UV03 / 0.079	UV02 / –0.068	UV05 / –0.046	UV20 / –0.042
Support plate failure time	UV12 / 0.285	UV07 / –0.172	UV15 / 0.120	UV28 / –0.111	UV14 / 0.074

While the SRCC provides with a direct ranking of importance (correlation), it is still necessary to corroborate those results, by using graphical aids, as scatter plots of the FOM in function of each uncertain

parameter or by constructing a Cobweb plot. As example, Fig. 34 shows the scatter plot of hydrogen mass and TCLMAX (UV07). It can be noted the positive monotonic, and practically linear, correlation between these two parameters. This result clearly agrees with the positive correlation value shown in Table 18.

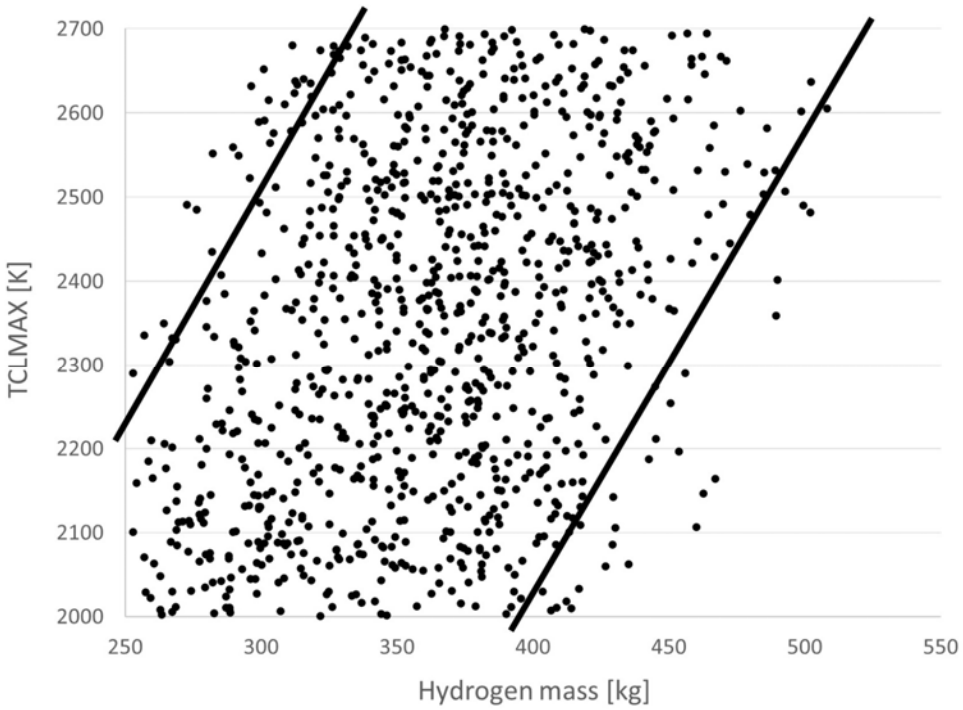

FIG. 34. Scatter plot of hydrogen mass and TCLMAX (UV07).

The degree of correlation calculated by the SRCC is generally divided in five ranges [45]: 0.0–0.09: negligible; 0.1–0.39: weak; 0.4–0.69: moderate; 0.7–0.89: strong; and 0.9–1.0: very strong. However, these boundaries have not been fixed. According to this ranking, with exception of UV01 for the FOM core damage criterion time, no other SRCC value reached even the moderate level, even though Fig. 34 shows clear correlation. Given this outcome, the MCF technique is applied as alternative methodology for the sensitivity analysis of the quantitative uncertain variables. This approach is applied by calculating percentile histograms. This method starts by dividing the input variables' values in the desired number of intervals (bins) over the whole range of variable variation. Ten bins are selected. Thus, within the intervals, an appropriate number of percentile ranges are created, based on the number of samples (code simulations) available, and the resulting values of the FOMs are accumulated in their corresponding percentile ranges. Ten percentiles are chosen because analysts are mostly interested in obtaining information of the FOMs in the 0–10% and 90–100% intervals.

As an example of the information that can be obtained from the application of the MCF technique, Fig. 35 shows the correlation between the uncertain variable temperature in time-at-temperature correlation for cladding rupture (TCLMAX, UV07) and the FOM hydrogen mass generated in the core. This figure clearly reflects the data from Fig. 34, that is, as TCLMAX increases, the percentile 90–100 also increases, but the percentile 0–10 decreases. For example, in the range 2,489.9–2,599.9 K, the percentile 90–100 reaches about 23%, but in this same interval the percentile 0–10 is less than 2 %. On the lower boundary occurs the

opposite. In the range 2,070.2–2,140.1 K, the percentile 90–100 is less than 5%, but the percentile 0–10 reaches 25%. Figure 34 also shows the 0–10% and 90–100% percentile histograms from the results of the uncertain variable VFCRCO (UV16), which is the variable with highest ranking of importance according the SRCC value in Table 18. The positive correlation is also clearly reflected in the figure.

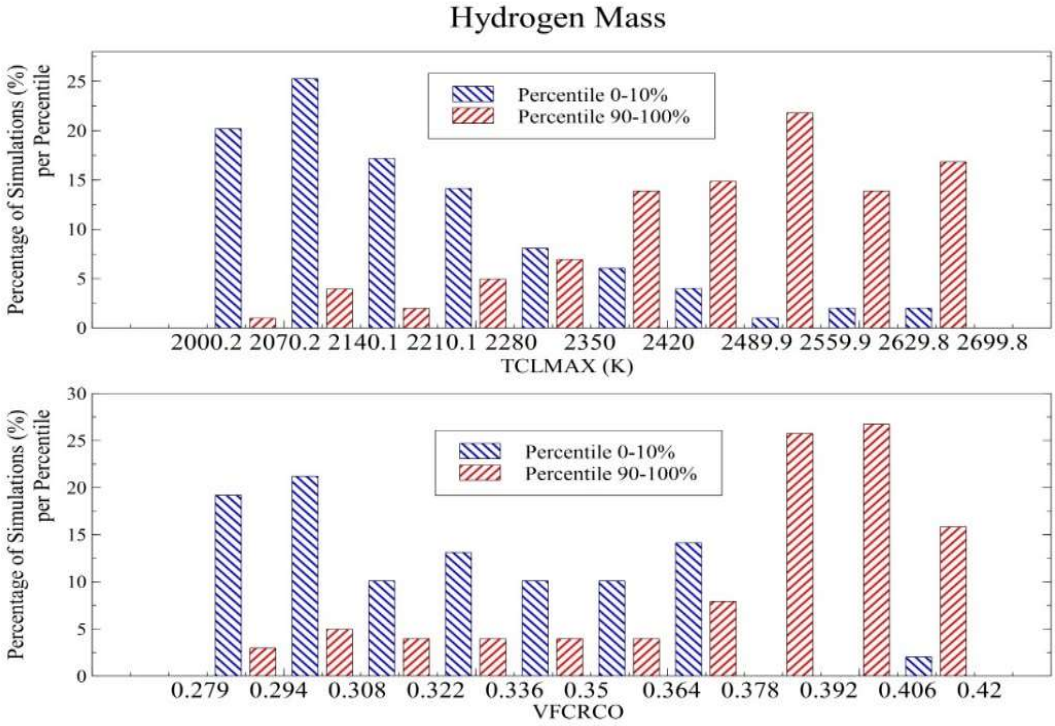

FIG. 35. MCF histograms of two percentiles for hydrogen mass as function of TCLMAX and VFCRCO.

One additional feature of MCF is that it can help determining if the correlation is nonlinear. This is important because it is recalled that the SRCC applies to monotonic correlations between the independent and dependent variables. Still, it does not provide information about what type of monotonic profile occurs. Therefore, by inspection of the histograms, one can determine nonlinear profiles. The percentile histograms in the MCF method can provide more insights into the FOMs, because one can correlate the uncertain variables over the whole range of parameter variation and/or at the bin level. For the uncertainty analysis, a new set of 1,000 MAAP5 simulations were run using the PDFs shown in Table 14, although seven of them crashed.

Figure 36 shows the resulting scatter plots of the six FOMs. The maximum, minimum, and average values are also presented.

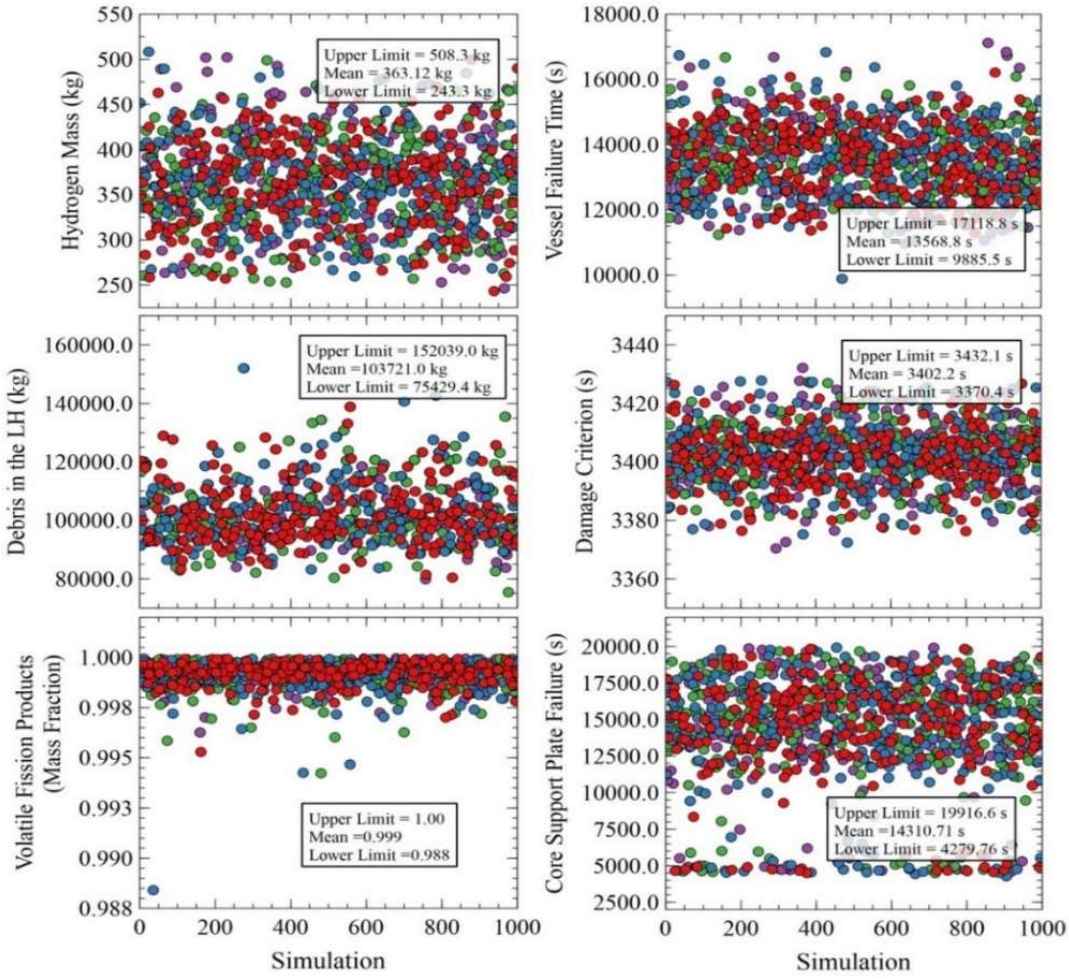

FIG. 36. Scatter plots of final values of the six figures of merit in the uncertainty analysis; .each dot represents one MAAP simulation. .

Figure 37 shows the 993 profiles of hydrogen accumulation throughout the accident scenario and the uncertainty band. The main change with respect to the use of only uniform PDFs for the uncertain parameters is a decrease of 39 kg in the maximum value. This change led to a decrease of 3.5 kg in the average hydrogen mass. Figure 37 shows that until the core heating period, the uncertainty band is narrow, in agreement with results from uncertainty analyses performed to study hydrogen generation in experimental facilities.

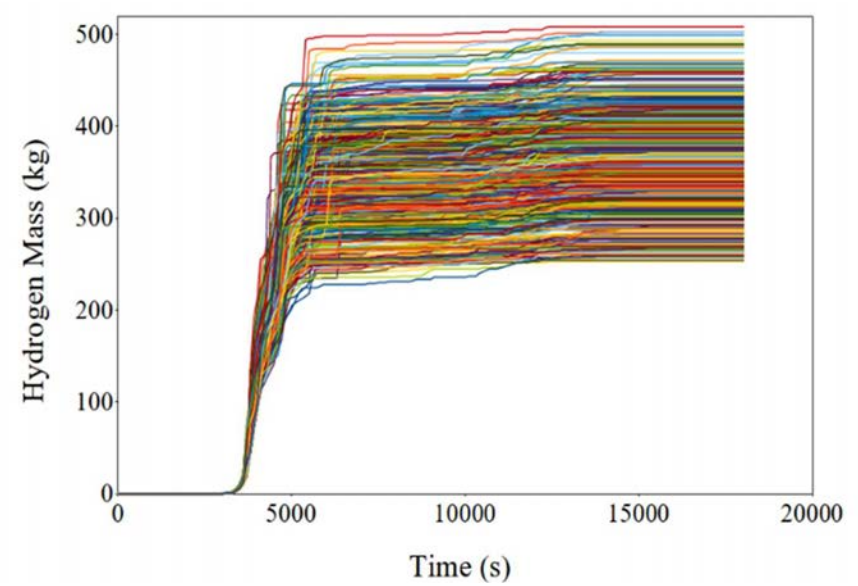

(a)

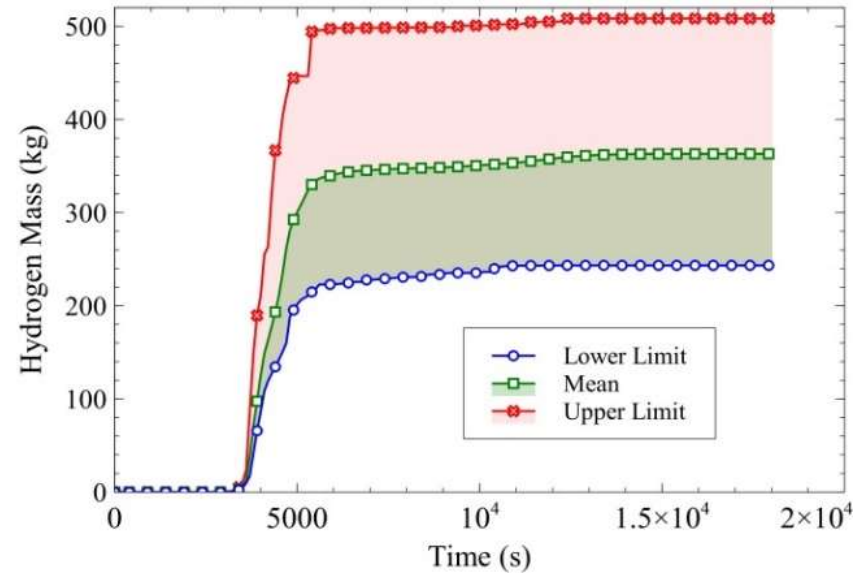

(b)

FIG. 37. Profiles of (a) hydrogen mass generated in the core and (b) resulting uncertainty band.

Another example of uncertainty analysis is given for the FOM volatile fission products mass fractions. Figure 38 shows the profiles of the mass fraction of fission products in the primary system and the resulting uncertainty band. The maximum and average values are basically the same as obtained in the sensitivity analysis. Only the minimum value changed from 0.995 in the sensitivity analysis to 0.988 in this uncertainty analysis.

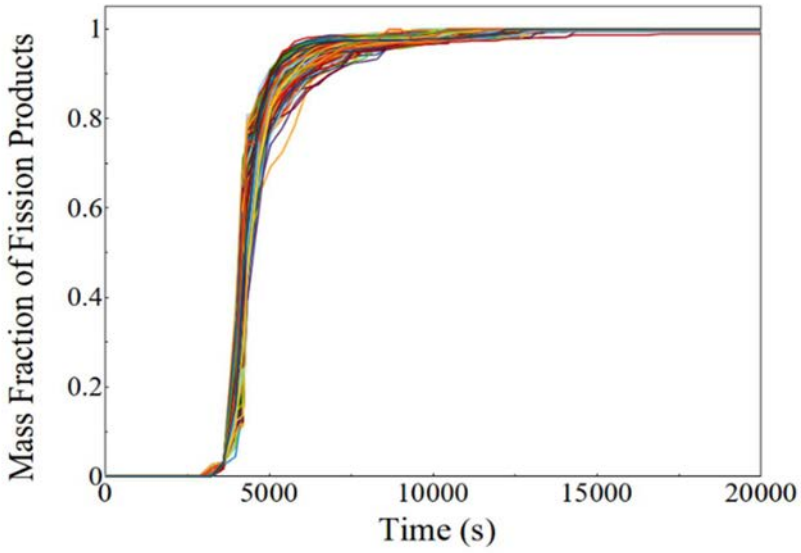

(a)

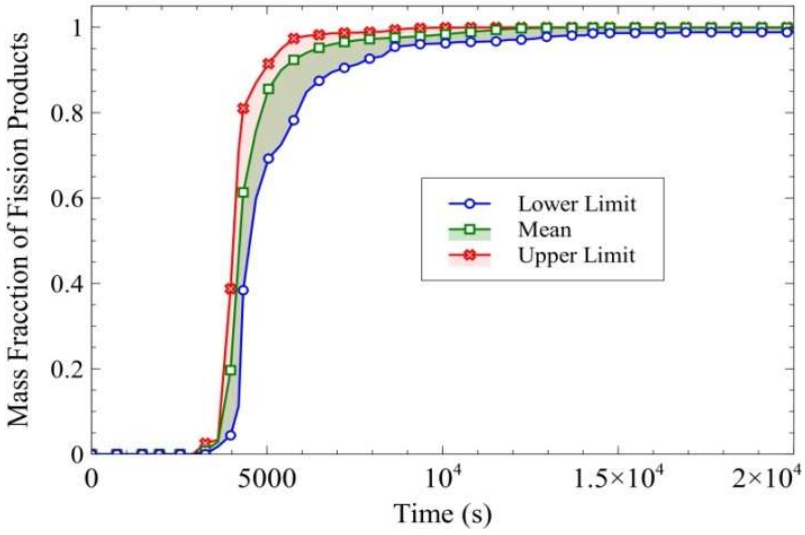

(b)

FIG. 38. Profiles of (a) total mass fraction of fission products in the primary system and (b) resulting uncertainty band.

Table 19 presents a summary of the main statistical parameters frequently used to characterize the results of FOMs [46]. Minimum, maximum, and average values were already shown in Fig. 36. Besides the parameters shown in Table 19, the characterization of FOMs is performed by looking at different PDFs that can be fitted with high degree of confidence.

TABLE 19. STATISTICAL CHARACTERIZATION OF THE FOMs[11]

FOM	Median	Standard deviation	Skewness	Kurtosis	Dispersion index	5th / 95th percentile
Hydrogen mass	364.8 kg	50.8 kg	0.088	–0.380	7.10 kg	279.6 / 444.8 kg
RPV failure time	13,587.6 s	1093.7 s	0.137	–0.200	88.16 s	11,860.2 / 15,317.1s
Volatile fission products mass fraction	0.9992	0.0007	–4.828	51.380	5.42×10^{-7}	0.9979 / 0.9999
Debris mass in lower head	101,924.0 kg	10,918.3 kg	0.777	0.957	1,149.33 kg	88,870.8 / 125,557.0 kg
Core damage time	3,402.3 s	10.4 s	–0.091	0.057	0.03 s	3,383.8 / 3,420.2 s

Figure 39 shows the histograms resulting from four FOMs and three different fitting PDFs. To finally determine which of the test PDFs should be selected as the most appropriate one, different acceptance criteria must be tested [47, 48]:

- FOM debris mass in lower head shown in Fig. 39 (top – left): its skewness value indicates that the data are moderately skewed on the positive direction. The kurtosis value is close to one, reflecting the short length of its distribution tails.
- FOM hydrogen mass generated in the core shown in Fig. 39 (top – right), its low value of skewness clearly reflects the symmetrical shape of the distribution data and its kurtosis value also reflects the low number of samples in the tails. These two values lead to consider a normal distribution as good fitting function for the data.
- A similar argument applies to the FOM RPV failure time shown in Fig. 39 (bottom – right).
- While for the FOM volatile fission products mass fractions shown in Fig. 39 (bottom – left) no values can be greater than one, the large kurtosis value and the large negative value of the skewness clearly reflect the data clustering above 0.9975, but with a long tail towards lower values.

[11] Kurtosis and skewness are statistical measures that describe the shape of a probability distribution.

Skewness measures the degree of asymmetry in the distribution. A distribution with a positive skew is one where the tail is longer on the right side of the distribution, and a negative skew is one where the tail is longer on the left side. A perfectly symmetrical distribution would have a skewness of zero.

Kurtosis measures the degree of peakedness or flatness in a distribution. A distribution with high kurtosis has a sharp peak and fat tails, while a distribution with low kurtosis has a flatter peak and thinner tails. A normal distribution has a kurtosis of three, which is sometimes referred to as mesokurtic. A distribution with a kurtosis greater than three is called leptokurtic, while one with a kurtosis less than three is called platykurtic.

Both skewness and kurtosis are important in statistics because they can provide insights into the underlying data generating process. For example, a high kurtosis may indicate that extreme values occur more frequently than would be expected under a normal distribution, while a positive skewness might suggest that the mean is higher than the median. Understanding the skewness and kurtosis of a distribution can be useful in selecting appropriate statistical methods and interpreting the results of statistical analyses.

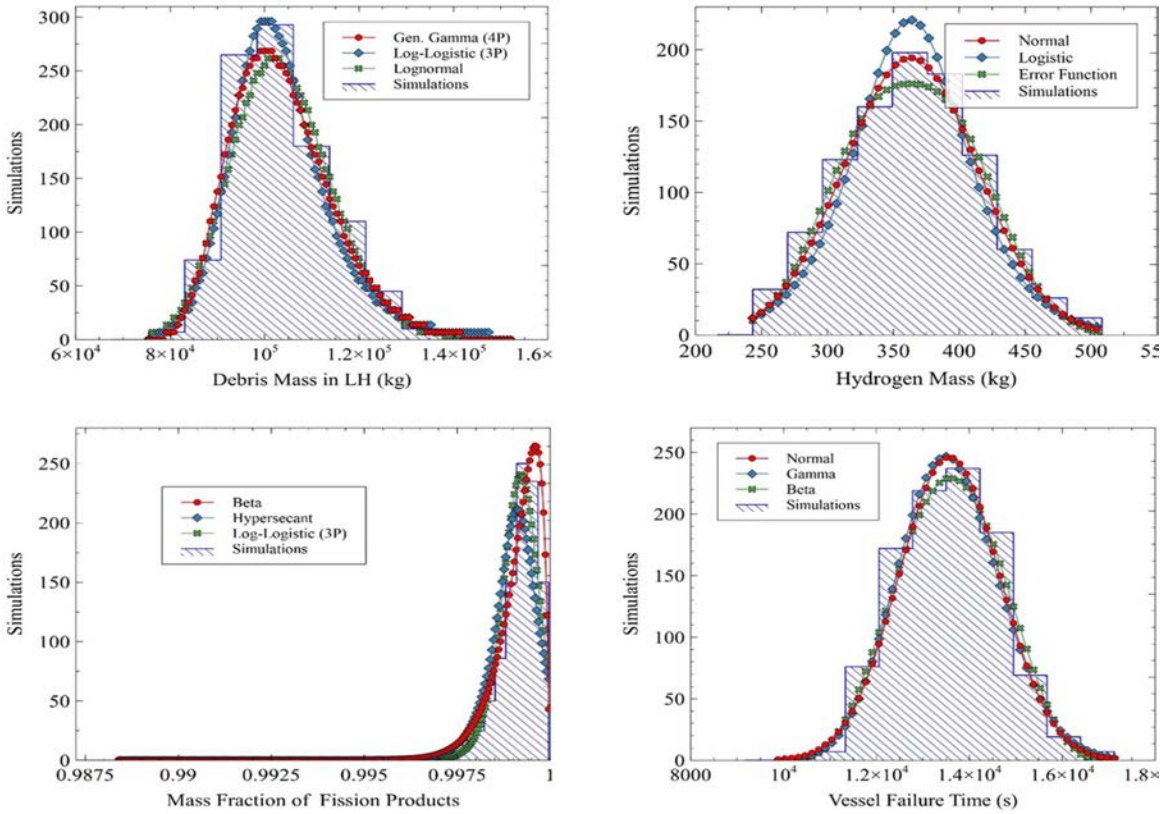

FIG. 39. FOMs PDFs and fitting functions.

2.3.4.7. Summary and conclusions

Uncertainty and sensitivity analysis of six FOMs are performed in the simulation of an unmitigated SBO occurring at a BWR5 with Mark II primary containment. The simulation scope is up to when the RPV would breach, thus only in-vessel phenomena are considered. The severe accident simulation tool was the code MAAP5. The six FOMs considered are: hydrogen mass; fission products mass fractions; time until core damage criterion; core support plate failure time; debris mass in the lower head; and RPV breach time.

Results of the six FOMs for the reference case can be summarized as follows: a) the mass of hydrogen generated in the core is 308.5 kg; b) about 65% of noble gases are released in the primary system in the early stages of the accident, but they leak to primary containment, while ~80% of Cs compounds still stay in the primary system at the time of RPV breach; c) the time predicted to reach 1,255 K and one-third of core level is 3,410 s, that is the criteria for core damage; d) the core support plate is considered to fail at about 10,007 s; e) about 110 tons of debris exists in the RPV lower head at the time of breach; and f) the RPV fails at 13,360 s, due to degradation of control rod drive tubes.

For the uncertainty and sensitivity analysis, 28 uncertain MAAP5 input variables are selected. These 28 uncertain parameters (variables) are used to investigate the range of valid application of different physical models that influence the sequence of the accident scenario. The sensitivity and uncertainty computational tool used was the home developed code AZTUSIA. For the sensitivity analysis, 992 accident simulations are carried out, while 993 simulations are used in the uncertainty analysis.

For the sensitivity analysis, the SRCC is calculated as a measure of the impact of the quantitative uncertain variables on different FOMs. Taking as an example the FOM hydrogen mass generated in core, the SRCC results show that the porosity of collapsed core region (UV16/VFCRCO) and the temperature in time-at-temperature correlation for cladding rupture (UV07/TCLMAX) are with the strongest impact. The calculation of correlation coefficients is not appropriate for the case of qualitative variables (code options), so such calculations are not carried out. However, the MCF technique can be applied to both quantitative and qualitative uncertainty values. Then, as alternative, the MCF technique was also applied, and these same results were confirmed when using quantitative uncertainty values. The application of the MCF technique for qualitative uncertainty values was not considered.

Regarding the uncertainty analysis, dispersion bands are calculated for all FOMs, along with their main statistical parameters frequently used to characterize them, as the maximum, minimum, average, standard deviation, skewness, kurtosis, etc. Additionally, the characterization of the FOMs was performed by reconstructing their PDF and then looking for different fitting distribution functions.

2.3.4.8. Lessons learned and best practices

The application of an integral uncertainty and sensitivity analysis to severe accident studies depends significantly on the accident simulation tool. MAAP5 has many input variables to choose different physical models that impact simulation results. Additionally, several of those input variables offer additional options. Therefore, it is necessary to include different model options as qualitative uncertain variables, as part of a robust sensitivity analysis, in conjunction with quantitative physical parameters associated to those option models. For uncertainty analysis, the statistical characterization of the FOMs provides with data to properly choose a fitting function to the FOMs PDF histogram data. While different fitting functions may closely match the PDF data, when appropriate, Gaussian, or other PDFs that can be transformed to Gaussian, are preferred because allows direct applications, as exceedance probability of the acceptance criteria with a selected confidence level.

Regarding best practices, a robust uncertainty and sensitivity analysis requires applying different approaches, because results from different techniques may contradict each other and/or do not reflect the correct FOM – uncertain variables correlation data. In provided analysis it is shown that the MCF technique is a complementary and/or an alternative approach for sensitivity analysis, because it can deal with both physical (quantitative variables) and code options or flags (qualitative variables).

It is also necessary to perform some tests to ensure the numerical stability of the results for the main parameters of the heat balance when the severe accident code in use has several user input parameters to control integration time steps. Similar tests need to be performed for the severe accident base case.

Development and review of SAMGs require support from severe accident simulation results because in the case of occurrence of an event beyond design basis, instrumentation may become unreliable. Thus, timing of key events or time windows to take mitigation actions would be determined from simulation results of the accident evolution.

From the sensibility analysis, it is shown that code option models do have a relevant impact on the FOMs. Additionally, the uncertainty results for some of the selected FOM showed that the wide range in which their values fall, it makes necessary a more detailed analysis of the selection of the input uncertain variables. Therefore, the uncertainty and sensitivity analysis has clearly shown its value and capability of providing with information of practical application, and in particular to help to the development and review of SAMGs.

3. SUMMARY AND CONCLUSIONS

The presented exercise was performed by one Regulatory Authority (CNSNS-Mexico) and three research and development institutions (CIEMAT-Spain, GAEC-Ghana and ININ-Mexico); this is quite relevant, since it shows the synergy that can be achieved to generate more robust and practical uncertainty and sensitivity methodologies, not only to gain confidence on the range of applicability of the simulation results, but also to increase the understanding about phenomenology of BWR severe accident progression, such as but not limited to core oxidation and degradation, dynamics of corium in the lower head, primary containment atmosphere conditions and transport of fission products. Consequently, significant improvement is expected in modelling and numerical implementation of these phenomena in the severe accident codes.

A robust uncertainty and sensitivity analysis requires applying different approaches, as results from different techniques may contradict or fail to reflect the correct FOM correlation data. Therefore, it is important to use a variety of methods and techniques to verify the results of the analysis and ensure their robustness. This can include using different sampling techniques, different sensitivity measures, and different statistical analyses. Furthermore, the application of an integral uncertainty and sensitivity analysis to severe accident simulation may require addressing both qualitative and quantitative uncertain variables. Qualitative variables may include model parameters or assumptions that have no numerical value, while quantitative variables are those that can be assigned a specific numerical value. Addressing both types of variables is important to ensure that all sources of uncertainty are accounted for in the analysis.

Selecting the input uncertain variables and their probability distribution functions is also a crucial step in uncertainty and sensitivity analysis. This selection has to be based on expert knowledge and experience with the simulation code, as well as the available experimental and/or observational data. It is important to select a set of uncertain variables that are most relevant to the FOM being analysed and that can be varied independently. The selection of appropriate probability distribution functions could also be based on sound technical criteria, such as the characteristics of the data and the nature of the uncertainties being analysed.

The participating organizations applied various severe accident analysis codes coupled with uncertainty and sensitivity tools. The challenges presented, in general, included the codes not converted into the final results, bifurcations and outliers, implying that further research is needed in finding better ways to address these challenges and in identifying how relevant expertise is important when interpreting the results.

To ensure the numerical stability of the results for the main parameters of the heat balance, it is important to perform tests to control integration time steps in the severe accident code. This can be done by varying the time step size and observing how the results change. If the results are significantly affected by the time step size, it may be necessary to adjust the time step size or implement a more sophisticated integration scheme.

In addition to controlling integration time steps, it is also important to perform an integral uncertainty and sensibility analysis for severe accident studies. This involves selecting uncertain code input variables and associated probability distribution functions to represent specific phenomena during the progression of the severe accident. These selections could be made based on robust technical criteria, such as the analyst's experience with the simulation code and knowledge of the state-of-the-art physical phenomena occurring during the accident scenario.

Focusing on a single FOM or a few FOMs can facilitate the integral uncertainty and sensitivity analysis procedure and improve understanding of the impact of uncertain variables at each stage of the accident evolution. However, it is important to keep in mind that the application of an uncertainty and sensitivity analysis methodology is not a straightforward process and requires careful consideration of the selection of uncertain variables and associated probability distribution functions. The uncertainty and sensitivity analysis of the same FOM (for example, generated hydrogen mass) using different codes can help determining specific key parameters behind the physical phenomena driving progression of the accident and the dynamics of the FOM itself. Such analysis becomes more difficult when the FOM involved is a variable resulting from multiple processes along the accident (for example, radionuclide release to the environment).

Finally, it is important to perform similar tests for the severe accident base case to ensure that the results are consistent and reliable across a range of scenarios. By performing these tests and analyses, one can ensure that the numerical results obtained from the severe accident code are stable, reliable, and can be used to inform safety assessments and decision making processes.

REFERENCES

[1] INTERNATIONAL ATOMIC ENERGY AGENCY, Status and Evaluation of Severe Accident Simulation Codes for Water Cooled Reactors, IAEA-TECDOC-1872, Vienna (2019).

[2] Herranz L.E., López C., Challenges and sensitivities in the modelling of Fukushima Daiichi Unit-1 unfolding with MELCOR 2.2, *Annals Nuclear Energy* 141, 107348, (2020). https://doi.org/10.1016/j.anucene.2020.107348

[3] Ross K., Phillips J., Gauntt R.O., Wagner K.C., MELCOR Best Practices as Applied in the State-of-the-Art Reactor Consequence Analyses (SOARCA) Project, NUREG/CR-7008, (2014).

[4] Bocanegra R., Towards a BEPU Methodology for Containment Safety Analyses. Ph.D. Dissertation, Universidad Politécnica de Madrid, Madrid, Spain, (2019).

[5] U.S. NRC, Transient and Accident Analysis Methods. Reg. Guide 1.203, (2005).

[6] Oberkampf W.L., Blottner F.G., Issues in Computational Fluid Dynamics Code Verification and Validation, AIAAJ 36 (5), (1998).

[7] Baccou J., et all., SAPIUM: A Generic Framework for a Practical and Transparent Quantification of Thermal-Hydraulic Code Model Input Uncertainty, *Nuclear Science and Engineering* 194 (8-9), (2020). https://doi.org/10.1080/00295639.2020.1759310

[8] Ghosh S.T., et all, Estimating Safety Valve Stochastic Failure-to-Close Probabilities for the Purpose of Nuclear Reactor Severe Accident Analysis, Proceedings of the ASME/NRC Pump and Valve Symposium, (2017).

[9] Walpole R.E., Myers R.H., Myers S.L., Ye K., Probability & Statistics for Engineers & Scientists, 9th ed., (2011).

[10] Yager R.R., Entropy and Specificity in a Mathematical Theory of Evidence, *International Journal of General Systems* 9 (4), pp. 249–260, (1983). DOI:10.1007/978-3-540-44792-4_11

[11] Helton J.C., Johnson J.D., Oberkampf W.L., Sallaberry C.J., Representation of Analysis Results Involving Aleatory and Epistemic Uncertainty, (2008).

[12] Sebastien D., Lecture Notes for Summer School FJOH, (2017).

[13] Laplace, Theorie Analytique des Probabilités, 2nd ed., Pair de France, (1814).

[14] Metropolis N., Ulam S., The Monte Carlo Method, *Journal of the American Statistical Association* 44 (247), pp. 335–341, (1949). DOI: 10.1080/01621459.1949.10483310

[15] Wilks S.S., Statistical Prediction with Special Reference to the Problem of Tolerance Limits, *The Annals of Mathematical Statistics,* (1942).

[16] Wilks S.S., Determination of Sample Sizes for Setting Tolerance Limits, *The Annals of Mathematical Statistics*, pp. 91–96, (1941).

[17] Pearson K., On the Theory of Contingency and Its Relation to Association and Normal Correlation, (1904).

[18] Spearman, C., Footrule' for Measuring Correlations, *British Journal of Psychology*, 1904–1920 2*,* **No. 1**, pp. 89–108, (1906).

[19] Sevón T., A MELCOR Model of Fukushima Daiichi Unit 1 Accident. Annals of Nuclear Energy 85, 1–11, (2015).

[20] Gauntt R. O., Bixler N., Wagner K.C., An Uncertainty Analysis of the Hydrogen Source Term for a Station Blackout Accident in Sequoyah Using MELCOR 1.8.5, Sandia National Laboratories, (2003).

[21] Rickard, M., Modeling of PWR LOCA Experiments in RELAP5 Based on PREMIUM Benchmark, MSc. Thesis, Chalmers University of Technology, Gothenburg, Sweden, (2013).
[22] Bohnhoff, W.J., et all., DAKOTA, A Multilevel Parallel Object-Oriented Framework for Design Optimization, Parameter Estimation, Uncertainty Quantification, and Sensitivity Analysis: Version 6.11. User's Manual, Albuquerque, Nov. (2019).
[23] Jacquemain, D., et al., PHEBUS FPT1 Final Report, Cadarache, France, (2000).
[24] Mattie, P., et all., U.S. Nuclear Regulatory Commission, State-of-the-Art Reactor Consequence Analyses Project: Uncertainty Analysis of the Unmitigated Long-Term Station Blackout of the Peach Bottom Atomic Power Station, NUREG/CR-7155, Washington, DC, (2016).
[25] Boafo, E.K., Numapau Gyamfi, E., Uncertainty Quantification in Support of Severe Accident Analysis Code User Confidence Using MELCOR-DAKOTA. *Journal of Nuclear Engineering and Radiation Science*, Vol. **8** / 031703-1 (2022). https://doi.org/10.1115/1.4053050
[26] Jones K., Vogt D., DAKOTA Uncertainty Plug-ins User´s Manual for SNAP, Applied Programming Technology, Inc., (2012).
[27] Straka M., Ward L., BWR PIRT and Assessment Matrices for BWR LOCA and Non-LOCA Events", SCIE-NRC-393-99, Washington, D.C.
[28] Larsen L., BWR Modeling and Model Assessment Session - 2. Determining Key Analysis Parameters", Inf. Sys. Lab., TRACE Workshop, (2011).
[29] Larsen L., BWR Modeling and Model Assessment Session – 3. Important BWR Phenomena", Inf. Sys. Lab., TRACE Workshop, (2011).
[30] GE Nuclear Energy, BWR/6 General Description of a Boiling Water Reactor, Oakland, (1980).
[31] Hessheimer M.F., Dameron R.A., Containment Integrity Research at Sandia National Laboratories - an Overview, NUREG/CR-6906, SAND2006-2274P, (2006).
[32] United States of America Nuclear Regulatory Commission, 10 CFR 50.2 Definitions, (2014).
[33] Electric Power Research Institute, Modular Accident Analysis Program 5 (MAAP5) Applications Guidance. Desktop Reference for Using MAAP5 Software – Phase 3 Report, Final Report 3002010658, Washington DC, (2017).
[34] Nuclear Energy Agency / Committee on the Safety of Nuclear Installations, Report on the Uncertainty Methods Study, NEA/CSNI/R(97)35 Vols. **1** and **2**, Paris, (1998).
[35] Glaeser H., Hofer E., Kloos M., Skorek T., GRS Analyses for CSNI Uncertainty Methods Study (UMS) in Report on the Uncertainty Methods Study, NEA/CSNI/R(97)35 Vol. **1**, Paris, (1998).
[36] Glaeser H., GRS Method for Uncertainty and Sensitivity Evaluation of Code Results and Applications, *Science and Technology of Nuclear Installations*, pp. 1–7, (2008). DOI:10.1155/2008/798901
[37] Bolado-Lavin R., Costescu-Badea A., Review of Sensitivity Analysis Methods and Experience for Geological Disposal of Radioactive Waste and Spent Nuclear Fuel, JRC 49536, EUR 23712EN, (2008).
[38] Lurie D., Abramson L., Vail J., Applying Statistics, NUREG-1475 Rev. 1, (2011).
[39] Reyes-Fuentes M., et all., AZTUSIA: A New Application Software for Uncertainty and Sensitivity Analysis for Nuclear Reactors, Reliability and System Safety, 209, 107441, (2021).
[40] Gómez-Torres A.M., et all., "Mexican Platform for Analysis and Design of Nuclear Reactors," in Proceedings of the International Congress on Advances in Nuclear Power Plants ICAPP, (2015).
[41] Zugazagoitia E., et all, Uncertainty and Sensitivity Analysis of a PWR LOCA Sequence Using Parametric and Non-Parametric Methods, Reliability Engineering and System Safety, 193, (2020).

[42] Martin R.P., An Evaluation Methodology Development and Application Process for Severe Accident Safety Issue Resolution, *Science and Technology of Nuclear Installations*, pp. 1–13, (2012). https://doi.org/10.1155/2012/735719

[43] Sakai N., et all., Validation of MAAP Model Enhancement for Fukushima Dai-ichi Accident Analysis with Phenomena Identification and Ranking Table (PIRT), *Journal of Nuclear Science and Technology*, 51, pp. 951–963, (2014). https://doi.org/10.1080/00223131.2014.901927

[44] Nuclear Energy Agency / Committee on the Safety of Nuclear Installations, Ability of Current Advanced Codes to Predict In-Vessel Core Melt Progression and Degraded Core Coolability - Benchmark Exercise on Three Mile Island-2 Plant. Final Report, NEA/CSNI/R 3, (2015).

[45] Schober P., Boer C., Schwarte L.A., Correlation Coefficients: Appropriate Use and Interpretation, Anesthesia & Analgesia, 126, 5, pp. 1763–1768, (2018).

[46] Fernández-Cosials K., et all Statistical Characterization of NPP Transients: Application to PWR LBLOCA, *Annals of Nuclear Energy*, 144, 107505, (2020). https://doi.org/10.1016/j.anucene.2020.107505

ABBREVATIONS

BWR	Boiling Water Reactor
BEPU	Best Estimate plus Uncertainty
CIEMAT	Centro de Investigaciones Energéticas, Medioambientales y Tecnológicas
CNSNS	Comisión Nacional de Seguridad Nuclear y Salvaguardias
DAKOTA	Design Analysis Kit for Optimization and Terascale Applications
GAEC	Ghana Atomic Energy Commission
IC	Isolation Condenser
ININ	Instituto Nacional de Investigaciones Nucleares
MAAP	Modular Accident Analysis Program
MCF	Monte Carlo Filtering
PCC	Partial Correlation Coefficient
PDF	Probability Density Function
PSCC	Pearson Simple Correlation Coefficient
PRCC	Partial Rank Correlation Coefficient
SBO	Station blackout
SNL	Sandia National Laboratory
SRCC	Spearman Rank Correlation Coefficient
SRV	Safety / Relief Valve
RCIC	Rector Core Isolation Cooling
RPV	Reactor Pressure Vessel

CONTRIBUTORS TO DRAFTING AND REVIEW

ALBRIGTH, L. I.	SNL (USA)
AMADOR-GARCÍA, R.	ININ (Mexico)
ANSAH-NAH, T.	GAEC (Ghana)
BOAFO, E. K.	GAEC (Ghana)
BOTCHWAY, E. K.	GAEC (Ghana)
DELVALLE-GALLEGOS, E.	IPN-ESFM (Instituto Politécnico Nacional – Escuela Superior de Física y Matemáticas Mexico)
GABRIELLI, F.	KIT (Germany)
GYAMFI, E. N.	GAEC (Ghana)
HERRANZ, L. E.	CIEMAT (Spain)
JEVREMOVIC, T.	IAEA
LUXAT, David L.	SNL (USA)
MARTÍNEZ-CABALLERO, E.	ININ (Mexico)
MASCARI, F.	ENEA (Italy)
ORTIZ-VILLAFUERTE, J.	ININ (Mexico)
QUERAL, C.	UPM (Universidad Politécnica de Madrid, Spain)
REYES-FUENTES, M.	IPN-ESFM (Instituto Politécnico Nacional – Escuela Superior de Física y Matemáticas Mexico)
REHMAN, ur H.	IAEA
SÁNCHEZ-MORA, H.	IPN-ESFM (Instituto Politécnico Nacional – Escuela Superior de Física y Matemáticas Mexico)

Research Coordination Meetings (RCMs)

1st RCM, IAEA Headquarters, Vienna, Austria, 14–17 October, 2019.

2nd RCM, IAEA Headquarters, Vienna, Austria, 20–22 October, 2020.

3rd RCM, IAEA Headquarters, Vienna, Austria, 8–10 November, 2021.

4th RCM, IAEA Headquarters, Vienna, Austria, 7–10 November, 2022.

IAEA
International Atomic Energy Agency

No. 27

ORDERING LOCALLY

IAEA priced publications may be purchased from the sources listed below or from major local booksellers.

Orders for unpriced publications should be made directly to the IAEA. The contact details are given at the end of this list.

NORTH AMERICA

Bernan / Rowman & Littlefield

15250 NBN Way, Blue Ridge Summit, PA 17214, USA
Telephone: +1 800 462 6420 • Fax: +1 800 338 4550
Email: orders@rowman.com • Web site: www.rowman.com/bernan

REST OF WORLD

Please contact your preferred local supplier, or our lead distributor:

Eurospan

1 Bedford Row
London
WC1R 4BU
United Kingdom

Trade Orders and Enquiries:

Tel: +44 (0)1235 465576
Email: trade.orders@marston.co.uk

Individual Customers:

Tel: +44 (0)1235 465577
Email: direct.orders@marston.co.uk
www.eurospanbookstore.com/iaea

For further information:

Tel. +44 (0) 207 240 0856
Email: info@eurospan.co.uk
www.eurospan.co.uk

Orders for both priced and unpriced publications may be addressed directly to:

Marketing and Sales Unit
International Atomic Energy Agency
Vienna International Centre, PO Box 100, 1400 Vienna, Austria
Telephone: +43 1 2600 22529 or 22530 • Fax: +43 1 26007 22529
Email: sales.publications@iaea.org • Web site: www.iaea.org/publications

24-02407E

International Atomic Energy Agency
Vienna
www.iaea.org